

Mathematical and computational methods for semiclassical Schrödinger equations

Shi Jin

*Department of Mathematics,
University of Wisconsin, Madison, WI 53706.
Email: jin@math.wisc.edu*

Peter Markowich

*Department of Applied Mathematics and Theoretical Physics,
University of Cambridge,
Wilberforce Road, Cambridge CB3 0WA.
Email: p.markowich@damtp.cam.ac.uk*

Christof Sparber

*Department of Mathematics, Statistics, and Computer Science,
University of Illinois at Chicago,
851 South Morgan Street, Chicago, Illinois 60607.
Email: sparber@math.uic.edu*

We consider time-dependent (linear and nonlinear) Schrödinger equations in a semiclassical scaling. These equations form a canonical class of (nonlinear) dispersive models whose solutions exhibit high frequency oscillations. The design of efficient numerical methods which produce an accurate approximation of the solutions, or, at least, of the associated physical observables, is a formidable mathematical challenge. In this article we shall review the basic analytical methods for dealing with such equations, including WKB-asymptotics, Wigner measures techniques and Gaussian beams. Moreover, we shall give an overview of the current state-of-the-art of numerical methods (most of which are based on the described analytical techniques) for the Schrödinger equation in the semiclassical regime.

1

¹ S. Jin was partially supported by NSF grant No. DMS-0608720, NSF FRG grant DMS-0757285, a Van Vleck Distinguished Research Prize and a Vilas Associate Award from the University of Wisconsin-Madison. C. Sparber was partially supported by the Royal Society through his University Research Fellowship. P. Markowich was supported by his Royal Society Wolfson Research Merit Award and by KAUST through his Investigator Award KUK-I1-007-43.

CONTENTS

1	Introduction	2
2	WKB analysis for semiclassical Schrödinger equations	5
3	Wigner transforms and Wigner measures	10
4	Finite difference methods for semiclassical Schrödinger equations	14
5	Time-splitting spectral methods for semiclassical Schrödinger equations	20
6	Moment closure methods	26
7	Level-set methods	31
8	Gaussian beam methods - Lagrangian approach	35
9	Gaussian beam methods - Eulerian approach	40
10	Asymptotic methods for discontinuous potentials	46
11	Schrödinger equations with matrix-valued potentials and surface hopping	52
12	Schrödinger equations with periodic potential	57
13	Numerical methods for the Schrödinger equation with periodic potentials	62
14	Schrödinger equation with random potentials	69
15	Nonlinear Schrödinger equations in the semiclassical regime	72
	References	79

1. Introduction

This goal of this article is to give an overview of the currently available numerical methods used in the study of *highly oscillatory* partial differential equations (PDEs) of Schrödinger type. This type of equations form a canonical class of (nonlinear) *dispersive* PDEs, i.e. equations in which waves of different frequency travel with different speed. The accurate and efficient numerical computation of such equations usually requires a lot of analytical insight and in particular this applies to the regime of high frequencies.

The following equation can be seen as a paradigm for the PDEs under consideration:

$$i\varepsilon\partial_t u^\varepsilon = -\frac{\varepsilon^2}{2}\Delta u^\varepsilon + V(x)u^\varepsilon; \quad u^\varepsilon(0, x) = u_{\text{in}}^\varepsilon(x), \quad (1.1)$$

for $(t, x) \in \mathbb{R} \times \mathbb{R}^d$, with $d \in \mathbb{N}$ denoting the spatial dimension. In addition, $\varepsilon \in (0, 1]$ denotes the small *semiclassical parameter* (the scaled Planck's constant), describing the microscopic/macroscopic scale ratio. Here, we already rescaled all physical parameters, such that only one dimensionless

parameter $\varepsilon \ll 1$ remains. The unknown $u^\varepsilon = u^\varepsilon(t, x) \in \mathbb{C}$ is the quantum mechanical wave function whose dynamics is governed by a static potential function $V = V(x) \in \mathbb{R}$ (time-dependent potentials $V(t, x)$ usually can also be taken into account without requiring too much extra work, but for the sake of simplicity we shall not do so here). In this article, several different classes of potentials, e.g., smooth, discontinuous, periodic, random, will be discussed, each of which requires a different numerical strategy. In addition, possible nonlinear effects can be taken into account (as we shall do in Section 15) by considering nonlinear potentials $V = f(|u^\varepsilon|^2)$.

In the absence of $V(x)$ a particular solution to the Schrödinger equation is given by a single plane wave

$$u^\varepsilon(t, x) = \exp\left(\frac{i}{\varepsilon}\left(\xi \cdot x - \frac{t}{2}|\xi|^2\right)\right),$$

for any given wave vector $\xi \in \mathbb{R}^d$. We see that u^ε features oscillations with frequency $1/\varepsilon$ in space and time, which *inhibit strong convergence* of the wave function in the *classical limit* $\varepsilon \rightarrow 0_+$. In addition, these oscillations pose a huge challenge in numerical computations of (2.1), particularly they strain computationally resources when run-off-the-mill numerical techniques are applied in order to numerically solve (1.1) in the *semiclassical regime* $\varepsilon \ll 1$. For the linear Schrödinger equation classical numerical analysis methods (like the stability-consistency concept) are sufficient to derive meshing strategies for discretizations (say, of finite difference, finite element or even time splitting spectral type) which guarantee (locally) strong convergence of the discrete wave functions when the semiclassical parameter ε is fixed (cf. (Chan, Lee and Shen 1986), (Chan and Shen 1987), (Wu 1996), (Dörfler 1998), extensions to nonlinear Schrödinger equations can be found in, e.g., (Delfour, Fortin and Payre 1981), (Taha and Ablowitz 1984), (Pathria and Morris 1990)). However, the classical numerical analysis strategies *cannot* be employed to investigate uniform in ε properties of discretization schemes in the semiclassical limit regime. As we shall detail in Section 4, even seemingly reasonable, i.e. stable and consistent, discretization schemes, which are heavily used in many practical application areas of Schrödinger-type equations, require *huge computational resources* in order to give accurate physical observables for $\varepsilon \ll 1$. The situation gets even worse when an accurate resolution of u^ε itself is required. To this end, we remark that time-splitting spectral methods tend to behave better than finite difference/finite element methods, as we shall see in more detail in Section 5.

In summary, there is clearly a big risk in using classical discretization techniques for Schrödinger calculations in the semiclassical regime. Certain schemes produce completely wrong observables under seemingly reasonable meshing strategies i.e. an asymptotic resolution of the oscillation is not

always enough. Even worse, in these cases there is no warning from the scheme (like destabilization) that something went wrong in the computation (since local error control is computationally not feasible in the semiclassical regime). The only safety anchor here lies in asymptotic mathematical analysis, such as *WKB analysis*, and/or a physical insight on the problem. They typically yield a (rigorous) asymptotic description of u^ε for small $\varepsilon \ll 1$ which consequently can be implemented on a numerical level, providing an *asymptotic numerical scheme* for the problem at hand. In this work, we shall discuss several asymptotic schemes, depending on the particular type of potentials V considered.

While one can not expect to be able to pass to the classical limit directly in the solution u^ε of (1.1), one should note that *densities of physical observables*, which are the quantities most interesting in practical applications, are typically better behaved as $\varepsilon \rightarrow 0$, since they are quadratic in the wave function (see Section 2.1 below). However, weak convergence of u^ε as $\varepsilon \rightarrow 0$ is *not* sufficient for passing to the limit in the observable densities (since weak convergence does not commute with nonlinear operations). This makes the analysis of the semiclassical limit a mathematically highly complex issue. Recently, much progress has been made in this area, particularly by using tools from micro-local analysis, such as *H-measures* (Tartar 1990) and *Wigner measures* (Lions and Paul 1993), (Markowich and Mauser 1993), (Gérard, Markowich, Mauser and Poupaud 1997). These techniques go far beyond classical WKB-methods, since the latter suffers from the appearance of *caustics* (see, e.g. (Sparber, Markowich and Mauser 2003) for a recent comparison of the two methods). In contrast to that, Wigner measure techniques reveal a kinetic equation on *phase space*, whose solution, the so-called *Wigner measure* associated to u^ε , does not exhibit caustics (see Section 3 for more details).

A word of caution is in order: First, a reconstruction of the asymptotic description for u^ε itself (for $\varepsilon \ll 1$) is in general not straightforward, since, typically, some phase information is lost when passing to the Wigner picture. Second, phase space techniques have proved to be very powerful in the linear case and in certain weakly nonlinear regimes, but they have not shown too much strength yet when applied to *nonlinear* Schrödinger equations in regime of supercritical geometric optics (see Section 15.2). There, classical WKB analysis (and in some special cases techniques for fully integrable systems) still prevails. The main mathematical reason for this is that the initial value problem for the linear Schrödinger equation propagates only one ε -scale of oscillations, provided the initial datum in itself is ε -oscillatory (as it is always assumed in WKB analysis). New (spatial) frequencies ξ may be generated during the time-evolution (typically, at caustics) but no new scales of oscillations will arise in the linear case. For nonlinear Schrödinger problems this is different, as new oscillation scales may be generated through

the nonlinear interaction of the solution with itself. Further, one should note that this important analytical distinction, i.e. no generation of new scales, but possible generation of new frequencies (in the linear case), may not be relevant on the numerically level, since, say, 100ε is analytically just a new frequency but numerically indeed a new scale.

Aside from semiclassical situations, modern research in the numerical solution of Schrödinger-type equations goes in a variety of directions, most importantly:

- (i) *Stationary problems* stemming from, e.g, material science. We mention band diagram computations (to be touched upon below in Sections 12 and 13) and density functional theory for approximating the full microscopic Hamiltonian (not to be discussed in this paper). The main difference between stationary and time-dependent semiclassical problems is given by the fact that in the former situation the spatial frequency is fixed, whereas in the latter (as already mentioned before) new frequencies may arise during the course of time.
- (ii) *Large spatial dimensions* $d \gg 1$, arising for example when the number of particles $N \gg 1$, since the quantum mechanical Hilbert space for N indistinguishable particles (without spin) is given by $L^2(\mathbb{R}^{3N})$. This is extremely important in quantum chemistry simulations of atomistic/molecular applications. Totally different analytical and numerical techniques need to be used and we shall not elaborate on these issues in this paper. We only remark that in case some of the particles are very heavy and can thus be treated classically (invoking the so-called Born-Oppenheimer approximation, cf. Section 11), a combination of numerical methods for both $d \gg 1$ and $\varepsilon \ll 1$ has to be used.

2. WKB analysis for semiclassical Schrödinger equations

2.1. Basic existence results and physical observables

We recall the basic existence theory for linear Schrödinger equations of the form

$$i\varepsilon\partial_t u^\varepsilon = -\frac{\varepsilon^2}{2}\Delta u^\varepsilon + V(x)u^\varepsilon; \quad u^\varepsilon(0, x) = u_{\text{in}}^\varepsilon(x). \quad (2.1)$$

For the sake of simplicity we assume the (real-valued) potential $V = V(x)$ to be continuous and bounded, i.e.

$$V \in C(\mathbb{R}^d; \mathbb{R}) : \quad |V(x)| \leq K.$$

The Kato-Rellich theorem then ensures that the Hamiltonian operator

$$H^\varepsilon := -\frac{\varepsilon^2}{2}\Delta + V(x), \quad (2.2)$$

is essentially self-adjoint on $D(-\Delta) = C_0^\infty \subset L^2(\mathbb{R}^d; \mathbb{C})$ and bounded from below by $-K$, see e.g. (Reed and Simon 1975). Its unique self-adjoint extension (to be denoted by the same symbol) therefore generates a strongly continuous semi-group $U^\varepsilon(t) = e^{-itH^\varepsilon/\varepsilon}$ on $L^2(\mathbb{R}^d)$, which ensures the global existence of a unique (mild) solution $u^\varepsilon(t) = U^\varepsilon(t)u_{\text{in}}$ of the Schrödinger equation (2.1). Moreover, since $U^\varepsilon(t)$ is unitary, it holds

$$\|u^\varepsilon(t, \cdot)\|_{L^2}^2 = \|u_{\text{in}}^\varepsilon\|_{L^2}^2, \quad \forall t \in \mathbb{R}.$$

In quantum mechanics this is interpreted as conservation of mass. In addition, we also have conservation of the *total energy*

$$E[u^\varepsilon(t)] = \frac{\varepsilon^2}{2} \int_{\mathbb{R}^d} |\nabla u^\varepsilon(t, x)|^2 dx + \int_{\mathbb{R}^d} V(x)|u^\varepsilon(t, x)|^2 dx, \quad (2.3)$$

which is the sum of the kinetic and the potential energies.

In general, expectation values of physical observables are computed via quadratic functionals of u^ε . To this end, denote by $a^W(x, \varepsilon D_x)$ the operator corresponding to a classical (phase space) observable $a \in C_b^\infty(\mathbb{R}^d \times \mathbb{R}^d)$, obtained via *Weyl-quantization*

$$a^W(x, \varepsilon D_x)f(x) := \frac{1}{(2\pi)^m} \iint_{\mathbb{R}^d \times \mathbb{R}^d} a\left(\frac{x+y}{2}, \varepsilon \xi\right) f(y) e^{i(x-y)\cdot\xi} d\xi dy, \quad (2.4)$$

where $\varepsilon D_x := -i\varepsilon \partial_x$. Then, the expectation value of a in the state u^ε at time $t \in \mathbb{R}$ is given by

$$a[u^\varepsilon(t)] = \langle u^\varepsilon(t), a^W(x, \varepsilon D_x)u^\varepsilon(t) \rangle_{L^2}. \quad (2.5)$$

where $\langle \cdot, \cdot \rangle_{L^2}$ denotes the usual scalar product on $L^2(\mathbb{R}^d; \mathbb{C})$.

Remark 2.1. The convenience in the Weyl-calculus lies in the fact that an (essentially) selfadjoint Weyl-operator $a^W(x, \varepsilon D_x)$ has a real-valued symbol $a(x, \xi)$, cf. (Hörmander 1985).

The quantum mechanical wave function u^ε can therefore be considered only an auxiliary quantity, whereas (real-valued) quadratic quantities of u^ε yield probability densities for the respective physical observables. The most basic quadratic quantities are the *particle density*

$$\rho^\varepsilon(t, x) := |u^\varepsilon(t, x)|^2, \quad (2.6)$$

and the *current density*

$$j^\varepsilon(t, x) := \varepsilon \operatorname{Im}(\overline{u^\varepsilon(t, x)} \nabla u^\varepsilon(t, x)). \quad (2.7)$$

It is easily seen that if u^ε solves (2.1), then the following conservation law holds

$$\partial_t \rho^\varepsilon + \operatorname{div} j^\varepsilon = 0. \quad (2.8)$$

In view of (2.3) we can also define the *energy density*

$$e^\varepsilon(t, x) := \frac{1}{2} |\varepsilon \nabla u^\varepsilon(t, x)|^2 + V(x) \rho^\varepsilon(t, x). \quad (2.9)$$

As will be seen (cf. Section 5), computing these observable densities numerically is usually less cumbersome than computing the actual wave function u^ε accurately. From the analytical point of view, however, we are facing the problem that the classical limit $\varepsilon \rightarrow 0$ can only be regarded as a weak limit (in a suitable topology), due to the oscillatory nature of u^ε . Quadratic operations defining densities of physical observables in general do not commute with weak limits and hence, it remains a challenging task to identify the (weak) limits of certain physical observables, or densities, respectively.

2.2. Asymptotic description of high frequencies

In order to gain a better understanding of the oscillatory structure of u^ε we invoke the following *WKB approximation*, cf. (Carles 2008) and the references given therein:

$$u^\varepsilon(t, x) \stackrel{\varepsilon \rightarrow 0}{\sim} a^\varepsilon(t, x) e^{iS(t, x)/\varepsilon}, \quad (2.10)$$

with real-valued phase S and (possibly) complex-valued amplitude a^ε , satisfying the asymptotic expansion

$$a^\varepsilon \stackrel{\varepsilon \rightarrow 0}{\sim} a + \varepsilon a_1 + \varepsilon^2 a_2 + \dots \quad (2.11)$$

Plugging the ansatz (2.10) into (2.1), one can determine an approximate solution to (2.1), by subsequently solving the equations obtained in each order of ε .

In leading order, i.e. terms of order $\mathcal{O}(1)$, one obtains a *Hamilton-Jacobi equation* for the phase function S :

$$\partial_t S + \frac{1}{2} |\nabla S|^2 + V(x) = 0; \quad S(0, x) = S_{\text{in}}(x). \quad (2.12)$$

This equation can be solved by the method of characteristics, provided $V(x)$ is sufficiently smooth, say $V \in C^2(\mathbb{R}^d)$. The characteristic flow is given by the following Hamiltonian system of ordinary differential equations

$$\begin{cases} \dot{x}(t, y) = \xi(t, y); & x(0, y) = y, \\ \dot{\xi}(t, y) = -\nabla_x V(x(t, y)); & \xi(0, y) = \nabla S_{\text{in}}(y). \end{cases} \quad (2.13)$$

Remark 2.2. The characteristic trajectories $y \mapsto x(t, y)$ obtained via (2.13) are usually interpreted as the *rays of geometric optics*. The WKB approximation considered here is therefore also regarded as the geometric optics limit of the wave field u^ε .

By the Cauchy-Lipschitz theorem, this system of ordinary differential equations can be solved at least locally in-time and consequently yields the phase function

$$S(t, x) = S(0, x) - \int_0^t \frac{1}{2} |\nabla S(\tau, y(\tau, x))|^2 + V(y(\tau, x)) \, d\tau.$$

where $y(\tau, x)$ denotes the inversion of the characteristic flow $X_t : y \mapsto x(t, y)$. This yields a smooth phase function $S \in C^\infty([-T, T] \times \mathbb{R}^d)$ up to some time $T > 0$ but possibly very small. The latter is due to the fact that in general characteristics will cross at some finite time $|T| < \infty$, in which case the flow map $X_t : \mathbb{R}^d \rightarrow \mathbb{R}^d$ is no longer one-to-one. The set of points at which X_t ceases to be a diffeomorphism is usually called *caustic set*. See Fig. 2.1 (taken from (Gosse, Jin and Li 2003)) for examples of caustic formulation.

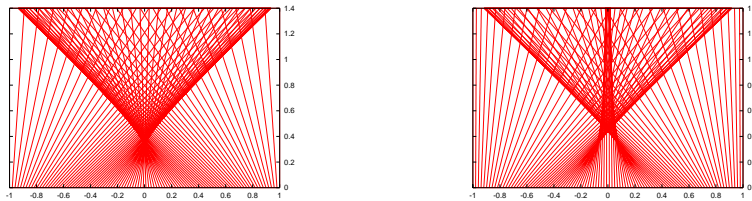


Figure 2.1. Caustics generated from initial data $\partial_x S_{\text{in}}(x) = -\sin(\pi x) |\sin(\pi x)|^{p-1}$. Left: $p = 1$, and the solution becomes triple valued. Right: $p = 2$, and we exhibit single-, triple- and quintuple-valued solutions.

Ignoring the problem of caustics for a moment one can proceed with our asymptotic expansion and obtain at order $\mathcal{O}(\varepsilon)$ the following transport equation for the leading order amplitude

$$\partial_t a + \nabla S \cdot \nabla a + \frac{a}{2} \Delta S = 0; \quad a(0, x) = a_{\text{in}}(x). \quad (2.14)$$

In terms of the leading order particle density $\rho := |a|^2$, this reads

$$\partial_t \rho + \text{div}(\rho \nabla S) = 0, \quad (2.15)$$

which is reminiscent of the conservation law (2.8).

The transport equation (2.14) is again solved by the methods of characteristics (as long as S is smooth, i.e. before caustics) and yields

$$a(t, x) = \frac{a_{\text{in}}(y(t, x))}{\sqrt{J_t(y(t, x))}}, \quad |t| \leq T. \quad (2.16)$$

where $J_t(y) := \det \nabla_y x(t, u)$ denotes the Jacobi determinant of the Hamiltonian flow. All higher order amplitudes a_n are then found to be solutions of inhomogeneous transport equations of the form

$$\partial_t a_n + \nabla S \cdot \nabla a_n + \frac{a_n}{2} \Delta S = \Delta a_{n-1}. \quad (2.17)$$

These equations are consequently solved by the method of characteristics. At least locally in-time (before caustics) this yields an approximate solution of WKB type

$$u_{\text{app}}^\varepsilon(t, x) = e^{iS(t,x)/\varepsilon} (a(t, x) + \varepsilon a_1(t, x) + \varepsilon^2 a_2(t, x) + \dots)$$

including amplitudes $(a_n)_{n=1}^N$ up to some order $N \in \mathbb{N}$. It is then straightforward to prove the following stability result:

Theorem 2.3. Assume that the initial data of (2.1) is given in WKB form

$$u_{\text{in}}^\varepsilon(x) = a_{\text{in}}(x) e^{iS_{\text{in}}(x)/\varepsilon} \quad (2.18)$$

with $S_{\text{in}} \in C^\infty(\mathbb{R}^d)$ and let $a_{\text{in}} \in \mathcal{S}(\mathbb{R}^d)$, i.e. smooth and rapidly decaying. Then for any closed time-interval $I \subset T$, before caustic onset, there exists a $C > 0$, independent of $\varepsilon \in (0, 1]$ such that

$$\sup_{t \in I} \|u^\varepsilon(t) - u_{\text{app}}^\varepsilon(t)\|_{L^2 \cap L^\infty} \leq C \varepsilon^N.$$

The first rigorous result of this type goes back to (Lax 1957). Its main drawback is the fact that the WKB solution breaks down at caustics, where S develops singularities. In addition, the leading order amplitude a blows up in $L^\infty(\mathbb{R}^d)$, in view of (2.16) and the fact that $\lim_{t \rightarrow T} J_t(y) = 0$. Of course, these problems are not present in the exact solution u^ε but are merely an artifact of the WKB ansatz (2.10). Caustics therefore indicate the appearance of new ε -oscillatory scales within u^ε , which are not captured by the simple oscillatory ansatz (2.10).

2.3. Beyond caustics

At least locally away from caustics, though, the solution can always be described by a superposition of WKB waves. This can be seen rather easily in the case of free dynamics where $V(x) = 0$. The corresponding solution of the Schrödinger equation (2.1) with WKB initial data is then explicitly given by

$$u^\varepsilon(t, x) = \frac{1}{(2\pi\varepsilon)^d} \iint_{\mathbb{R}^d \times \mathbb{R}^d} a_{\text{in}}(y) e^{i\varphi(x,y,\xi,t)/\varepsilon} dy d\xi, \quad (2.19)$$

with phase function

$$\varphi(x, y, \xi, t) := (x - y) \cdot \xi + \frac{t}{2} |\xi|^2 + S_{\text{in}}(y). \quad (2.20)$$

The representation formula (2.19) comprises an oscillatory integral, whose main contributions stem from *stationary phase points* at which $\partial_{y,\xi}\varphi(x,t) = 0$. In view of (2.20) this yields

$$\xi = \nabla S, \quad y = x - t\xi,$$

The corresponding map $y \mapsto x(t,y)$ is the characteristic flow of the free Hamilton Jacobi equation

$$\partial_t S + \frac{1}{2}|\nabla S|^2 = 0; \quad S(0,x) = S_{\text{in}}(x)$$

Reverting the relation $y \mapsto x(t,y)$ yields the required stationary phase points $\{y_j(t,x)\}_{j \in \mathbb{N}} \in \mathbb{R}^d$ for the integral (2.19). Assuming for simplicity that there are only finitely many such points, then

$$\begin{aligned} u^\varepsilon(t,x) &= \frac{1}{(2\pi\varepsilon)^d} \iint_{\mathbb{R}^d \times \mathbb{R}^d} a_{\text{in}}(y) e^{i\varphi(x,y,\xi,t)/\varepsilon} dy d\xi \\ &\underset{\varepsilon \rightarrow 0}{\sim} \sum_{j=1}^J \frac{a_{\text{in}}(y_j(t,x))}{\sqrt{J_t(y_j(t,x))}} e^{iS(y_j(t,x))/\varepsilon + i\pi m_j/4}, \end{aligned} \quad (2.21)$$

with constant phase shifts $m_j \in \mathbb{N}$ (usually referred to as the Keller-Maslov index). The right hand side of this expression is usually referred to as *multi-phase WKB approximation*. The latter can be interpreted as an asymptotic description of interfering wave trains in u^ε .

Remark 2.4. The case of non-vanishing $V(x)$, although similar in spirit, is much more involved in general. In order to determine asymptotic description of u^ε beyond caustics, one needs to invoke the theory of *Fourier integral operators*, see e.g. (Duistermaat 1996). In particular it is in general very hard to determine the precise form and number of caustics appearing throughout the time-evolution of $S(t,x)$, which is why there is an extensive amount of papers on numerical schemes for ‘capturing caustics’, see e.g. (Benamou and Sollic 2000), or (Benamou, Lafitte, Sentis and Sollic 2003) and the references therein.

3. Wigner transforms and Wigner measures

3.1. The Wigner transformed picture of quantum mechanics

Whereas WKB type methods aim for approximate solutions of u^ε , the goal of this section is to directly identify the weak limits of physical observable densities as $\varepsilon \rightarrow 0$. To this end, one defines the so-called *Wigner transform* of u^ε , as given in (Wigner 1932):

$$w^\varepsilon[u^\varepsilon](x,\xi) := \frac{1}{(2\pi)^d} \int_{\mathbb{R}^d} u^\varepsilon\left(x + \frac{\varepsilon}{2}\eta\right) \overline{u^\varepsilon}\left(x - \frac{\varepsilon}{2}\eta\right) e^{i\xi \cdot \eta} d\eta. \quad (3.1)$$

Plancherel's theorem together with a simple change of variables yields

$$\|w^\varepsilon\|_{L^2(\mathbb{R}^{2d})} = \varepsilon^{-d}(2\pi)^{-d/2}\|u^\varepsilon\|_{L^2(\mathbb{R}^d)}^2.$$

The real-valued Wigner transform $w^\varepsilon \in L^2(\mathbb{R}_x^d \times \mathbb{R}_\xi^d)$ can be interpreted as a phase-space description of the quantum state u^ε . In contrast to classical phase-space distributions, w^ε in general also takes negative values (except for Gaussian wave-functions).

Applying this transformation to the Schrödinger equation (2.1), the time-dependent Wigner function $w^\varepsilon(t, x, \xi) \equiv w^\varepsilon[u^\varepsilon(t)](x, \xi)$ is easily seen to satisfy

$$\partial_t w^\varepsilon + \xi \cdot \nabla_x w^\varepsilon - \Theta^\varepsilon[V]w^\varepsilon = 0; \quad w^\varepsilon(0, x, \xi) = w_{\text{in}}^\varepsilon(x, \xi), \quad (3.2)$$

where $\Theta^\varepsilon[V]$ is a pseudo-differential operator, taking into account the influence of $V(x)$. Explicitly it is given by

$$\Theta^\varepsilon[V]f(x, \xi) := \frac{i}{(2\pi)^d} \iint_{\mathbb{R}^d \times \mathbb{R}^d} \delta V^\varepsilon(x, y) f(x, \xi') e^{i\eta(\xi - \xi')} d\eta d\xi', \quad (3.3)$$

where the symbol δV^ε reads

$$\delta V^\varepsilon := \frac{1}{\varepsilon} \left(V\left(x - \frac{\varepsilon}{2}y\right) - V\left(x + \frac{\varepsilon}{2}y\right) \right).$$

Note that in the free case where $V(x) = 0$, the Wigner equation becomes the free transport equation of classical kinetic theory. Moreover, if $V \in C^1(\mathbb{R}^d)$ we obviously have that

$$\delta V^\varepsilon \xrightarrow{\varepsilon \rightarrow 0} y \cdot \nabla_x V,$$

in which case the $\varepsilon \rightarrow 0$ limit of (3.2) formally becomes the classical *Liouville equation* on phase space, see (3.7) below.

The most important feature of the Wigner transform is that it allows for a simple computation of quantum mechanical expectation values of physical observables. Namely,

$$\langle u^\varepsilon(t), a^W(x, \varepsilon D)u^\varepsilon(t) \rangle_{L^2} = \iint_{\mathbb{R}^d \times \mathbb{R}^d} a(x, \xi) w^\varepsilon(t, x, \xi) dx d\xi, \quad (3.4)$$

where $a(x, \xi)$ is the classical symbol of the operator $a^W(x, \varepsilon D_x)$. In addition, at least formally (since $w^\varepsilon \notin L^1(\mathbb{R}^d \times \mathbb{R}^d)$ in general), the particle density (2.6) can be computed via

$$\rho^\varepsilon(t, x) = \int_{\mathbb{R}^d} w^\varepsilon(t, x, \xi) d\xi,$$

and the current density (2.7) is given by

$$j^\varepsilon(t, x) = \int_{\mathbb{R}^d} \xi w^\varepsilon(t, x, \xi) d\xi.$$

Similarly, the energy density (2.9) is

$$e^\varepsilon(t, x) = \int_{\mathbb{R}^d} H(x, \xi) w^\varepsilon(t, x, \xi) \, d\xi,$$

where the classical (phase space) Hamiltonian function is denoted by

$$H(x, \xi) = \frac{1}{2}|\xi|^2 + V(x). \quad (3.5)$$

Remark 3.1. It can be proved that the Fourier transform of w^ε w.r.t. ξ satisfies $\widehat{w}^\varepsilon \in C_0(\mathbb{R}_y^d; L^1(\mathbb{R}_x^d))$ and likewise for the Fourier transformation of w^ε w.r.t. $x \in \mathbb{R}^d$. This allows to define the integrals of w^ε via a limiting process after convolving w^ε with Gaussians, see (Lions and Paul 1993) for more details.

3.2. Classical limit of Wigner transforms

The main point in the formulae given above is that the right hand side of (3.4) involves only linear operations of w^ε which is compatible with weak limits. To this end, we recall the main result proved in (Lions and Paul 1993) and (Gérard et al. 1997):

Theorem 3.2. Let $u^\varepsilon(t)$ be uniformly bounded in $L^2(\mathbb{R}^d)$ w.r.t. ε , that is

$$\sup_{0 < \varepsilon \leq 1} \|u^\varepsilon(t)\|_{L^2} < +\infty, \quad \forall t \in \mathbb{R}.$$

Then, the set of Wigner functions $\{w^\varepsilon(t)\}_{0 < \varepsilon \leq 1} \subset \mathcal{S}'(\mathbb{R}_x^d \times \mathbb{R}_\xi^d)$ is weak- $*$ compact and thus, up to extraction of subsequences

$$w^\varepsilon[u^\varepsilon] \xrightarrow{\varepsilon \rightarrow 0} w^0 \equiv w \quad \text{in } L^\infty([0, T]; \mathcal{S}'(\mathbb{R}_x^d \times \mathbb{R}_\xi^d)) \text{ w} - *,$$

where the limit $w(t) \in \mathcal{M}^+(\mathbb{R}_x^d \times \mathbb{R}_\xi^d)$ is called the *Wigner measure*. If, in addition $\forall t : (\varepsilon \nabla u(t)) \in L^2(\mathbb{R}^d)$ uniformly w.r.t. ε , then we also have

$$\begin{aligned} \rho^\varepsilon(t, x) &\xrightarrow{\varepsilon \rightarrow 0} \rho(t, x) = \int_{\mathbb{R}^d} w(t, x, d\xi), \\ j^\varepsilon(t, x) &\xrightarrow{\varepsilon \rightarrow 0} j(t, x) = \int_{\mathbb{R}^d} \xi w(t, x, d\xi). \end{aligned}$$

Note that although $w^\varepsilon(t)$ in general also takes negative values its weak limit $w(t)$ is indeed a non-negative measure on phase space.

Remark 3.3. The limiting phase space measures $w(t) \in \mathcal{M}^+(\mathbb{R}_x^d \times \mathbb{R}_p^d)$ are also often referred to as *semiclassical measures* and are closely related to the so-called *H-measures* used in homogenization theory (Tartar 1990). The fact that their weak limits are non-negative can be seen by considering the corresponding *Husimi transformation*, i.e.

$$w_{\text{H}}^\varepsilon[u^\varepsilon] := w^\varepsilon[u^\varepsilon] *_x G^\varepsilon *_\xi G^\varepsilon,$$

where we denote

$$G^\varepsilon(\cdot) := (\pi\varepsilon)^{-d/4} e^{-|\cdot|^2/\varepsilon}.$$

The Husimi transform w_H^ε is non-negative a.e. and has the same limit points as the Wigner function w^ε , cf. (Markowich and Mauser 1993).

This result allows to exchange limit and integration on the limit on the right hand side of (3.4) to obtain

$$\langle u^\varepsilon, a^W(x, \varepsilon D_x) u^\varepsilon \rangle_{L^2} \xrightarrow{\varepsilon \rightarrow 0} \iint_{\mathbb{R}^d \times \mathbb{R}^d} a(x, \xi) w(t, x, \xi) dx d\xi.$$

The Wigner transformation and its associated Wigner measure therefore are highly useful tools to compute the classical limit of the expectation values of physical observables. In addition it is proved in (Lions and Paul 1993) (Gérard et al. 1997), that $w(t, x, \xi)$ is the *push-forward* under the flow corresponding to the classical Hamiltonian $H(x, \xi)$, i.e.

$$w(t, x, \xi) = w_{\text{in}}(F_{-t}(x, \xi)),$$

where w_{in} is the initial Wigner measure and $F_t : \mathbb{R}^{2d} \rightarrow \mathbb{R}^{2d}$ is the phase space flow given by

$$\begin{cases} \dot{x} = \nabla_\xi H(x, \xi), & x(0, y, \zeta) = y, \\ \dot{\xi} = -\nabla_x H(x, \xi), & \xi(0, y, \zeta) = \zeta. \end{cases} \quad (3.6)$$

In other words $w(t, x, \xi)$ is a distributional solution of the classical *Liouville equation* on phase space, i.e.

$$\partial_t w + \{H, w\} = 0, \quad (3.7)$$

where

$$\{a, b\} := \nabla_\xi a \cdot \nabla_x b - \nabla_x a \cdot \nabla_\xi b$$

denotes the *Poisson bracket*. Note that in the case where $H(x, \xi)$ is given by (3.5), this yields

$$\partial_t w + \xi \cdot \nabla_\xi w - \nabla_x V(x) \cdot \nabla_x w = 0, \quad (3.8)$$

with characteristic equations given by the Newton trajectories:

$$\dot{x} = \xi, \quad \dot{\xi} = -\nabla_x V(x).$$

Strictly speaking we require $V \in C_b^1(\mathbb{R}^d)$, in order to define w as a distributional solution of (3.8). Note however, in contrast to WKB techniques, the equation for the limiting Wigner measure (3.8) is globally well posed, i.e. one does not experience problems of caustics. This is due to the fact that the Wigner measure $w(t, x, \xi)$ lives on phase space.

3.3. Connection between Wigner measures and WKB analysis

A particularly interesting situation occurs for $u_{\text{in}}^\varepsilon$ given in WKB form (2.18). The corresponding Wigner measure is found to be

$$w^\varepsilon[u_{\text{in}}^\varepsilon] \xrightarrow{\varepsilon \rightarrow 0} w_{\text{in}} = |a_{\text{in}}(x)|^2 \delta(\xi - \nabla S_{\text{in}}(x)), \quad (3.9)$$

i.e. a mono-kinetic measure concentrated on the initial velocity $v = \nabla S_{\text{in}}$. In this case the phase space flow F_t is projected onto physical space \mathbb{R}^d , yielding X_t , the characteristic flow of the Hamilton-Jacobi equation (2.12). More precisely, the following result has been proved in (Sparber et al. 2003):

Theorem 3.4. Let $w(t, x, \xi)$ be the Wigner measure of the exact solution u^ε to (2.1) with WKB initial data. Then

$$w(t, x, \xi) = |a(t, x)|^2 \delta(\xi - \nabla S(t, x))$$

if and only if $\rho = |a|^2$ and $v = \nabla S$ are smooth solutions of the leading order WKB system given by (2.12) and (2.15).

This theorem links the theory of Wigner measures with the WKB approximation before caustics. After caustics, the Wigner measure in general is no longer mono-kinetic. However, it can be shown, cf. (Sparber et al. 2003), (Jin and Li 2003) that for generic initial data $u_{\text{in}}^\varepsilon$ and locally away from caustics, the Wigner measure can be decomposed as

$$w(t, x, \xi) = \sum_{j=1}^J |a_j(t, x)|^2 \delta(\xi - v_j(t, x)), \quad (3.10)$$

which is consistent with the multi-phase WKB approximation given in (2.21).

4. Finite difference methods for semiclassical Schrödinger equations

4.1. Basic setting

A basic numerical scheme for solving linear partial differential equations is the well-known *finite difference method* (FD), to be discussed in this section (see e.g. (Strikwerda 1989) for a general introduction). In the following, we shall be mainly interested in its performance as $\varepsilon \rightarrow 0$. To this end, we shall allow for more general Schrödinger type PDEs in the form (Markowich and Poupaud 1999)

$$i\varepsilon \partial_t u^\varepsilon = H^W(x, \varepsilon D_x) u^\varepsilon; \quad u^\varepsilon(0, x) = u_{\text{in}}^\varepsilon(x), \quad (4.1)$$

where H^W denotes the Weyl-quantization of a classical real-valued phase space Hamiltonian $H(x, \xi) \in C^\infty(\mathbb{R}^d \times \mathbb{R}^d)$, which is supposed to grow at most quadratically in x and ξ . For the following we assume that the symbol

is a polynomial of order $K \in \mathbb{N}$ in ξ with C^∞ -coefficients $H_k(x)$, i.e.

$$H(x, \xi) = \sum_{|k| \leq K} H_k(x) \xi^k \quad ,$$

where $k = (k_1, \dots, k_d) \in \mathbb{N}^d$ denotes a multi-index with $|k| := k_1 + \dots + k_d$. The differential operator $H(x, \varepsilon D_x)^W$ can now be written as

$$H(x, \varepsilon D_x)^W \varphi(x) = \sum_{|k| \leq K} \varepsilon^{|k|} D_y^k \left(H_k \left(\frac{x+y}{2} \right) \varphi(y) \right) \Big|_{y=x} . \quad (4.2)$$

In addition, assume the following:

$$H(x, \varepsilon D_x)^W \text{ is essentially self-adjoint on } L^2(\mathbb{R}^d), \quad (A1)$$

and, for simplicity:

$$\forall k, \alpha \in \mathbb{N}^d \text{ with } |k| \leq K \exists C_{k,\alpha} > 0 : |\partial_x^\alpha H_k(x)| \leq C_{k,\alpha} \quad \forall x \in \mathbb{R}^d. \quad (A2)$$

Under these conditions $H(x, \varepsilon D_x)^W$ can be shown (Kitada 1980) to generate a unitary (strongly continuous) semi-group of operators $U^\varepsilon(t) = e^{-itH^W/\varepsilon}$, which provides a unique global-in-time solution $u^\varepsilon = u^\varepsilon(t) \in L^2(\mathbb{R}^d)$. Next, let

$$\Gamma := \left\{ \gamma = \ell_1 r_1 + \dots + \ell_m r_m \mid \ell_j \in \mathbb{Z} \text{ for } 1 \leq j \leq d \right\} \subseteq \mathbb{R}^d$$

be the lattice generated by the linearly independent vectors $r_1, \dots, r_d \in \mathbb{R}^d$. For a multi-index $k \in \mathbb{N}^d$ we construct a discretization of order N of the operator ∂_x^k as follows:

$$\partial_x^k \varphi(x) \approx \frac{1}{h^{|k|}} \sum_{\gamma \in \Gamma_k} a_{\gamma,k} \varphi(x + h\gamma). \quad (4.3)$$

Here $\Delta x = h \in (0, h_0]$ is the mesh-size, $\Gamma_k \subseteq \Gamma$ is the finite set of discretization points and $a_{\gamma,k} \in \mathbb{R}$ are coefficients satisfying

$$\sum_{\gamma \in \Gamma_k} a_{\gamma,k} \gamma^\ell = k! \delta_{\ell,k}, \quad 0 \leq |\ell| \leq N + |k| - 1 \quad (B1)$$

where $\delta_{\ell,k} = 1$, if $\ell = k$, and zero otherwise. It is an easy exercise to show that the local discretization error of (4.3) is $\mathcal{O}(h^N)$ for all smooth functions if (B1) holds. For a detailed discussion of the linear problem (B1) (i.e. possible choices of the coefficients $a_{\gamma,k}$) we refer to (Markowich and Poupaud 1999).

4.2. Spatial discretization

We shall now define the corresponding finite difference discretization of $H(x, \varepsilon D_x)^W$ by applying (4.3) directly to (4.2). To this end, we denote

$$H_{h,\varepsilon}(x, \xi) = \sum_{|k| \leq K} \varrho^{|k|} (-i)^{|k|} \sum_{\gamma \in \Gamma_k} a_{\gamma,k} H_k(x) e^{i\gamma \cdot \xi / \varrho} \quad (4.4)$$

with $\varrho = \frac{\varepsilon}{h}$, the ratio between the small semiclassical parameter ε and the mesh size h . Then we obtain the finite difference discretization of (4.2) in the form

$$\begin{aligned} H(x, \varepsilon D_x)^W \varphi(x) &\approx H_{h,\varepsilon}(x, \varepsilon D_x)^W \varphi(x) = \\ &= \sum_{|k| \leq K} \varrho^{|k|} (-i)^{|k|} \sum_{\gamma \in \Gamma_k} a_{\gamma,k} H_k\left(x + \frac{h\gamma}{2}\right) \varphi(x + h\gamma). \end{aligned}$$

In view of (4.4), the discretization $H_{h,\varepsilon}(x, \varepsilon D_x)^W$ is seen to be a bounded operator on $L^2(\mathbb{R}^d)$ and self-adjoint if

$$i^{|k|} \sum_{\gamma \in \Gamma_k} a_{\gamma,k} e^{i\gamma \cdot \xi} \quad \text{is real-valued for } 0 \leq |k| \leq K. \quad (B2)$$

We shall now collect several properties of such finite difference approximations, proved in (Markowich, Pietra and Pohl 1999). We start with a spatial consistency result.

Lemma 4.1. Let (A1), (B1), (B2) hold and $\varphi \in \mathcal{S}(\mathbb{R}_x^d \times \mathbb{R}_\xi^d)$. Then, for $\varrho = \frac{\varepsilon}{h} \xrightarrow{\varepsilon, h \rightarrow 0} \infty$

$$H_{h,\varepsilon} \varphi \xrightarrow{\varepsilon, h \rightarrow 0} H \varphi \quad \text{in } \mathcal{S}(\mathbb{R}_x^d \times \mathbb{R}_\xi^d). \quad (4.5)$$

For a given $\varepsilon > 0$, choosing h such that $\varrho = \frac{\varepsilon}{h} \rightarrow \infty$ corresponds to asymptotically resolving the oscillations of wavelength $\mathcal{O}(\varepsilon)$ in the solution $u^\varepsilon(t, x)$ to the Schrödinger type equation (4.1). In the case $\varrho = \text{const}$, i.e. putting a fixed number of grid-points per oscillation, the symbol $H_{h,\varepsilon}(x, \xi) \equiv H_\varrho(x, \xi)$ is independent of h and ε , i.e.

$$H_\varrho(x, \xi) = \sum_{|k| \leq K} \varrho^{|k|} \sum_{\gamma \in \Gamma_k} a_{\gamma,k} (-i)^{|k|} H_k(x) e^{i\gamma \cdot \xi / \varrho}. \quad (4.6)$$

In the case $\varrho \xrightarrow{\varepsilon, h \rightarrow 0} 0$, which corresponds to a scheme ignoring the ε -oscillations, we find

$$H_{h,\varepsilon} \underset{h, \varepsilon \rightarrow 0}{\sim} \sum_{\gamma \in \Gamma_0} a_{\gamma,0} \cos\left(\frac{\gamma \cdot \xi}{\varrho}\right) H_0(x),$$

and hence $H_{h,\varepsilon}(x, \varepsilon D_x)^W$ *does not* approximate $H(x, \varepsilon D_x)^W$. We thus cannot expect reasonable numerical results in this case (which will not be investigated further).

4.3. Temporal discretization and violation of gauge invariance

For the temporal discretization one can employ the *Crank-Nicolson scheme* with time-step $\Delta t > 0$. This is a widely used time-discretization scheme for the Schrödinger equation, featuring some desirable properties (see below). We shall comment on the temporal discretizations below. The scheme reads

$$\varepsilon \frac{u_{n+1}^\sigma - u_n^\sigma}{\Delta t} + iH_{h,\varepsilon}(x, \varepsilon D_x)^W \left(\frac{1}{2}u_{n+1}^\sigma + \frac{1}{2}u_n^\sigma \right) = 0, \quad n = 0, 1, 2, \dots \quad (4.7)$$

subject to initial data $u_{\text{in}}^\sigma = u_{\text{in}}^\varepsilon(x)$, where from now on, we shall denote the vector of small parameters by $\sigma = (\varepsilon, h, \Delta t)$. Note that the self-adjointness of $H_{h,\varepsilon}(x, \varepsilon D_x)^W$ implies that the operator

$$1 + isH_{h,\varepsilon}(x, \varepsilon D_x)^W$$

is invertible on $L^2(\mathbb{R}^d)$ for all $s \in \mathbb{R}$. Therefore the scheme (4.7) gives well-defined approximations u_n^σ for $n = 1, 2, \dots$ if $u_{\text{in}}^\varepsilon \in L^2(\mathbb{R}^d)$. Moreover we remark that it is sufficient to evaluate (4.7) at $x \in h\Gamma$ in order to obtain discrete equations for $u_n^\sigma(h\gamma)$, $\gamma \in \Gamma$.

Remark 4.2. For practical computations, one needs to impose artificial ‘far-field’ boundary conditions. Their impact, however, will not be taken into account in the subsequent analysis.

By taking the L^2 scalar product of (4.7) with $(\frac{1}{2}u_{n+1}^\sigma + \frac{1}{2}u_n^\sigma)$, one can directly infer the following stability result:

Lemma 4.3. The solution of (4.7) satisfies

$$\|u_n^\sigma\|_{L^2} = \|u_{\text{in}}^\varepsilon\|_{L^2}, \quad n = 0, 1, 2, \dots$$

In other words, the physically important property of mass-conservation also holds on the discrete level.

On the other hand, the scheme can be seen to *violate the gauge invariance* of (4.1). More precisely, one should note that expectation values of physical observables, as defined in (2.5), are invariant under the substitution (gauge transformation)

$$v^\varepsilon(t, x) = u^\varepsilon(t, x)e^{i\omega t/\varepsilon}, \quad \omega \in \mathbb{R}.$$

In other words, the average value of the observable in the state u^ε is equal to its average value in the state v^ε .

Remark 4.4. Note that in view of (3.1) the Wigner-function is seen to be also invariant under this substitution, i.e.

$$\forall \omega \in \mathbb{R} : w^\varepsilon[u^\varepsilon(t)] = w^\varepsilon[u^\varepsilon(t)e^{i\omega t/\varepsilon}] \equiv w^\varepsilon[v^\varepsilon(t)].$$

On the other hand, using this gauge-transformation the Schrödinger equation (4.1) transforms to

$$i\varepsilon\partial_t v^\varepsilon = \left(H(x, \varepsilon D_x)^W + \omega \right) v^\varepsilon; \quad v^\varepsilon(0, x) = u_{\text{in}}^\varepsilon(x), \quad (4.8)$$

which implies that the zeroth order term $H_0(x)$ in (4.2) is replaced by $H_0(x) + \omega$ while the other coefficients $H_k(x), k \neq 0$, remain unchanged. In physical terms, $H_0(x)$ corresponds to a scalar (static) potential $V(x)$. The corresponding force field obtained via $F(x) = \nabla H_0(x) = \nabla(H_0(x) + \omega)$ is unchanged by the gauge transformation and thus (4.8) can be considered (physically) *equivalent* to (4.1). The described situation, however, is completely different for the difference scheme outlined above: Indeed, a simple calculation shows that the *discrete gauge transformation*

$$v_n^\sigma = u_n^\sigma e^{i\omega t_n/\varepsilon}$$

does *not commute* with the discretization (4.7), up to adding a real constant to the potential. Thus, the discrete approximations of average values of observables *depend on the gauging of the potential*. In other words, the discretization method is not time-transverse invariant.

4.4. Stability-consistency analysis for (FD) in the semiclassical limit

The consistency-stability concept of classical numerical analysis provides a framework for the convergence analysis of finite difference discretizations of linear partial differential equations. Thus, for $\varepsilon > 0$ *fixed* it is easy to prove that the scheme (4.7) is convergent of order N in space and order 2 in time if the exact solution $u^\varepsilon(t, x)$ is sufficiently smooth. Therefore, again for fixed $\varepsilon > 0$, we conclude convergence of the same order for average-values of physical observables provided $a(x, \xi)$ is smooth.

However, due to the oscillatory nature solutions to (4.1) the local discretization error of the finite difference schemes and, consequently, also the global discretization error, in general tend to infinity as $\varepsilon \rightarrow 0$. Thus, the classical consistency-stability theory does not provide *uniform results* in the classical limit. Indeed, under the reasonable assumption that, for all multi-indices j_1 and $j_2 \in \mathbb{N}^d$:

$$\frac{\partial^{|j_1|+|j_2|}}{\partial t^{j_1} \partial x^{j_2}} u^\varepsilon(t, x) \stackrel{\varepsilon \rightarrow 0}{\sim} \varepsilon^{-|j_1|-j_2} \quad \text{in } L^2(\mathbb{R}^d),$$

locally uniformly in $t \in \mathbb{R}$, the classical stability-consistency analysis gives the following bound for the global L^2 -discretization error:

$$\mathcal{O}\left(\frac{(\Delta t)^2}{\varepsilon^3}\right) + \mathcal{O}\left(\frac{h^N}{\varepsilon^{N+1}}\right).$$

The situation is further complicated by the fact that for any fixed $t \in \mathbb{R}$,

the solution $u^\varepsilon(t, \cdot)$ of (4.1) and its discrete counterpart u_n^σ , in general converge only *weakly* in $L^2(\mathbb{R}^d)$ as $\varepsilon \rightarrow 0$, respectively, $\sigma \rightarrow 0$. Thus, the limit processes $\varepsilon \rightarrow 0$, $\sigma \rightarrow 0$ *do not commute* with the quadratically nonlinear operation (2.5), needed to compute the expectation value of physical observables $a[u^\varepsilon(t)]$.

In practice, one is therefore interested in finding conditions on the mesh size h and the time-step Δt , depending on ε in such a way, that the expectation values of physical observables in discrete form approximate $a[u^\varepsilon(t)]$ uniformly as $\varepsilon \rightarrow 0$. To this end, let $t_n = n\Delta t$, $n \in \mathbb{N}$, and denote

$$a^\sigma(t_n) := \langle a(\cdot, \varepsilon D_x)^W u_n^\sigma, u_n^\sigma \rangle.$$

The function $a^\sigma(t)$, $t \in \mathbb{R}$, is consequently defined by piecewise linear interpolation of the values $a^\sigma(t_n)$. We seek conditions on h, k such that, for all $a \in \mathcal{S}(\mathbb{R}_x^m \times \mathbb{R}_\xi^m)$,

$$\lim_{h, \Delta t \rightarrow 0} (a^\sigma(t) - a[u^\varepsilon(t)]) = 0 \quad \text{uniformly in } \varepsilon \in (0, \varepsilon_0], \quad (4.9)$$

and locally uniformly in $t \in \mathbb{R}$. A rigorous study of this problem will be given by using the theory of Wigner measures applied in a discrete setting. Denoting the Wigner-transformation (on the scale ε) of the finite difference solution u_n^σ by

$$w^\sigma(t_n) := w^\varepsilon[u_n^\sigma]$$

and defining, as before, $w^\sigma(t)$, for any $t \in \mathbb{R}$, by the piecewise linear interpolation of $w^\sigma(t_n)$, we conclude that (4.9) is equivalent to proving, locally uniformly in t :

$$\lim_{h, \Delta t \rightarrow 0} (w^\sigma(t) - w^\varepsilon(t)) = 0 \quad \text{in } \mathcal{S}'(\mathbb{R}_x^d \times \mathbb{R}_\xi^d), \text{ uniformly in } \varepsilon \in (0, \varepsilon_0], \quad (4.10)$$

where $w^\varepsilon(t)$ is the Wigner-transform of the solution $u^\varepsilon(t)$ of (4.1). We shall now compute the accumulation points of the sequence $\{w^\sigma(t)\}_\sigma$ as $\sigma \rightarrow 0$. We shall see that for any given sub-sequence $\{\sigma_n\}_{n \in \mathbb{N}}$, the set of Wigner-measures of the difference schemes

$$\mu(t) := \lim_{n \rightarrow \infty} w^{\sigma_n}(t),$$

depends *decisively* on the relative sizes of ε, h and Δt . Clearly, in those cases in which $\mu = w$, where w denotes the Wigner measure of the exact solution $u^\varepsilon(t)$, the desired property (4.10) follows. On the other hand (4.10) does not hold if the measures μ and w are different. Such a Wigner measure-based study of finite difference schemes has been conducted in (Markowich et al. 1999), (Markowich and Poupaud 1999). The main result given in there is as follows:

Theorem 4.5. Fix a scale $\varepsilon > 0$ and denote by μ , the Wigner measure of

the discretization (4.7) as $\sigma \rightarrow 0$. Then it holds:

Case 1. If $h/\varepsilon \rightarrow 0$ (or, equivalently, $\varrho \rightarrow \infty$) and if, either:

(i) $\Delta t/\varepsilon \rightarrow 0$, then μ satisfies:

$$\partial_t \mu + \{H, \mu\} = 0; \quad \mu(0, x, \xi) = w_{\text{in}}(x, \xi)$$

(ii) $\Delta t/\varepsilon \rightarrow \omega \in \mathbb{R}^+$, then μ solves

$$\frac{\partial}{\partial t} \mu + \left\{ \frac{2}{\omega} \arctan \left(\frac{\omega}{2} H \right), \mu \right\} = 0; \quad \mu(0, x, \xi) = w_{\text{in}}(x, \xi)$$

(iii) $\Delta t/\varepsilon \rightarrow \infty$ and if in addition there exists $C > 0$ such that $|H(x, \xi)| \geq C$, $\forall x, \xi \in \mathbb{R}^d$, then μ is constant in time, i.e.

$$\mu(t, x, \xi) \equiv \mu_{\text{in}}(x, \xi), \quad \forall t \in \mathbb{R}.$$

Case 2. If $h/\varepsilon \rightarrow 1/\varrho \in \mathbb{R}^+$, then the assertions (i)-(iii) hold true, with H replaced by H_ϱ defined in (4.6).

The proof of this result proceeds similarly to the derivation of the phase space Liouville equation (3.7), in the continuous setting. Note that Theorem 4.5 implies that, as $\varepsilon \rightarrow 0$, expectation values for physical observables in the state $u^\varepsilon(t)$, computed via the Crank-Nicolson finite difference scheme, are asymptotically correct only if *both* spatial *and* temporal oscillations of wavelength ε are accurately resolved.

Remark 4.6. Time-irreversible finite difference schemes, such as the explicit (or implicit) Euler scheme, behave even worse, as they require $\Delta t = o(\varepsilon^2)$ in order to guarantee asymptotically correct numerically computed observables, cf. (Markowich et al. 1999).

5. Time-splitting spectral methods for semiclassical Schrödinger equations

5.1. Basic setting, first and second order splittings

As have been discussed before, finite difference methods do now perform well in computing the solution to semiclassical Schrödinger equations. An alternative is given by time-splitting trigonometric spectral methods which shall be discussed in this sub-section (see also (McLachlan and Quispel 2002) for a broad introduction on splitting methods). For the sake of notation, we shall introduce the method only in the case of one space dimension $d = 1$. Generalizations to $d > 1$ are straightforward for tensor product grids and the results remain valid without modifications.

In the following, we shall therefore study the one-dimensional version of equation (2.1), i.e.

$$i\varepsilon \partial_t u^\varepsilon = -\frac{\varepsilon^2}{2} \partial_{xx} u^\varepsilon + V(x) u^\varepsilon; \quad u^\varepsilon(0, x) = u_{\text{in}}^\varepsilon(x), \quad (5.1)$$

for $x \in [a, b]$, $0 < a < b < +\infty$, equipped with periodic boundary conditions

$$u^\varepsilon(t, a) = u^\varepsilon(t, b), \quad \partial_x u^\varepsilon(t, a) = \partial_x u^\varepsilon(t, b), \quad \forall t \in \mathbb{R}.$$

We choose the spatial mesh size $\Delta x = h > 0$ with $h = (b - a)/M$ for some $M \in 2\mathbb{N}$, and a ε -independent time-step $\Delta t \equiv k > 0$. The spatio-temporal grid-points are then given by

$$x_j := a + jh, \quad j = 1, \dots, M, \quad t_n := nk, \quad n \in \mathbb{N}.$$

In the following, let $u_j^{\varepsilon, n}$ be the numerical approximation of $u^\varepsilon(x_j, t_n)$ and $\mathbf{u}^{\varepsilon, n}$ be the vector with components $u_j^{\varepsilon, n}$, for $j = 1, \dots, M$.

First-order time-splitting spectral method (SP1)

The Schrödinger equation (5.1) is solved by a splitting method, based on the following two-steps:

Step 1. From time $t = t_n$ to time $t = t_{n+1}$ first solve the free Schrödinger equation

$$i\varepsilon \partial_t u^\varepsilon + \frac{\varepsilon^2}{2} \partial_{xx} u^\varepsilon = 0. \quad (5.2)$$

Step 2. On the same-time interval, i.e. $t \in [t_n, t_{n+1}]$, solve the ordinary differential equation (ODE)

$$i\varepsilon \partial_t u^\varepsilon - V(x)u^\varepsilon = 0, \quad (5.3)$$

with the solution obtained from Step 1 as initial data for Step 2. (5.3) can be solved *exactly* since $|u(t, x)|$ is left invariant under (5.3),

$$u(t, x) = |u(0, x)| e^{iV(x)t}.$$

In Step 1, the linear equation (5.2) will be discretized in space by a (pseudo-)spectral method (see e.g. (Fornberg 1996) for a general introduction) and consequently integrated in time *exactly*. More precisely, one obtains at time $t = t_{n+1}$:

$$u(t_{n+1}, x) \approx u_j^{\varepsilon, n+1} = e^{iV(x_j)k/\varepsilon} u_j^{\varepsilon, *}, \quad j = 0, 1, 2, \dots, M.$$

with initial value $u_j^{\varepsilon, 0} = u_{\text{in}}^\varepsilon(x_j)$, and

$$u_j^{\varepsilon, *} = \frac{1}{M} \sum_{\ell=-M/2}^{M/2-1} e^{i\varepsilon k \gamma_\ell^2 / 2} \widehat{u}_\ell^{\varepsilon, n} e^{i\gamma_\ell(x_j - a)},$$

where $\gamma_\ell = \frac{2\pi\ell}{b-a}$ and $\widehat{u}_\ell^{\varepsilon, n}$ denoting the Fourier coefficients of $u^{\varepsilon, n}$, i.e.

$$\widehat{u}_\ell^{\varepsilon, n} = \sum_{j=1}^M u_j^{\varepsilon, n} e^{-i\gamma_\ell(x_j - a)}, \quad \ell = -\frac{M}{2}, \dots, \frac{M}{2} - 1.$$

Note that the only time discretization error of this method is the splitting error, which is *first order* in $k = \Delta t$, for any *fixed* $\varepsilon > 0$.

Strang splitting (SP2)

In order to obtain a scheme which is second order in time (for fixed $\varepsilon > 0$), one can use the *Strang splitting method*, i.e. on the time-interval $[t_n, t_{n+1}]$ we compute,

$$u_j^{\varepsilon, n+1} = e^{iV(x_j)k/2\varepsilon} u_j^{\varepsilon, **}, \quad j = 0, 1, 2, \dots, M-1,$$

where

$$u_j^{\varepsilon, **} = \frac{1}{M} \sum_{\ell=-M/2}^{M/2-1} e^{i\varepsilon k \gamma_\ell^2 / 2} \widehat{u}_\ell^{\varepsilon, *} e^{i\gamma_\ell(x_j-a)},$$

with $\widehat{u}_\ell^{\varepsilon, *}$ denoting the Fourier coefficients of $u^{\varepsilon, *}$ given by

$$u_j^{\varepsilon, *} = e^{iV(x_j)k/2\varepsilon} u_j^{\varepsilon, n}.$$

Again, the overall time discretization error comes solely from the splitting, which is now (formally) second order in $\Delta t = k$ for fixed $\varepsilon > 0$.

Remark 5.1. Extensions to higher order (in time) splitting schemes can be found in the literature, see e.g. (Bao and Shen 2005). For rigorous investigations about the long time error estimates of such splitting schemes we refer to (Dujardin and Faou 2007a), (Dujardin and Faou 2007b) and the references given therein.

In comparison to finite difference methods, the main advantage of such splitting schemes is that they are *gauge invariant* (cf. the discussion in Section 4 above). Concerning the *stability* of the time-splitting spectral approximations with variable potential $V = V(x)$, one can prove (see (Bao, Jin and Markowich 2002)) the following lemma, in which we denote $U = (u_1, \dots, u_M)^\top$ and $\|\cdot\|_{l^2}$ the usual discrete l^2 -norm on the interval $[a, b]$, i.e.

$$\|U\|_{l^2} = \left(\frac{b-a}{M} \sum_{j=1}^M |u_j|^2 \right)^{1/2}.$$

Lemma 5.2. The time-splitting spectral schemes (SP1) and (SP2) are unconditionally stable, i.e. for any mesh size h and any time-step k , it holds:

$$\|U^{\varepsilon, n}\|_{l^2} = \|U^{\varepsilon, 0}\|_{l^2} \equiv \|U_{\text{in}}^\varepsilon\|_{l^2}, \quad n \in \mathbb{N},$$

and consequently

$$\|u_{\text{int}}^{\varepsilon, n}\|_{L^2(a,b)} = \|u_{\text{int}}^{\varepsilon, 0}\|_{L^2(a,b)}, \quad n \in \mathbb{N},$$

where $u_{\text{int}}^{\varepsilon,n}$ denotes the trigonometric polynomial interpolating

$$\{(x_1, u_1^{\varepsilon,n}), (x_1, u_1^{\varepsilon,n}), \dots, (x_M, u_M^{\varepsilon,n})\}.$$

In other words, time-splitting spectral methods satisfy mass-conservation on a fully discrete level.

5.2. Error estimate of (SP1) in the semiclassical limit

To get a better understanding of the stability of spectral methods in the classical limit $\varepsilon \rightarrow 0$, we shall establish the error estimates for (SP1). Assume that the potential $V(x)$ is $(b-a)$ -periodic, smooth, and satisfies

$$\left\| \frac{d^m}{dx^m} V \right\|_{L^\infty[a,b]} \leq C_m, \quad (\text{A})$$

for some constant $C_m > 0$. Under this assumptions it can be shown that the solution $u^\varepsilon = u^\varepsilon(t, x)$ of (5.1) is $(b-a)$ periodic and smooth. In addition, we assume

$$\left\| \frac{\partial^{m_1+m_2}}{\partial t^{m_1} \partial x^{m_2}} u^\varepsilon \right\|_{C([0,T]; L^2[a,b])} \leq \frac{C_{m_1+m_2}}{\varepsilon^{m_1+m_2}}, \quad (\text{B})$$

for all $m, m_1, m_2 \in \mathbb{N} \cup \{0\}$. Thus, we assume that the solution oscillates in space and time with wavelength ε , but not smaller.

Remark 5.3. The latter is known to be satisfied if the initial data $u_{\text{in}}^\varepsilon$ only invokes oscillations of wavelength ε (but not smaller).

Theorem 5.4. Let $V(x)$ satisfy assumption (A) and $u^\varepsilon(t, x)$ be a solution of (5.1) satisfying (B). Denote by $u_{\text{int}}^{\varepsilon,n}$ the interpolation of the discrete approximation obtained via (SP1). Then, if

$$\frac{\Delta t}{\varepsilon} = \mathcal{O}(1), \quad \frac{\Delta x}{\varepsilon} = \mathcal{O}(1),$$

as $\varepsilon \rightarrow 0$, we have that for all $m \in \mathbb{N}$ and $t_n \in [0, T]$:

$$\|u^\varepsilon(t_n) - u_{\text{int}}^{\varepsilon,n}\|_{L^2(a,b)} \leq G_m \frac{T}{\Delta t} \left(\frac{\Delta x}{\varepsilon(b-a)} \right)^m + \frac{CT\Delta t}{\varepsilon}, \quad (5.4)$$

where $C > 0$ is independent of ε and m and $G_m > 0$ is independent of ε , Δx , Δt .

The proof of this theorem is given in (Bao et al. 2002), where a similar result is also shown for (SP2). Now, let

$Dt > 0$ be a desired error bound such that

$$\|u^\varepsilon(t_n) - u_{\text{int}}^{\varepsilon,n}\|_{L^2[a,b]} \leq \delta,$$

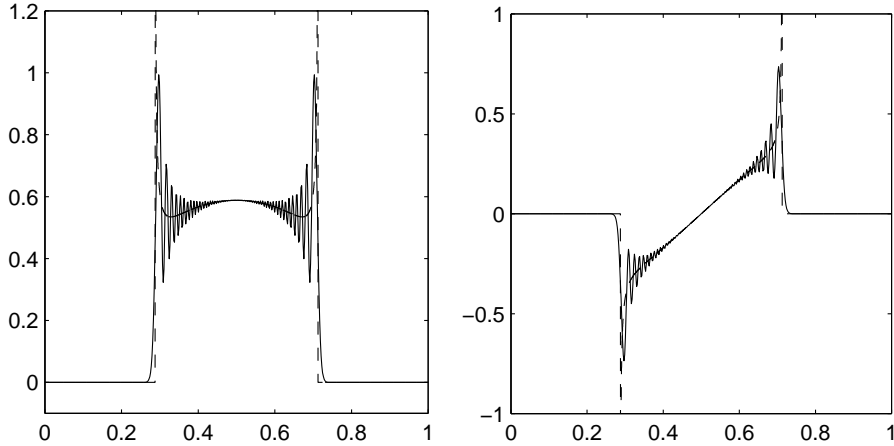


Figure 5.2. Numerical solution of ρ^ε (left) and j^ε (right) at $t = 0.54$ as given in Example 5.5. In the picture the solution computed by using SP2 for $\varepsilon = 0.0008$, $h = \frac{1}{512}$, is superimposed with the limiting ρ and j , obtained by taking moments of the Wigner measure solution of (3.8).

holds, uniformly in ε . Then Theorem 5.4 suggests the following meshing strategy on $\mathcal{O}(1)$ -time and space intervals:

$$\frac{\Delta t}{\varepsilon} = \mathcal{O}(\delta), \quad \frac{\Delta x}{\varepsilon} = \mathcal{O}\left(\delta^{1/m}(\Delta t)^{1/m}\right), \quad (5.5)$$

where $m \geq 1$ is an arbitrary integer, assuming that G_m does not increase too fast as $m \rightarrow \infty$. This meshing is already more efficient than what is needed for finite differences. In addition, as will be seen below, the conditions (5.5) can be strongly relaxed if, instead of resolving the solution $u^\varepsilon(t, x)$, one is only interested in the accurate numerical computation of quadratic observable densities (and thus asymptotically correct expectation values).

Example 5.5. This is an example from (Bao et al. 2002). The Schrödinger equation (2.1) is solved with $V(x) = 10$ and the initial data

$$\begin{aligned} \rho_{\text{in}}(x) &= \exp(-50(x - 0.5)^2), \\ \mathcal{S}_{\text{in}}(x) &= -\frac{1}{5} \ln(\exp(5(x - 0.5)) + \exp(-5(x - 0.5))), \quad x \in \mathbb{R}. \end{aligned}$$

The computational domain is restricted to $[0, 1]$ equipped with periodic boundary conditions. Figure 5.2 shows the solution of the limiting position density ρ and current density j obtained by taking moments of w , satisfying the Liouville equation (3.8). This has to be compared with the oscillatory ρ^ε and j^ε , obtained by solving the Schrödinger equation (2.1) using SP2. As one can see these oscillations are average out in the *weak limits* ρ, j .

5.3. *Accurate computation of quadratic observable densities using time-splitting*

We shall again invoke the theory of Wigner functions and Wigner measures. To this end, let $u^\varepsilon(t, x)$ be the solution of (5.1) and $w^\varepsilon(t, x, \xi)$ the corresponding Wigner transform. Having in mind the results of Section 3, we see that the first order splitting scheme (SP1), corresponds to the following time-splitting scheme for the Wigner equation (3.2):

Step 1. For $t \in [t_n, t_{n+1}]$, first solve the linear transport equation

$$\partial_t w^\varepsilon + \xi \partial_x w^\varepsilon = 0. \quad (5.6)$$

Step 2. On the same time-interval, solve the non-local (in space) ordinary differential equation

$$\partial_t w^\varepsilon - \Theta^\varepsilon[V]w^\varepsilon = 0, \quad (5.7)$$

with initial data obtained from Step 1 above.

In (5.6), the only possible ε -dependence stems from the initial data. In addition, in (5.7) the limit $\varepsilon \rightarrow 0$ can be easily carried out (assuming sufficient regularity of the potential $V(x)$) with $k = \Delta t$ fixed. In doing so, one consequently obtains a time-splitting scheme of the limiting Liouville equation (3.8) as follows:

Step 1. For $t \in [t_n, t_{n+1}]$ solve

$$\partial_t w + \xi \partial_x w^0 = 0.$$

Step 2. Using the outcome of Step 1 as initial data, solve, on the same time-interval:

$$\partial_t w - \partial_x V \partial_\xi w^0 = 0.$$

Note that in this scheme *no error* is introduced other than the splitting error, since the time-integrations are performed exactly.

These considerations, which can easily be made rigorous (for smooth potentials), show that a *uniform time-stepping* (i.e. an ε -independent $k = \Delta t$) of the form

$$\Delta t = \mathcal{O}(\delta)$$

combined with the spectral mesh-size control given in (5.5) yields the following error

$$\|w^\varepsilon(t_n) - w_{\text{int}}^{\varepsilon, n}\|_{L^2(a, b)} \leq \delta,$$

uniformly in Δt as $\varepsilon \rightarrow 0$. Essentially this implies that a fixed number of grid points in every spatial oscillation of wavelength ε combined with

ε -independent time-stepping is sufficient, to guarantee the accurate computation of (expectation values of) physical observables in the classical limit. This strategy is therefore clearly superior to finite difference schemes, which require $k/\varepsilon \rightarrow 0$ and $h/\varepsilon \rightarrow 0$, even if one only is interested in computing physical observables.

Remark 5.6. Time-splitting methods have been proved particularly successful in nonlinear situations, see the references given in Section 15.4 below.

6. Moment closure methods

We have seen before that a direct numerical calculation of u^ε is numerically very expensive, in particular in higher dimensions, due to the mesh and time step constraint (5.5). In order to circumvent this problem, the asymptotic analysis presented in Sections 2 and 3 can be invoked in order to design asymptotic numerical methods which allow for an efficient numerical simulation in the limit $\varepsilon \rightarrow 0$.

The initial value problem (3.8)-(3.9) is the starting point of the numerical methods to be described below. Most recent computational methods are derived from, or closely related to, this equation. The main advantage is that (3.8)-(3.9) correctly describes the limit of quadratic densities of u^ε (which in itself exhibits oscillations of wave-length $\mathcal{O}(\varepsilon)$) and thus allows a numerical mesh size *independent of* ε . However, we are facing the following major difficulties in the numerical approximation:

- (i) *High dimensionality:* The Liouville equation (3.8) is defined in phase space, thus the memory requirement exceeds the current computational capability in $d \geq 3$ spatial dimensions.
- (ii) *Measure valued initial data:* The initial data (3.9) is a delta measure and the solution at later time remains one (for single-valued solution) or summation of several delta functions (for multivalued solution (3.10)).

In the past few years, several new numerical methods have been introduced to overcome these difficulties. In the following, we shall briefly describe the basic ideas in these methods.

6.1. The concept of multi-valued solutions

In order to overcome the problem of high dimensionality one aims to approximate $w(t, x, p)$ by using averaged quantities depending only on t, x . This is a well-known technique in classical kinetic theory, usually referred to as *moment closure*. A basic example for it is provided by the result of Theorem 3.4, which tells us that, as long as the WKB analysis of Section 2.2 is valid (i.e. before the appearance of the first caustic), the Wigner measure is given by a mono-kinetic distribution on phase space, i.e.

$$w(t, x, \xi) = \rho(t, x)\delta(\xi - v(t, x))$$

where one identifies $\rho = |a|^2$ and $v = \nabla S$. The latter solve the *pressure-less Euler system*

$$\begin{aligned} \partial_t \rho + \operatorname{div}(\rho v) &= 0, & \rho(0, x) &= |a_{\text{in}}|^2(x), \\ \partial_t v + (v \cdot \nabla)v + \nabla V &= 0, & v(0, x) &= \nabla S_{\text{in}}(x), \end{aligned} \quad (6.1)$$

which, for smooth solutions, is equivalent to the system of transport equation (2.14) coupled with the Hamilton-Jacobi equation (2.12), obtained through the WKB approximation. Thus instead of solving the Liouville equation on phase space $\mathbb{R}_t \times \mathbb{R}_x^d$. Of course, this can only be done until the appearance of the first caustic, or, equivalently, the emergence of shocks in (6.1).

In order to go beyond that one might be tempted to use numerical methods based on the unique viscosity solution, cf. (Crandall and Lions 1983), for (6.1). However, the latter does not provide the correct asymptotic description—the multivalued solution—of the wave function $u^\varepsilon(t, x)$ beyond caustics. Instead, one has to pass to so-called *multi-valued solutions*, based on higher order moment closure methods. This fact is illustrated in Fig. 6.3, which shows the difference between viscosity solutions and multivalued solutions. The top figures are the two different solutions for the following eiconal equation (in fact, the zero level set of S):

$$\partial_t S + |\nabla_x S| = 0, \quad x \in \mathbb{R}^2. \quad (6.2)$$

This equation, corresponding to $H(\xi) = |\xi|$, arises in the geometric optics limit of the wave equation and models two circular fronts moving outward in the normal direction with speed 1, cf. (Osher and Sethian 1988). As one can see the main difference occurs when the two fronts merge. Similarly, the bottom figures shows the difference between the viscosity and the multivalued solution to the Burgers equation

$$\partial_t v + \frac{1}{2} \partial_x v^2 = 0, \quad x \in \mathbb{R}. \quad (6.3)$$

This is nothing but the second equation in the system (6.1) for $V(x) = 0$ and written in divergence form. The solution begins as a sinusoidal function and then forms a shock. Clearly, the solutions are different after the shock formation.

6.2. Moment-closure

The moment closure idea was first introduced by (Brenier and Corrias 1998) in order to define multi-valued solutions to Burgers' equation and seems to be the natural choice in view of the multi-phase WKB expansion given in (2.21). The method has then been used numerically in (Engquist and Runborg 1996) (see also (Engquist and Runborg 2003) for a broad review) and (Gosse 2002) to study multivalued solutions in the geometrical optics

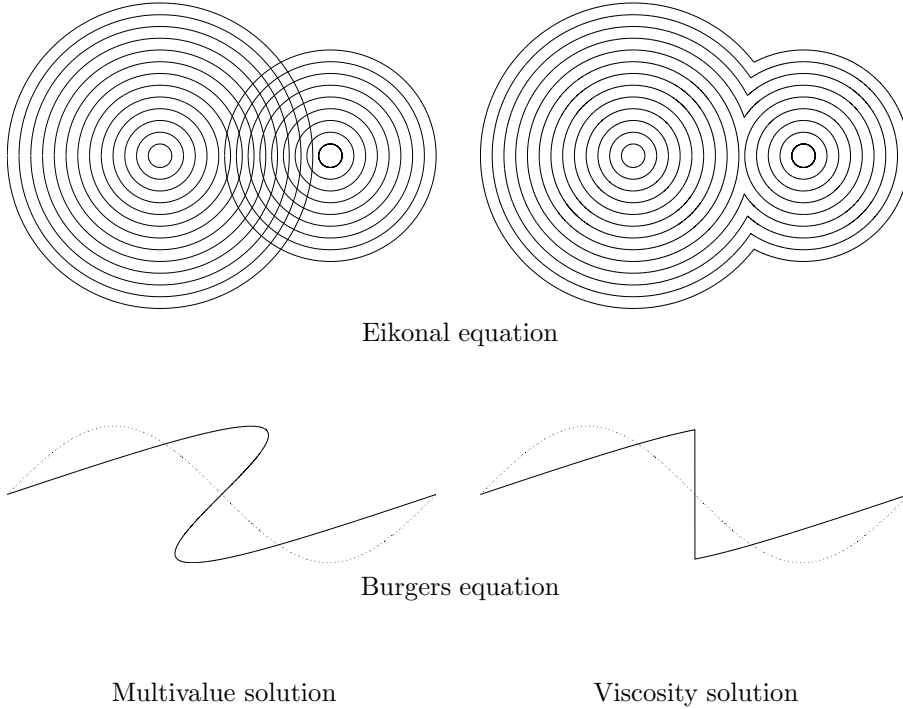


Figure 6.3. Multivalued solution (left) vs. viscosity solution (right). Top figures are the zero level set curves (at different times) of solutions to the eikonal equation (6.2). The bottom figures are the two solutions to the Burgers' equation (6.3) before and after the formation of a shock.

regime of hyperbolic wave equations. A closely related method is given in (Benamou 1999), where a direct computation of multi-valued solutions to Hamilton-Jacobi equations is performed. For the semiclassical limit of the Schrödinger equation, this was done in (Jin and Li 2003) and then (Gosse et al. 2003).

In order to describe the basic idea, let $d = 1$ and define

$$m_\ell(t, x) = \int_{\mathbb{R}} \xi^\ell w(t, x, \xi) \, d\xi, \quad \ell = 1, 2, \dots, L \in \mathbb{N}, \quad (6.4)$$

i.e. the ℓ -th moment (in velocity) of the Wigner measure. By multiplying the Liouville equation (3.8) by ξ^ℓ and integrating over \mathbb{R}_ξ , one obtains the

following moment system

$$\begin{aligned} \partial_t m_0 + \partial_x m_1 &= 0, \\ \partial_t m_1 + \partial_x m_2 &= -m_0 \partial_x V, \\ &\dots\dots\dots \\ \partial_t m_{L-1} + \partial_x m_L &= -(L-1)m_{L-2} \partial_x V. \end{aligned}$$

Note that this system is *not closed*, since the equation determining the ℓ -th moment involves the $(\ell + 1)$ -st moment.

The δ -closure

As already mentioned in (3.10), locally away from caustics the Wigner measure of u^ε as $\varepsilon \rightarrow 0$ can be written as

$$w(t, x, \xi) = \sum_{j=1}^J \rho_j(t, x) \delta(\xi - v_j(t, x)), \quad (6.5)$$

where the number of velocity branches J in principle can be determined a-priori from $\nabla S_{\text{in}}(x)$. For example, in $d = 1$, it is the total number of inflection point of $v(0, x)$, see (Gosse et al. 2003). Using this particular form (6.5) of w with $L = 2J$ provides a closure condition for the moment system above. More, precisely, one can express the last moment m_{2J} as a function of all of the lower order moments (Jin and Li 2003), i.e.

$$m_{2J} = g(m_0, m_1, \dots, m_{2J-1}) \quad (6.6)$$

This consequently yields a system of $2J \times 2J$ equations (posed in physical space), which effectively provides a solution of the Liouville equation, before the generation of a new phase, yielding a new velocity v_j , $j > J$. It was shown in (Jin and Li 2003) that this system is only *weakly hyperbolic*, in the sense that the Jacobian matrix of the flux is a Jordan Block, with only J distinct eigenvalues v_1, v_2, \dots, v_J . This system is equivalent to J pressure-less gas equations (6.1) for (ρ_j, v_j) respectively. In (Jin and Li 2003) the explicit flux function g in (6.6) was given for $J \leq 5$. For larger J a numerical procedure was proposed for evaluating g .

Since the moment system is only weakly hyperbolic, with phase jumps which are *under-compressive shocks* (Gosse et al. 2003), standard shock capturing schemes such as the Lax-Friedrichs scheme and the Godunov scheme face severe numerical difficulties as in the computation of the pressure-less gas dynamics, cf. (Bouchut, Jin and Li 2003), (Engquist and Runborg 1996), or (Jiang and Tadmor 1998). Following the ideas of (Bouchut et al. 2003) for the pressure-less gas system, a kinetic scheme derived from the Liouville equation (3.8) with the closure condition (6.6), was used in (Jin and Li 2003) for this moment system.

The Heaviside closure

Another type of closure was introduced by Brenier and Corrias (Brenier and Corrias 1998) using the following ansatz, called *H-closure*:

$$w(t, x, \xi) = \sum_{j=1}^J (-1)^{j-1} H(v_j(t, x) - \xi), \quad (6.7)$$

to obtain the J -branch velocities v_j , with $j = 1, \dots, J$. This type of closure-condition for (3.8) arises from an entropy-maximization principle, see (Levermore 1996). Using (6.7) one arrives at (6.6) with $L = J$. The explicit form of the corresponding function $g(m_0, \dots, m_{2J-1})$ for $J < 5$ is available analytically in (Runborg 2000). Note that this method decouples the computation of velocities v_j from the densities ρ_j . In fact, to obtain the latter, (Gosse 2002) has proposed to solve the following linear conservation law (see also (Gosse and James 2002) and (Gosse et al. 2003)):

$$\partial_t \rho_j + \partial_x(\rho_j v_j) = 0, \quad \text{for } j = 1, \dots, N.$$

The numerical approximation to this linear transport with variable or even discontinuous flux is not straightforward. In (Gosse et al. 2003) a semi-Lagrangian method that uses the method of characteristics was used, requiring the time step to be sufficiently small for the case of non-zero potentials.

The corresponding method is usually referred to as *H-closure*. Note that in $d = 1$ the *H-closure* system is a non-strictly rich hyperbolic system, whereas the δ -closure system described before is only weakly hyperbolic. Thus one expects a better numerical resolution from the *H-closure* approach, which, however, is much harder to implement in the higher dimension. In $d = 1$, the mathematical equivalence of the two moment systems was proved in (Gosse et al. 2003).

Remark 6.1. Multivalued solutions also arise in the high-frequency approximation of *nonlinear* waves, for example, in the modeling of electron transport in vacuum electronic devices, see e.g. (Granstein, Parker and Armstrong 1999). There the underlying equations are the Euler-Poisson equations, which is a nonlinearly coupled hyperbolic-elliptic system. The multivalued solution of the Euler-Poisson system also arises for electron sheet initial data and can be characterized by a weak solution of the Vlasov-Poisson equation, see (Majda, Majda and Zheng 1994). Similarly, the work of (Li, Wohlbier, Jin and Booske 2004) uses the moment closure ansatz (6.6) for the Vlasov-Poisson system, see also (Wohlbier, Jin and Sengele 2005). For multivalued (or multiphase) solution of the semiclassical limit of nonlinear dispersive waves using the closely related method of *Whitham's modulation theory* we refer to (Whitham 1974), (Flaschka, Forrest and McLaughlin 1980). Finally, we mention that multivalued solutions

also arise in supply chain modeling, see, e.g, (Armbruster, Marthaler and Ringhofer 2003).

In summary, the moment closure approach yields an Eulerian method defined in the physical space which offers a greater efficiency compared to the computation on phase space. However, when the number of phases $J \in \mathbb{N}$ becomes very large and/or in dimensions $d > 1$, the moment systems become very complex and thus difficult to solve. In addition, in high space dimension, it is very difficult to estimate *a-priori* the total number of phases needed to construct the moment system. Thus it remains an interesting and challenging open problem to develop more efficient and general physical space based numerical methods for the multivalued solutions.

7. Level-set methods

7.1. Eulerian approach

Level-set methods have been recently introduced for computing multi-valued solutions in the context of geometric optics and semiclassical analysis. These methods are rather general and applicable to any (scalar) multi-dimensional quasilinear hyperbolic system or Hamilton-Jacobi equation (see below). We shall now review the basic ideas, following the lines of (Jin and Osher 2003). The original mathematical formulation is classical, see for example (Courant and Hilbert 1962).

Computation of the multi-valued phase

Consider a general d -dimensional Hamilton-Jacobi equation of the form

$$\partial_t S + H(x, \nabla S) = 0; \quad S(0, x) = S_{\text{in}}(x). \quad (7.1)$$

For example, in present context of semiclassical analysis for Schrödinger equations,

$$H(x, \xi) = \frac{1}{2}|\xi|^2 + V(x),$$

while for applications in geometrical optics (i.e. the high frequency limit of the wave equation)

$$H(x, \xi) = c(x)|\xi|,$$

with $c(x)$ denoting the local sound (or wave) speed. Introducing, as before, a velocity $v = \nabla S$ and taking the gradient of (7.1) one gets an equivalent equation (at least for smooth solutions) in the form (Jin and Xin 1998):

$$\partial_t v + (\nabla_\xi H(x, v) \cdot \nabla)v + \nabla_x H(x, v) = 0; \quad v(0, x) = \nabla_x S_{\text{in}}(x). \quad (7.2)$$

Then, in $d \geq 1$ spatial dimensions, define *level-set functions* ϕ_j , for $j = 1, \dots, d$, via

$$\forall (t, x) \in \mathbb{R} \times \mathbb{R}^d : \quad \phi_j(t, x, \xi) = 0 \quad \text{at} \quad \xi = v_j(t, x).$$

In other words, the (intersection of the) zero level-sets of all $\{\phi_j\}_{j=1}^d$ yields the graph of the multivalued solution $v_j(t, x)$ of (7.2). Using (7.2) it is easy to see that ϕ_j solves the following initial value problem:

$$\partial_t \phi_j + \{H(x, \xi), \phi_j\} \phi_j = 0; \quad \phi_j(x, \xi, 0) = \xi_j - v_j(0, x), \quad (7.3)$$

which is nothing but the phase space Liouville equation. Note that in contrast to (7.2), this equation is *linear* and thus can be solved *globally in-time*. In doing so, one obtains, for all $t \in \mathbb{R}$, the multi-valued solution to (7.2), needed in the asymptotic description of physical observables. See also (Cheng, Liu and Osher 2003).

Computation of the particle density

It remains to compute the classical limit of the particle density $\rho(t, x)$. To do so, a simple idea was introduced in (Jin, Liu, Osher and Tsai 2005a). This method is equivalent to a decomposition of the measure-valued initial data (3.9) for the Liouville equation. More precisely, a simple argument based on the method of characteristics (see (Jin, Liu, Osher and Tsai 2005b)), shows that the solution to (3.8)-(3.9) can be written as

$$w(t, x, \xi) = \psi(t, x, \xi) \prod_{j=1}^d \delta(\phi_j(t, x, \xi)),$$

where $\phi_j(t, x, \xi) \in \mathbb{R}^n$, $j = 1, \dots, d$, solves (7.3) and the auxiliary function $\psi(t, x, \xi)$ again satisfies the Liouville equation (3.8), subject to initial data:

$$\psi(0, x, \xi) = \rho_{\text{in}}(x)$$

The first two moments of w w.r.t. ξ (corresponding to the particle ρ and current-density $J = \rho u$) can then be recovered through

$$\begin{aligned} \rho(t, x) &= \int_{\mathbb{R}^d} \psi(t, x, \xi) \prod_{j=1}^d \delta(\phi_j(t, x, \xi)) \, d\xi, \\ u(t, x) &= \frac{1}{\rho(t, x)} \int_{\mathbb{R}^d} \xi \psi(t, x, \xi) \prod_{j=1}^d \delta(\phi_j(t, x, \xi)) \, d\xi. \end{aligned}$$

Thus the only time one has to deal with the delta measure is at the numerical output, while during the time-evolution one simply solves for ϕ_j and ψ , both of which are smooth L^∞ -functions. This avoids the singularity problem mentioned earlier, and gives numerical methods with much better resolution than solving directly (3.8), (3.9), e.g., by approximating the initial delta-function numerically. An additional advantage of this level-set approach is that one *only needs* to care about *the zero level-sets* of ϕ_j . Thus the technique of local level-set methods developed in (Adalsteinsson and Sethian

1995) and (Peng, Merriman, Osher, Zhao and Kang 1999) can be used. One thereby restricts the computational domain to a narrow band around the zero level set, in order to reduce the computational cost to $\mathcal{O}(N \ln N)$, for N computational points in the physical space. This is a nice alternative for dimension reduction of the Liouville equation. When solutions for many initial data need to be computed, fast algorithms can be used, see (Fomel and Sethian 2002), or (Ying and Candès 2006).

Example 7.1. This example is from (Jin et al. 2005b). Consider (2.1) in $d = 1$ with periodic potential $V(x) = \cos(2x + 0.4)$, and WKB initial data corresponding to

$$S_{\text{in}}(x) = \sin(x + 0.15),$$

$$\rho_{\text{in}}(x) = \frac{1}{2\sqrt{\pi}} \left[\exp\left(-\left(x + \frac{\pi}{2}\right)^2\right) + \exp\left(-\left(x - \frac{\pi}{2}\right)^2\right) \right].$$

Figure 7.4 shows the time-evolution of the velocity and the corresponding density computed by the level set method described above. The velocity eventually develops some small oscillations with higher frequency, which require a finer grid to resolve.

Remark 7.2. The outlined ideas have been extended to general linear symmetric hyperbolic systems in (Jin et al. 2005a). So far, however, level-set methods have not been formulated for nonlinear equations, except for the one-dimensional Euler-Poisson equations (Liu and Wang 2007), where a three-dimensional Liouville equation has to be used in order to calculate the corresponding one-dimensional multivalued solutions.

7.2. The Lagrangian phase flow method

While the Eulerian level-set method is based on solving the Liouville equation (3.8) on a fixed mesh, the *Lagrangian (or particle) method*, is based on solving the Hamiltonian system (3.6), which is nothing but the characteristic flow of the Liouville equation (3.7). In geometric optics this idea is referred to as *ray tracing*, cf. (Cervený 2001), and the curves $x(t, y, \zeta), \xi(t, y, \zeta) \in \mathbb{R}^d$ obtained by solving (3.6), are usually called *bi-characteristics*.

Remark 7.3. Note that finding an efficient way to numerically solve Hamiltonian ODEs, such as (3.6), is a problem of great (numerical) interests in its own right, see, e.g., (Leimkuhler and Reich 2004).

Here we shall briefly describe a fast algorithm, called the *phase flow method* in (Ying and Candès 2006), which is very efficient if multiple initial data, as it is often the case in practical applications, are to be propagated by the Hamiltonian flow (3.6). Let $F_t : \mathbb{R}^{2d} \rightarrow \mathbb{R}^{2d}$ be the *phase flow* defined

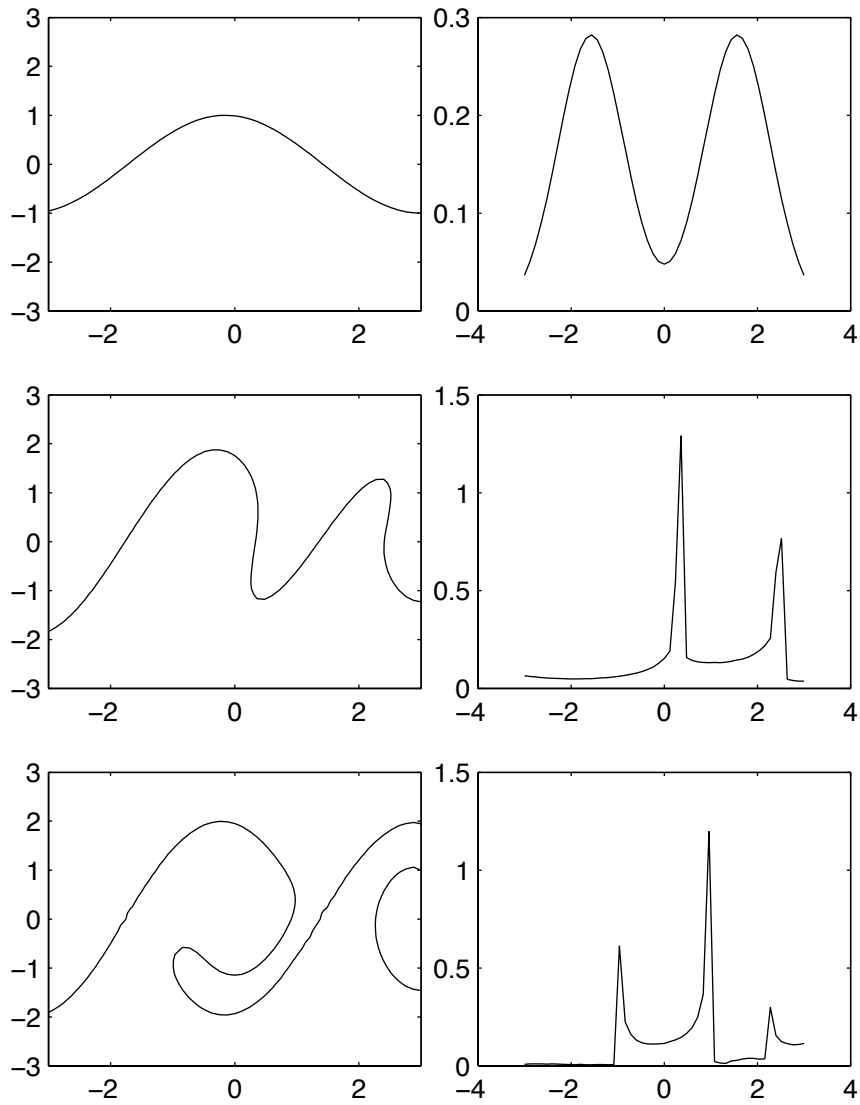


Figure 7.4. Example 7.1. The left column shows the multivalued velocity v at time $T = 0.0, 6.0,$ and 12.0 . The right column shows the corresponding density ρ .

by

$$F_t(y, \zeta) = (x(t, y, \zeta), \xi(t, y, \zeta)), \quad t \in \mathbb{R}.$$

A manifold $\mathcal{M} \subset \mathbb{R}_x^d \times \mathbb{R}_\xi^d$ is said to be *invariant* if $F_t(\mathcal{M}) \subset \mathcal{M}$. For the autonomous ODEs, such as (3.6), a key property of the phase map is the one parameter group structure, $F_t \circ F_s = F_{t+s}$.

Instead of integrating (3.6) for each individual initial condition (y, ζ) , up to, say, time T the phase flow method constructs the complete phase map F_T . To this end, one first constructs the F_t for small times using standard ODE integrators and then builds up the phase map for larger times via a local interpolation scheme together with the group property of the phase flow. Specifically, fix a small time $\tau > 0$ and suppose that $T = 2^n \tau$.

Step 1. Begin with a uniform or quasi-uniform grid on \mathcal{M} .

Step 2. Compute an approximation of the phase map F_τ at time τ . The value of F_τ at each grid point is computed by applying a standard ODE or Hamiltonian integrator with a single time step of length τ . The value of F_τ at any other point is defined via a local interpolation.

Step 3. For $k = 1, \dots, n$, construct $F_{2^k \tau}$ using the group relation $F_{2^k \tau} = F_{2^{k-1} \tau} \circ F_{2^{k-1} \tau}$. Thus, for each grid point (y, ζ) ,

$$F_{2^k \tau}(y, \zeta) = F_{2^{k-1} \tau}(F_{2^{k-1} \tau}(y, \zeta))$$

while $F_{2^k \tau}$ is defined via a local interpolation at any other point.

When the algorithm terminates, one obtains an approximation of the whole phase map at time $T = 2^n \tau$. This method is clearly much faster than solving each for initial condition, independently.

8. Gaussian beam methods - Lagrangian approach

A common numerical problem with all numerical approaches based on the Liouville-equation with mono-kinetic initial data (3.8), (3.9), is that the particle density $\rho(t, x)$ blows up at caustics. Another problem is the *loss of phase information* when passing through a caustic point, i.e. the loss of the Keller-Maslov index (Maslov 1981). To this end, we recall that the Wigner measure only sees the gradient of the phase, see (3.10). The latter can be fixed by incorporating this index into a level-set method as it was done in (Jin and Yang 2008). Nevertheless, one still faces the problem that any numerical method based on the Liouville equation is unable handle wave interference effects. The *Gaussian beam method* (or Gaussian wave packet approach, as it is called in quantum chemistry, cf. (Heller 2006)), is an efficient approximate method that allows an accurate computation of the

wave amplitude around caustics, and in addition captures the desired phase information. This, by now, classical method has been developed in (Popov 1982), (Ralston 1982) and (Hill 1990), and has seen increasing activities in recent years. In the following, we shall describe the basic ideas, starting with its classical Lagrangian formulation.

8.1. Lagrangian dynamics of Gaussian beams

Similar to the WKB method, the approximate Gaussian beam solution is given in the form

$$\varphi^\varepsilon(t, x, y) = A(t, y)e^{iT(t, x, y)/\varepsilon}, \quad (8.1)$$

where the variable $y = y(t, y_0)$ will be determined below and the phase $T(t, x, y)$ is given

$$T(t, x, y) = S(t, y) + p(t, y) \cdot (x - y) + \frac{1}{2}(x - y)^\top M(t, y)(x - y) + \mathcal{O}(x - y|^3).$$

This is reminiscent of the Taylor expansion of the phase S around the point y , upon identifying $p = \nabla S \in \mathbb{R}^d$, $M = \nabla^2 S$, the *Hessian matrix*. The idea is now to allow the phase T so be *complex-valued* (in contrast to WKB analysis) and choose the imaginary part of $M \in \mathbb{C}^{n \times n}$ *positive definite* so that (8.1) has indeed a Gaussian profile.

Plugging the ansatz (8.1) into the Schrödinger equation (2.1), and ignoring the higher order terms in both ε and $(y - x)$, one obtains the following system of ODEs:

$$\frac{dy}{dt} = p, \quad \frac{dp}{dt} = -\nabla_y V, \quad (8.2)$$

$$\frac{dM}{dt} = -M^2 - \nabla_y^2 V, \quad (8.3)$$

$$\frac{dS}{dt} = \frac{1}{2}|p|^2 - V, \quad \frac{dA}{dt} = -\frac{1}{2}(\text{Tr}(M))A, \quad (8.4)$$

where p, V, M, S and A have to be understood as functions of $(t, y(t, y_0))$. The latter defines the *center of a Gaussian beam*. The equations (8.2)-(8.4) can be considered as the the Lagrangian formulation of the Gaussian beam method, with (8.2) furnishing a classical the ray-tracing algorithm. We further note that (8.3) is a *Riccati equation* for M . We the main properties of (8.3), (8.4) in the following Theorem, the proof of which can be found in (Ralston 1982) (see also (Jin, Wu and Yang 2008b)):

Theorem 8.1. Let $P(t, y(t, y_0))$ and $R(t, y(t, y_0))$ be the (global) solutions of the equations

$$\frac{dP}{dt} = R, \quad \frac{dR}{dt} = -(\nabla_y^2 V)P, \quad (8.5)$$

with initial conditions

$$P(0, y_0) = \text{Id}, \quad R(0, y_0) = M(0, y_0), \quad (8.6)$$

where Id is the identity matrix and $\text{Im}(M(0, y_0))$ is positive definite. Assume that $M(0, y_0)$ is symmetric. Then, for each initial position y_0 , it holds:

- (i) $P(t, y(t, y_0))$ is invertible for all $t > 0$.
- (ii) The solution to equation (8.3) is given by

$$M(t, y(t, y_0)) = R(t, y(t, y_0))P^{-1}(t, y(t, y_0)) \quad (8.7)$$

- (iii) $M(t, y(t, y_0))$ is symmetric and $\text{Im}(M(t, y(t, y_0)))$ is positive definite for all $t > 0$.
- (iv) The Hamiltonian $H = \frac{1}{2}|p|^2 + V$ is conserved along the y -trajectory as is $(A^2 \det P)$, i.e. $A(t, y(t, y_0))$ can be computed via

$$A(t, y(t, y_0)) = ((\det P(t, y(t, y_0)))^{-1} A^2(0, y_0))^{1/2}, \quad (8.8)$$

where the square root is taken as the principle value.

In particular, since $(A^2 \det P)$ is a conserved quantity, we infer that A *does not blow up* along the time-evolution (provided it initially bounded).

8.2. Lagrangian Gaussian beam summation

It should be noted that a single Gaussian beam given by (8.1) is *not* an asymptotic solution of (2.1), since its $L^2(\mathbb{R}^{2d})$ norm goes to zero, in the classical limit $\varepsilon \rightarrow 0$. Rather, one needs to sum over several Gaussian beams, the number of which is $\mathcal{O}(\varepsilon^{-1/2})$. This is referred to as the *Gaussian beam summation*, see for example (Hill 1990). In other words, one first needs to approximate a given initial data through Gaussian beam profiles. For WKB initial data (2.18), a possible way to do so, is given by the next theorem proved by (Tanushev 2008).

Theorem 8.2. Let the initial data be given by

$$u_{\text{in}}^\varepsilon(x) = a_{\text{in}}(x)e^{iS_{\text{in}}(x)/\varepsilon},$$

with $a_{\text{in}} \in C^1(\mathbb{R}^d) \cap L^2(\mathbb{R}^d)$ and $S_{\text{in}} \in C^3(\mathbb{R}^d)$, and define

$$\varphi^\varepsilon(x, y_0) = a_{\text{in}}(y_0)e^{iT(x, y_0)/\varepsilon},$$

where

$$T(x, y_0) = T_\alpha(y_0) + T_\beta \cdot (x - y_0) + \frac{1}{2}(x - y_0)^\top T_\gamma (x - y_0),$$

$$T_\alpha(y_0) = S_{\text{in}}(y_0), \quad T_\beta(y_0) = \nabla_x S_{\text{in}}(y_0), \quad T_\gamma(y_0) = \nabla_x^2 S_{\text{in}}(y_0) + i\text{Id}.$$

Then

$$\left\| u_{\text{in}}^\varepsilon - (2\pi\varepsilon)^{-d/2} \int_{\mathbb{R}^d} r_\theta(\cdot - y_0) \varphi^\varepsilon(\cdot, y_0) \, dy_0 \right\|_{L^2} \leq C\varepsilon^{\frac{1}{2}},$$

where $r_\theta \in C_0^\infty(\mathbb{R}^d)$, $r_\theta \geq 0$ is a truncation function with $r_\theta \equiv 1$ in a ball of radius $\theta > 0$ around the origin and C is a constant related to θ .

In view of Theorem 8.2, one can specify the initial data for (8.2)-(8.4) as

$$y(0, y_0) = y_0, \quad p(0, y_0) = \nabla_x S_{\text{in}}(y_0), \quad (8.9)$$

$$M(0, y_0) = \nabla_x^2 S_{\text{in}}(y_0) + i \text{Id}, \quad (8.10)$$

$$S(0, y_0) = S_{\text{in}}(y_0), \quad A(0, y_0) = a_{\text{in}}(y_0). \quad (8.11)$$

Then, the the Gaussian beam solution approximating the exact solution of (2.1) is given by

$$u_G^\varepsilon(t, x) = (2\pi\varepsilon)^{-d/2} \int_{\mathbb{R}^d} r_\theta(x - y(t, y_0)) \varphi^\varepsilon(t, x, y(t, y_0)) dy_0.$$

In discretized form this reads

$$u_G^\varepsilon(t, x) \approx (2\pi\varepsilon)^{-d/2} \sum_{j=1}^{N_{y_0}} r_\theta(x - y(t, y_0^j)) \varphi^\varepsilon(t, x, y_0^j) \Delta y_0,$$

where the y_0^j are equidistant mesh points, and N_{y_0} is the number of the beams initially centered at y_0^j .

Remark 8.3. Note that the cut-off error introduced via r_θ becomes large when the truncation parameter θ is taken too small. On the other hand, a big θ for wide beams makes the error in the Taylor expansion of T large. As far as we know, it is still an open mathematical problem to determine an optimal size of θ when beams spread. However, for narrow beams one can take a fairly large θ which makes the cut-off error almost zero. For example, a one-dimensional constant solution can be approximated through

$$1 = \int_{\mathbb{R}} \frac{1}{\sqrt{2\pi\varepsilon}} \exp\left(\frac{-(x - y_0)^2}{2\varepsilon}\right) dy_0 \approx \sum_j \frac{\Delta y_0}{\sqrt{2\pi\varepsilon}} \exp\left(\frac{-(x - y_0^j)^2}{2\varepsilon}\right),$$

in which $r_\theta \equiv 1$.

8.3. Higher order Gaussian beams

The above Gaussian beam method can be extended to higher order in ε , see (Tanushev 2008), (Jin et al. 2008b), (Liu and Ralston 2010). For notational convenience we shall only consider the case $d = 1$. Consider the Schrödinger equation (2.1) with initial data

$$u_{\text{in}}^\varepsilon(x) = e^{iS_{\text{in}}(x)/\varepsilon} \sum_{j=0}^N \varepsilon^j a_j(x), \quad x \in \mathbb{R}.$$

Let a ray $y(t, y_0)$ start at a point $y_0 \in \mathbb{R}$. Expand $S_{\text{in}}(x)$ in a Taylor series around y_0 :

$$S_{\text{in}}(x) = \sum_{\beta=0}^{k+1} S_{\beta}(y_0)(x - y_0)^{\beta} + \mathcal{O}(|x - y_0|^{\beta+1}).$$

Then, a single k -th order Gaussian beam takes the form

$$\varphi_k^{\varepsilon}(t, x, y) = \sum_{j=1}^{[k/2]-1} \varepsilon^j A_j(t, y) e^{iT(t, x, y)/\varepsilon}$$

where the phase is given by

$$T(t, x, y) = T_0(t, y) + p(t, y)(x - y) + \frac{1}{2}M(t, y)(x - y)^2 + \sum_{\beta=3}^{k+1} \frac{1}{\beta!} T_{\beta}(t, y)(x - y)^{\beta}$$

and the amplitude reads

$$A_j = \sum_{\beta=0}^{k-2j-1} \frac{1}{\beta!} A_{j,\beta}(t, y)(x - y)^{\beta}.$$

Here the bi-characteristic curves $(y(t, y_0), p(t, y(t, y_0)))$ satisfy the Hamiltonian system (8.2) with initial data

$$y(0, y_0) = y_0, \quad p(0, y_0) = \partial_y S_0(y_0)$$

In addition, the equations for the phase coefficients along the bi-characteristic curves are given by

$$\begin{aligned} \frac{dT_0}{dt} &= \frac{p^2}{2} - V, \\ \frac{dM}{dt} &= -M^2 - \partial_y^2 V, \\ \frac{dT_{\beta}}{dt} &= - \sum_{\gamma=2}^{\beta} \frac{(\beta-1)!}{(\gamma-1)!(\beta-\gamma)!} T_{\gamma} T_{\beta-\gamma+2} - \partial_y^{\beta} V, \end{aligned}$$

for $\beta = 3, \dots, k+1$. These equations are equipped with the following initial data

$$T_0(0, y_0) = S_0(y_0), \quad M(0, y_0) = \partial_y^2 S_0(y_0) + i \text{Id}, \quad T_{\beta}(0, y_0) = S_{\beta}(y_0).$$

Finally, the amplitude coefficients are obtained recursively by solving the transport equations for $A_{j,\beta}$ with $\beta \leq k - 2j - 1$, starting from

$$\frac{dA_{0,0}}{dt} = -\frac{1}{2} \text{Tr}(M(t, z)) A_{0,0} \tag{8.12}$$

with initial data

$$A_{j,\beta}(0, y_0) = a_\beta(y_0)$$

In $d = 1$, the k -th order Gaussian beam superposition is thus formed by

$$u_{G,k}^\varepsilon(t, x) = (2\pi\varepsilon)^{-1/2} \int_{\mathbb{R}} r_\theta(x - y(t, y_0)) \varphi_k^\varepsilon(t, x, y(t, y_0)) dy_0 \quad (8.13)$$

where, as before, $r_\theta \in C_0^\infty(\mathbb{R}; \mathbb{R})$, is some cut-off function. For this type of approximation, the following theorem was proved in (Liu, Runborg and Yanushev n.d.):

Theorem 8.4. If $u^\varepsilon(t, x)$ denotes the exact solution to the Schrödinger equation (2.1) and $u_{G,k}^\varepsilon$ is the k -th order Gaussian beam superposition, then

$$\sup_{|t| < T} \|u^\varepsilon(t, \cdot) - u_{G,k}^\varepsilon(t, \cdot)\| \leq C(T)\varepsilon^{k/2}, \quad (8.14)$$

for any $T > 0$.

9. Gaussian beam methods - Eulerian approach

9.1. Eulerian dynamics of Gaussian beams

The Gaussian beam method can be reformulated in an Eulerian framework. To this end, let us first define the linear Liouville operator as

$$\mathcal{L} = \partial_t + \xi \cdot \nabla_y - \nabla_y V \cdot \nabla_\xi.$$

In addition, we shall denote

$$\Phi := (\phi_1, \dots, \phi_d),$$

where ϕ_j is the level set function defined in (7.1) and (7.3). Using this, it was shown in (Jin et al. 2005b) and (Jin and Osher 2003), that one can obtain from the original Lagrangian formulation (8.2)-(8.4), the following (inhomogeneous) Liouville equations for velocity, phase and amplitude, respectively:

$$\mathcal{L}\Phi = 0, \quad (9.1)$$

$$\mathcal{L}S = \frac{1}{2}|\xi|^2 - V, \quad (9.2)$$

$$\mathcal{L}A = \frac{1}{2}\text{Tr}((\nabla_\xi \Phi)^{-1} \nabla_y \Phi) A. \quad (9.3)$$

In addition, if one introduces the following new quantity, cf. (Jin et al. 2005b):

$$f(t, y, \xi) = A^2(t, y, \xi) \det(\nabla_\xi \Phi),$$

then $f(t, y, \xi)$ again satisfies the Liouville equation, i.e.

$$\mathcal{L}f = 0. \quad (9.4)$$

Two more inhomogeneous Liouville equations, which are the Eulerian version of (8.5) for P and R , were introduced in (Leung, Qian and Burrige 2007) to construct the Hessian matrix. More precisely, one finds

$$\mathcal{L}R = -(\nabla_y^2 V)P, \quad (9.5)$$

$$\mathcal{L}P = R. \quad (9.6)$$

Note that the equations (9.1)–(9.4) are *real*, while (9.5) and (9.6) are *complex* and consist of $2n^2$ equations.

Gaussian beam dynamics using complex level set functions

In (Jin et al. 2008b) the following observation was made. Taking the gradient of the equation (9.1) with respect to y and ξ separately, one has

$$\mathcal{L}(\nabla_y \Phi) = \nabla_y^2 V \nabla_\xi \Phi, \quad (9.7)$$

$$\mathcal{L}(\nabla_\xi \Phi) = -\nabla_y \Phi, \quad (9.8)$$

Comparing (9.5), (9.6) with (9.7), (9.8), one observes that $-\nabla_y \Phi$ and $\nabla_\xi \Phi$ satisfy the *same* equations as R and P , respectively. Since the Liouville operator is linear, one can allow Φ to be *complex-valued* and impose for $-\nabla_y \Phi$, $\nabla_\xi \Phi$ the same initial conditions as for R and P , respectively. By doing so,

$$R = -\nabla_x \Phi, \quad P = \nabla_\xi \Phi.$$

holds true for any time $t \in \mathbb{R}$. In view of (8.6) and (8.10), this suggests the following initial condition for Φ :

$$\Phi_0(y, \xi) = -iy + (\xi - \nabla_y S_0). \quad (9.9)$$

With this observation, now one can solve (9.1) for *complex* Φ , subject to initial data (9.9). Then the matrix M can be constructed by

$$M = -\nabla_y \Phi (\nabla_\xi \Phi)^{-1} \quad (9.10)$$

where the velocity $v = \nabla_y S$ is given by the intersection of the zero-level contours of the *real* part of Φ , i.e. for each component ϕ_j ,

$$\text{Re}(\phi_j(t, y, \xi)) = 0, \quad \text{at} \quad \xi = v(t, y) = \nabla_y S. \quad (9.11)$$

Note that in order to compute v , S and M one only needs to solve d *complex-valued homogeneous Liouville equations* (9.1). The Eulerian level set method of (Jin et al. 2008b) (on complex phase space) can then be summarized as follows:

Step 1. Solve (9.1) for Φ *complex*, with initial condition (9.9) and obtain

the velocity v by the intersection of the zero-level sets of $\operatorname{Re} \phi_j$, $j = 1, \dots, n$.

Step 2. Use $-\nabla_y \Phi$ and $\nabla_\xi \Phi$ to construct M by (9.10) (note that these quantities are already available from the first step after discretizing the Liouville equation for Φ).

Step 3. Integrate the velocity v along the zero-level sets (Gosse 2002), (Jin and Yang 2008) to get the phase S . To do so, one performs a numerical integration *following each branch* of the velocity. The integration constants are obtained by the boundary condition and the fact that the multivalued phase is continuous when passing from one branch to the other. For example, if one considers a bounded domain $[a, b]$ in $d = 1$ space dimension, the phase function is given by

$$S(t, x) = -V(a)t - \frac{1}{2} \int_0^t v^2(\tau, a) \, d\tau + \int_a^x v(t, y) \, dy + S(0, a). \quad (9.12)$$

For more details on this and its extension to higher dimensions, see (Jin and Yang 2008).

Step 4. Solve (9.4) with the initial condition

$$f_0(y, \xi) = A_0^2(y, \xi).$$

Then amplitude A is given by

$$A = (\det(\nabla_\xi \Phi)^{-1} f)^{1/2}, \quad (9.13)$$

where the square root has to be understood as the principle value. (We also refer to (Jin, Wu and Yang 2011) for a more elaborated computation of A .)

Note that all functions appearing in Steps 2–4 only need to be solved locally around the zero-level sets of $\operatorname{Re} \phi_j$, $j = 1, \dots, n$. Thus, the entire algorithm can be implemented using the local level set methods of (Osher, Cheng, Kang, Shim and Tsai 2002) and (Peng et al. 1999). For a given mesh size Δy , the computational cost is therefore $\mathcal{O}((\Delta y)^{-d} \ln(\Delta y)^{-1})$, about the same as the local level set methods for geometrical optics computation, see (Jin et al. 2005b).

Remark 9.1. If one is only interested in computing the classical limit of (the expectation values of) physical observables, one observes that the only term in (9.12) which affects a quadratic observable density for fixed time t is $\int_a^x v(t, y) \, dy$. Thus, as long as one is only interested in physical observables, one can simply take

$$S(t, x) = \int_a^x v(t, y) \, dy \quad (9.14)$$

in the numerical simulations.

That M and A are indeed well-defined via (9.10) and (9.13) is justified by the following theorem (which can be seen as the Eulerian version of Theorem 8.1) proved in (Jin et al. 2008b):

Theorem 9.2. Let $\Phi = \Phi(t, y, \xi) \in \mathbb{C}$ be the solution of (9.1) with initial data (9.9). Then, the following properties hold:

- (i) $\nabla_\xi \Phi$ is non-degenerate for all $t \in \mathbb{R}$.
- (ii) $\text{Im}(-\nabla_y \Phi (\nabla_\xi \Phi)^{-1})$ is positive definite for all $t \in \mathbb{R}$, $y, \xi \in \mathbb{R}^d$.

Although $\det(\text{Re}(\nabla_\xi \Phi)) = 0$ at caustics, the complexified Φ makes $\nabla_\xi \Phi$ *non-degenerate*, and the amplitude A , defined in (9.13), *does not blow-up* at caustics.

9.2. Eulerian Gaussian beam summation

As before we are facing the problem of Gaussian beam summation, i.e. in order to reconstruct the full solution u^ε a superposition of single Gaussian beams has to be considered. To this end, we define a single Gaussian beam, obtained through the Eulerian approach, by

$$\tilde{\varphi}^\varepsilon(t, x, y, \xi) = A(t, y, \xi) e^{iT(t, x, y, \xi)/\varepsilon}, \quad (9.15)$$

where A is solved via (9.13) and

$$T(t, x, y, \xi) = S(t, y, \xi) + \xi \cdot (x - y) + \frac{1}{2}(x - y)^\top M(t, y, \xi)(x - y).$$

Then, the wave function is constructed via the following *Eulerian Gaussian beam summation* formula, cf. (Leung et al. 2007):

$$\tilde{u}_G^\varepsilon(t, x) = (2\pi\varepsilon)^{-d/2} \iint_{\mathbb{R}^d \times \mathbb{R}^d} r_\theta(x - y) \tilde{\varphi}^\varepsilon(t, x, y, \xi) \prod_{j=1}^d \delta(\text{Re}(\phi_j)) \, d\xi \, dy,$$

which is consistent to the Lagrangian summation formula (8.2).

Indeed, the above given double-integral for u_G^ε can be evaluated as a single integral in y as follows: We again denote by v_j , $j = 1, \dots, J$ the j -th branch of the multi-valued velocity and write

$$\tilde{u}_G^\varepsilon(t, x) = (2\pi\varepsilon)^{-d/2} \int_{\mathbb{R}^d} r_\theta(x - y) \sum_{j=1}^J \frac{\tilde{\varphi}^\varepsilon(t, x, y, v_k)}{|\det(\text{Re}(\nabla_\xi \Phi)_{\xi=v_j})|} \, dy. \quad (9.16)$$

However, since $\det(\text{Re}(\nabla_\xi \Phi)) = 0$ at caustics, a direct numerical integration of (9.16) loses accuracy around caustics. To get a better accuracy, one can

split (9.16) into two parts

$$I_1 = \sum_{j=1}^J \int_{\Omega_1} (2\pi\varepsilon)^{-d/2} r_\theta(x-y) \frac{\tilde{\varphi}^\varepsilon(t, x, y, v_k)}{|\det(\operatorname{Re}(\nabla_\xi \Phi)_{\xi=v_j})|} dy, \quad (9.17)$$

$$I_2 = \sum_{j=1}^J \int_{\Omega_2} (2\pi\varepsilon)^{-d/2} r_\theta(x-y) \frac{\tilde{\varphi}^\varepsilon(t, x, y, v_k)}{|\det(\operatorname{Re}(\nabla_\xi \Phi)_{\xi=v_j})|} dy, \quad (9.18)$$

where

$$\begin{aligned} \Omega_1 &:= \{y : |\det(\operatorname{Re}(\nabla_p \phi)(t, y, p_j))| \geq \tau\}, \\ \Omega_2 &:= \{y : |\det(\operatorname{Re}(\nabla_p \phi)(t, y, p_j))| < \tau\}, \end{aligned}$$

with τ being a small parameter. The latter is chosen sufficiently small in order to minimize the cost of computing (9.18), yet large enough to make I_1 a *regular integral*.

The regular integral I_1 can then be approximated by a standard quadrature rule, such as the trapezoid quadrature rule, while the *singular integral* I_2 is evaluated by the semi-Lagrangian method introduced in (Leung et al. 2007).

Remark 9.3. When the velocity contours are complicated due to large numbers of caustics, the implementation of the local semi-Lagrangian method is hard. In such situations one can use a discretized δ -function method for numerically computing (9.18) as was done in (Wen 2010). In this method one needs to numerically solve (9.2) in order to obtain the phase function, since all values of ϕ_j near the support of $\delta(\operatorname{Re}(\phi_j))$ are needed to evaluate (9.18).

Example 9.4. This is an example from (Jin et al. 2008b). It considers the free motion of particles in $d = 1$ with $V(x) = 0$. The initial conditions for the Schrödinger equation (2.1) are induced by

$$\rho_{\text{in}}(x) = \exp(-50x^2), \quad v_{\text{in}}(x) = \partial_x S_0(x) = -\tanh(5x).$$

Fig. 9.5 shows the l_∞ errors between the square modulus of u^ε , the exact solution of the Schrödinger equation (2.1), and the approximate solution constructed: (i) by the level set method described in Section 7; (ii) the level set method with Keller-Maslov index built in, cf. (Jin and Yang 2008), and (iii) the Eulerian Gaussian beam method described above. As one can see, method (ii) improves the geometric optics solution (i) away from caustics, while Gaussian beam method offers a uniformly small error even near the caustics.

Compared to the Lagrangian formulation based on solving the ODE system (8.2)-(8.4), the Eulerian Gaussian beam method has the advantage of maintaining a good numerical accuracy since they are based on solving PDEs

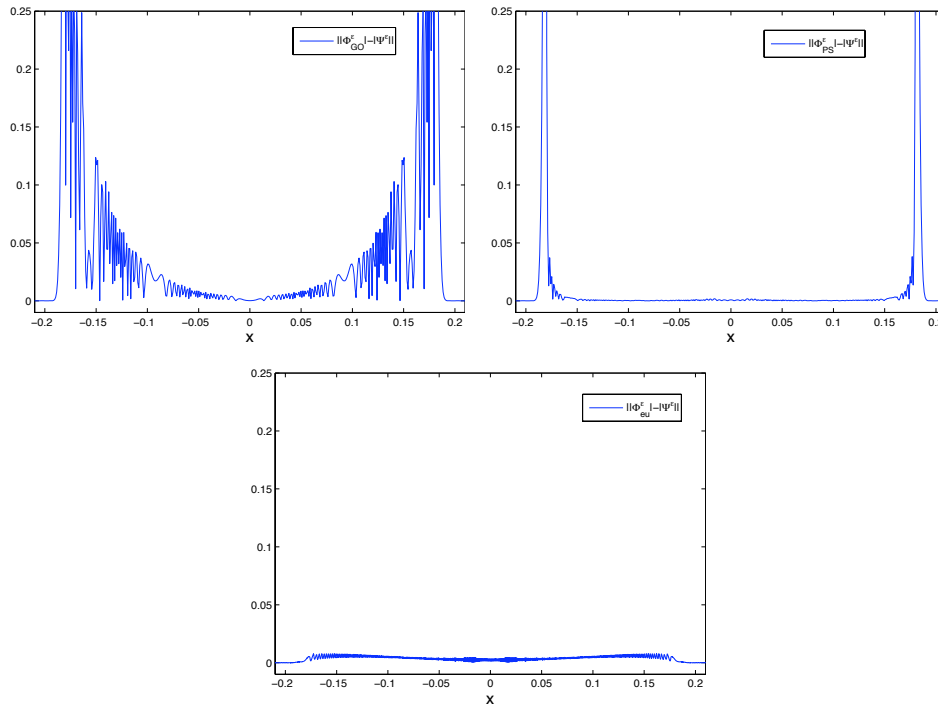


Figure 9.5. Example 9.4. Errors between the solution of the Schrödinger equation when compared to the geometrical optics solution (top left), the geometrical optics with phase-shift built in (top right), and the Gaussian beam method (bottom). Caustics are around $x = \pm 0.18$.

on fixed grids. Moreover, higher order (in ε) Eulerian Gaussian beam methods have been constructed, see (Liu and Ralston 2010) and (Jin et al. 2011).

Remark 9.5. Research on the Gaussian beam methods is of great recent interest in the applied math community, see, e.g, (Leung et al. 2007), (Jin et al. 2008b), (Leung and Qian 2009) for Eulerian formulations, (Tanushev 2008), (Motamed and Runborg n.d.), (Liu and Ralston 2010), (Bougacha, Akian and Alexandre 2009), (Liu et al. n.d.) for error estimates, and (Tanushev, Engquist and Tsai 2009), (Ariel, Engquist, Tanushev and Tsai n.d.), (Qian and Ying 2010), and (Yin and Zheng n.d.) for initial data decompositions.

9.3. Frozen Gaussian approximations

The construction of Gaussian beam approximation is based on the truncation of the Taylor expansion of the phase $T(t, x, y)$ (8.1) around the beam center y , hence it *loses accuracy* when the width of the beam becomes large,

i.e. when the imaginary part of $M(t, y)$ in (8.1) becomes small so that the Gaussian function is *not localized* any more. This happens for example when the solution of the Schrödinger equation spreads (namely, the ray determined by (8.2) diverges), which can be seen as the time-reversed situation of caustic-formation. The corresponding loss in the numerical computation can be overcome by re-initialization every once in a while, see (Tanushev et al. 2009), (Ariel et al. n.d.), (Qian and Ying 2010), and (Yin and Zheng n.d.). However, this approach increases the computational complexity in particular, when beams spread quickly.

The *frozen Gaussian approximation* (as it is referred to in quantum chemistry), first proposed in (Heller 1981), uses *Gaussian functions with fixed widths* to approximate the exact solution u^ε . More precisely, instead of using Gaussian beams only in the physical space, the frozen Gaussian approximation uses a *superposition* of Gaussian functions in *phase space*. That's why the method is also known under the name *coherent state approximation*. To this end, one first decomposes the initial data into several Gaussian functions in phase space

$$\psi^\varepsilon(y_0, p_0) = \int_{\mathbb{R}^d} u_{\text{in}}^\varepsilon(y) e^{-(ip_0 \cdot (y-y_0) - \frac{1}{2}|y-y_0|^2)/\varepsilon} dy,$$

and then propagates the center of each function $(y(t), p(t))$ along the Hamiltonian flow (8.2), subject to initial data at (y_0, p_0) . The frozen Gaussian beam solution takes the form

$$u_{\text{FG}}^\varepsilon(t, x) = (2\pi\varepsilon)^{-3d/2} \iint_{\mathbb{R}^d \times \mathbb{R}^d} a(t, y_0, p_0) \psi(y_0, p_0) e^{(ip(t) \cdot (x-y(t)) - \frac{1}{2}|x-y(t)|^2)/\varepsilon} dp_0 dy_0,$$

where the complex valued amplitude $a(t, y_0, p_0)$, is the so-called *Herman-Kluk pre-factor*, cf. (Herman and Kluk 1984). Since the width of the Gaussians is fixed, one does not encounter the problem of beam spreading here. However, since this method is based in the phase space, the computational cost is considerably higher than the standard Gaussian beam methods. For subsequent developments in this direction, see (Herman and Kluk 1984), (Kay 1994), (Kay 2006), (Robert 2010), (Swart and Rousse 2009), (Lu and Yang n.d.).

10. Asymptotic methods for discontinuous potentials

Whenever a medium is heterogeneous, the potential V can be discontinuous, creating a sharp potential barrier or interface where waves can be partially reflected and transmitted (as in the Snell-Descartes' law of refraction). This gives rise to new mathematical and numerical challenges not present in the smooth potential case. Clearly, the semiclassical limit (3.8)

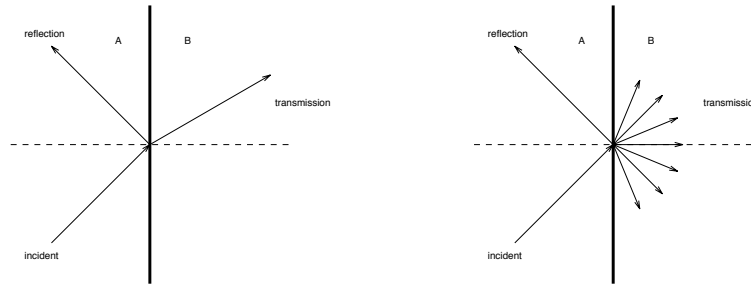


Figure 10.6. Wave transmissions and reflections through an interface

and (3.9) does not hold at the barrier. Whenever V is discontinuous, the Liouville equation (3.8) contains characteristics which are discontinuous or even measure-valued. To this end, we recall that the characteristics curves $(x(t), \xi(t))$ are determined by the Hamiltonian system (3.6). The latter is a nonlinear system of ODEs whose right hand side is not Lipschitz due to the singularity in $\nabla_x H(x, \xi)$ and thus the classical well-posedness theory for the Cauchy problem of the ODEs fails. Even worse, the coefficients in the Liouville equation in general are not even BV (i.e. of bounded variation), for which almost everywhere solutions were introduced by (DiPerna and Lions 1989) and (Ambrosio 2004). Analytical studies of semiclassical limits in situations with interface were carried out in, e.g., (Bal, Keller, Papanicolaou and Ryzhik 1999b), (Miller 2000), (Nier 1995), (Nier 1996), and (Benedetto, Esposito and Pulvirenti 2004) using more elaborate Wigner transformation techniques, such as *two-scale Wigner measures*.

10.1. The interface condition

In order to allow for discontinuous potentials, one first needs to introduce a notion of solutions of the underlying singular Hamiltonian system (3.6). This can be done by providing *interface conditions for reflection and transmission*, based on Snell's law. The solution so constructed will give the correct transmission and reflection of waves through the barrier, obeying the laws of geometrical optics.

Fig. 10.6 (taken from (Jin, Liao and Yang 2008a)) shows typical cases of wave transmissions and reflections through an interface. When the interface is rough, or in higher dimension, the scattering can be diffusive, in which the transmitted or reflected waves can move in all directions (see the right picture). However, in this section we will not discuss the diffusive interface, which was treated analytically in (Bal et al. 1999b) and numerically in (Jin et al. 2008a).

An Eulerian interface condition

In (Jin and Wen 2006a), an interface condition is provided, connecting the Liouville equations at both sides of a given (sharp) interface. Let us focus here on the case of only space dimension $d = 1$ and consider a particle moving with velocity $\xi > 0$ towards the barrier. The interface condition at a given fixed time t is given by:

$$w(t, x^+, \xi^+) = \alpha_T w(t, x^-, \xi^-) + \alpha_R w(t, x^+, -\xi^+) \quad (10.1)$$

Here the superscripts “ \pm ” represent the right and left limits of the quantities, $\alpha_T \in [0, 1]$ and $\alpha_R \in [0, 1]$ are the transmission and reflection coefficients respectively, satisfying $\alpha_R + \alpha_T = 1$. For a sharp interface $x^+ = x^-$, while ξ^+ and ξ^- are connected by the *Hamiltonian preserving* condition:

$$H(x^+, \xi^+) = H(x^-, \xi^-) \quad (10.2)$$

The latter is motivated as follows: In classical mechanics, the Hamiltonian $H = \frac{1}{2}\xi^2 + V(x)$ is conserved along the particle trajectory, even across the barrier. In this case, $\alpha_T, \alpha_R = 0$ or 1 , i.e., a particle can be either completely transmitted or completely reflected. In geometric optics (corresponding to $H(x, \xi) = c(x)|\xi|$), condition (10.2) is equivalent to Snell’s Law of Refraction for a flat interface (Jin and Wen 2006b), i.e. waves can be *partially* transmitted or reflected.

Remark 10.1. In practical terms, the coefficients α_T and α_R are determined from the original Schrödinger equation (2.1) *before* the semiclassical limit is taken. Usually one invokes stationary scattering theory to do so. Thus (10.1) represents a *multi-scale* coupling between the (macroscopic) Liouville equation and the (microscopic) Schrödinger (or wave) equation. Furthermore, by incorporating the diffraction coefficients, determined from the *Geometrical Theory of Diffraction* developed in (Keller and Lewis 1995), into the interface condition, one could even simulate diffraction phenomena near boundaries, interfaces or singular geometries (Jin and Yin 2008b) (Jin and Yin 2008a) (Jin and Yin n.d.).

The well-posedness of the initial value problem of the singular Liouville equation with the interface condition (10.1) was established in (Jin and Wen 2006a), using the method of characteristics. To determine a solution at (x, p, t) one traces back along the characteristics determined by the Hamiltonian system (3.6) until hitting the interface. At the interface, the solution bifurcates with the interface condition (10.1), one corresponds to the transmission and the other reflection, and this process continues until one arrives at $t = 0$. The interface condition (10.1) thus provides a generalization of the method of characteristics.

A Lagrangian Monte-Carlo particle method for the interface

A notion of the solution of the (discontinuous) Hamiltonian system (3.6) was introduced in (Jin 2009) (see also (Jin and Novak 2006)) using a *probability* interpretation. One thereby solves the system (3.6) using a standard ODE or Hamiltonian solver, but at the interface, the following *Monte-Carlo solution* can be constructed (we shall only give solution in the case of $\xi^- > 0$; the other case is similar):

- (i) With probability α_R , the particle (wave) is reflected with

$$x \mapsto x, \quad \xi^- \mapsto -\xi^-. \quad (10.3)$$

- (ii) With probability α_T , the particle (wave) is transmitted, with

$$x \mapsto x, \quad \xi^+ \text{ is obtained from } \xi^- \text{ using (10.2)} \quad (10.4)$$

Although the original problem is deterministic, this probabilistic solution allows one to go beyond the interface with the new value of (x, ξ) defined in (10.3)-(10.4). This is the Lagrangian formulation of the solution determined by using the interface condition (10.1). This is the basis of a (Monte-Carlo based) particle method for thin quantum barriers introduced in (Jin and Novak 2007).

10.2. Modification of the numerical flux at the interface

A typical one-dimensional semi-discrete finite difference method for the Liouville equation (3.7) is

$$\partial_t w_{ij} + \xi_j \frac{w_{i+\frac{1}{2},j}^- - w_{i-\frac{1}{2},j}^+}{\Delta x} - DV_i \frac{w_{i,j+\frac{1}{2}} - w_{i,j-\frac{1}{2}}}{\Delta \xi} = 0.$$

Here w_{ij} is the cell average or pointwise value of $w(t, x_i, \xi_j)$ at fixed t . The *numerical fluxes* $w_{i+\frac{1}{2},j}, w_{i,j+\frac{1}{2}}$ are typically defined by a (first, or higher order) upwind scheme, and DV_i is some numerical approximation of $\partial_x V$ at $x = x_i$.

When V is discontinuous, such schemes face difficulties when the Hamiltonian is discontinuous, since ignoring the discontinuity of V in the actual numerical computation will result in solutions which are inconsistent with the notion of the physically relevant solution, defined in the preceding subsection. Even with a smoothed Hamiltonian, it is usually impossible (at least in the case of *partial* transmission and reflection) to obtain transmission and reflection with the correct transmission and reflection coefficients. A smoothed V will also give a severe time step constraint like $\Delta t \sim O(\Delta x \Delta \xi)$, see, e.g., (Cheng, Kang, Osher, Shim and Tsai 2004). This is a parabolic type CFL condition, despite the fact that we are solving a hyperbolic problem.

A simple method to solve this problem was introduced in (Jin and Wen

2005) and (Jin and Wen 2006a). The basic idea is to build the *interface condition* (10.1) *into the numerical flux*, as follows: Assume V is discontinuous at $x_{i+1/2}$. First one should avoid discretizing V across the interface at $x_{i+1/2}$. One possible discretization is

$$DV_k = \frac{V_{k+1/2}^- - V_{k-1/2}^+}{\Delta x}, \quad \text{for } k = i, i+1,$$

where, for example,

$$V_{k+1/2}^\pm = \lim_{x \rightarrow x_{k+1/2}^\pm} V(x).$$

The numerical flux in the ξ direction, $W_{i,j\pm 1/2}$, can be the usual numerical flux (for example, the upwind scheme or its higher order extension). To define the numerical flux $w_{i+1/2,j}^\pm$, without loss of generality, consider the case $\xi_j > 0$. Using upwind scheme, $w_{i+\frac{1}{2},j}^- = w_{ij}$. However,

$$\begin{aligned} w_{i+1/2,j}^+ &= w(x_{i+1/2}^+, \xi_j^+) = \alpha_T w(x_{i+1/2}^-, \xi_j^-) + \alpha_R w(x_{i+1/2}^+, -\xi_j^+) \\ &= \alpha_T w_i(\xi_j^-) + \alpha_R w_{i+1,-j}. \end{aligned}$$

while ξ^- is obtained from (10.2) with $\xi_j^+ = \xi_j$. Since ξ^- may not be a grid point, one has to define it approximately. A simple approach is to locate the two cell centers that bound it, then use a linear interpolation to evaluate the needed numerical flux at ξ_j^- . The case of $\xi_j < 0$ is treated similarly. The detailed algorithm to generate the numerical flux is given (Jin and Wen 2005) (Jin and Wen 2006a).

This numerical scheme overcomes the aforementioned analytic and numerical difficulties. In particular, it possesses the following properties:

- (i) It produces the correct physical solution crossing the interface (as defined in the previous subsection). In particular, in the case of geometric optics, this solution is consistent to Snell-Descartes' Law of Refraction at the interface.
- (ii) It allows a *hyperbolic* CFL condition $\Delta t = \mathcal{O}(\Delta x, \Delta \xi)$.

The idea outlined above, has its origin in so-called *well-balanced kinetic schemes* for shallow water equations with bottom topography, cf (Perthame and Simeoni 2001). It has been applied to compute the semiclassical limit of the linear Schrödinger equation with potential barriers in (Jin and Wen 2005) and the geometrical optics limit with complete transmission/reflection in (Jin and Wen 2006b), for thick interfaces, and (Jin and Wen 2006a), for sharp interfaces. Positivity, and both l^1 and l^∞ stabilities were also established, under a hyperbolic CFL condition. For piecewise constant Hamiltonians, an l^1 -error estimate of the first order finite difference of this type was established in (Wen 2009), following (Wen and Jin 2009).

Remark 10.2. Let us remark that this approach has also been extended to high frequency elastic waves (Jin and Liao 2006), and high frequency waves in random media with diffusive interfaces (Jin et al. 2008*a*). When the initial data are measure-valued, such as (3.9), the level set method introduced in (Jin et al. 2005*b*) becomes difficult for interfaces where waves undergo *partial* transmissions and reflections, since one needs to increase the number of level set functions each time a wave hits the interface. A novel method to get around this problem has been introduced in (Wei, Jin, Tsai and Yang 2010). It involves two main ingredients:

- (i) The solutions involving partial transmissions and partial reflections are decomposed into a finite sum of solutions, obtained by solving problems involving only *complete transmissions* or *complete reflections*. For the latter class of problems, the method of (Jin et al. 2005*b*) applies.
- (ii) Consequently, a re-initialization technique is introduced such that waves coming from multiple transmissions and reflections can be combined seamlessly as new initial value problems. This is implemented by rewriting the sum of several delta functions as one delta measure with a suitable weight, which can be easily implemented numerically.

10.3. Semiclassical computation of quantum barriers

A correct modeling of electron transport in nano-structures, such as resonant tunneling diodes, superlattices or quantum dots, requires the treatment of quantum phenomena in highly localized regions within the devices (so-called *quantum wells*), while the rest of the device can be dealt with by classical mechanics. However, solving the Schrödinger equation in the entire physical domain is usually too expensive, and thus, it is attractive to use a *multi-scale approach* as given in (Ben Abdallah, Degond and Gamba 2002). That is, solving the quantum mechanics only in the quantum well, and couple the solution to classical mechanics outside the well. To this, end, the following semiclassical approach for thin quantum barriers was proposed in (Jin and Novak 2006):

Step 1. Solve the time-independent Schrödinger equation (either analytically, or numerically) for the local barrier-well to determine the scattering data, i.e. the transmission and reflection coefficients α_T, α_R .

Step 2. Solve the classical Liouville equation elsewhere, using the scattering data generated in Step 1 and the the interface condition (10.1) given above.

The results for $d = 1$ and $d = 2$ given in (Jin and Novak 2006) (Jin and Novak 2007) demonstrate the validity of this approach whenever the well is

either *very thin* (i.e. of the order of only a few ε 's) or *well-separated*. In higher dimension, the interface condition (10.1) needs to be implemented in the direction normal to interface, and the interface condition may be *nonlocal* for diffusive transmissions or reflections (Jin and Novak 2007). This method correctly captures both, the transmitted and the reflected quantum waves and the results agree (in the sense of weak convergence) with the solution obtained by directly solving the Schrödinger equation with small ε . Since one obtains the quantum scattering information only in a preprocessing step (i.e. Step 1), the rest of the computation (Step 2) is classical, and thus the overall computational cost is the same as for computing classical mechanics. Nevertheless, purely quantum mechanical effects, such as tunneling can be captured.

If the interference needs to be accounted for, then such Liouville based approaches are not appropriate. One attempt was made in (Jin and Novak 2010) for one-dimensional problems, where a *complex* Liouville equation is used together with interface condition using (*complex-valued*) *quantum scattering data* obtained from solving the stationary Schrödinger equation. Its extension to multi-dimensional problem remains to be done. A more general approach could use the Gaussian beam methods, which do capture the phase information. This is an interesting line of research yet to be pursued.

11. Schrödinger equations with matrix-valued potentials and surface hopping

Closely related problems to those mentioned in the Section 10 arise in the study of semiclassical Schrödinger equations with *matrix-valued potentials*. This type of potentials can be seen as a caricature of the full many-body quantum dynamics of molecular dynamics. Using the celebrated *Born-Oppenheimer approximation* to decouple the dynamics of the electrons from the one for the much heavier nuclei, see, e.g., (Spohn and Teufel 2001), one finds that the electrons are subject to external forces which can be modeled by system of Schrödinger equations for the nuclei along the electronic energy surfaces. The nucleonic Schrödinger system has matrix valued potentials, which will be treated in this section.

To this end, we consider the following typical situation. Namely, a time-dependent Schrödinger equation with $\mathbb{R}^{2 \times 2}$ -matrix valued potential, see, e.g., (Spohn and Teufel 2001), or (Teufel 2003):

$$i\varepsilon \partial_t u^\varepsilon = \left(-\frac{\varepsilon^2}{2} \Delta_x + V(x) \right) u^\varepsilon, \quad u^\varepsilon(0, x) = u_{\text{in}}^\varepsilon \in L^2(\mathbb{R}^2, \mathbb{C}^2), \quad (11.1)$$

for $(t, x) \in \mathbb{R}^+ \times \mathbb{R}^2$ and $\Delta_x = \text{diag}(\Delta_{x_1} + \Delta_{x_2}, \Delta_{x_1} + \Delta_{x_2})$. The unknown

$u^\varepsilon(t, x) \in \mathbb{C}^2$ and V is a *symmetric matrix* of the form

$$V(x) = \frac{1}{2} \operatorname{tr} V(x) + \begin{pmatrix} v_1(x) & v_2(x) \\ v_2(x) & -v_1(x) \end{pmatrix}, \quad (11.2)$$

with $v_1(x), v_2(x) \in \mathbb{R}$. The matrix V then has two eigenvalues

$$\lambda^{(\pm)}(x) = \operatorname{tr} V(x) \pm \sqrt{v_1(x)^2 + v_2(x)^2}.$$

Remark 11.1. In the born-Oppenheimer approximation, the dimensionless semiclassical parameter $\varepsilon > 0$ is given by $\varepsilon = \sqrt{\frac{m}{M}}$, where m and M are the masses of an electron and a nucleus respectively (Spohn and Teufel 2001). Then, all oscillations are roughly characterized by the frequency $1/\varepsilon$, which typically ranges between one hundred and one thousand.

11.1. Wigner matrices and the classical limit for matrix-valued potentials

In this section, we shall discuss the influence of matrix-valued potentials on the semiclassical limit of the Schrödinger equations (11.1). Introduce the *Wigner matrix* as defined in (Gérard et al. 1997):

$$W^\varepsilon[u^\varepsilon](x, \xi) = (2\pi)^{-2} \int_{\mathbb{R}^2} \psi^\varepsilon(x - \frac{\varepsilon}{2}\eta) \otimes \bar{\psi}^\varepsilon(x + \frac{\varepsilon}{2}\eta) e^{i\eta \cdot \xi} dy, \quad (x, \xi) \in \mathbb{R}_x^2 \times \mathbb{R}_\xi^2.$$

We also denote by W denote the corresponding (weak) limit

$$W^\varepsilon[u^\varepsilon] \xrightarrow{\varepsilon \rightarrow 0} W \in L^\infty(\mathbb{R}; \mathcal{M}^+(\mathbb{R}_x^2 \times \mathbb{R}_\xi^2; \mathbb{R}^2)).$$

In order to describe the the dynamics of the limiting matrix-valued measure $W(t, x, \xi)$, first note that the complex 2×2 matrix-valued symbol of (11.1) is given by

$$P(x, \xi) = \frac{i}{2} |\xi|^2 + iV(x).$$

The two eigenvalues of $-iP(x, \xi)$ are

$$\lambda_{1,2}(x, \xi) = \frac{|\xi|^2}{2} + \operatorname{tr} V(x) \pm \sqrt{v_1(x)^2 + v_2(x)^2} = \frac{|\xi|^2}{2} + \lambda^\pm(x).$$

These eigenvalues λ_n , $n = 1, 2$, govern the time-evolution of the limiting measure $W(t)$, as proved in (Gérard et al. 1997). They act as the correct classical Hamiltonian function on phase space, corresponding to the two energy levels, respectively. In the following, we shall say that two energy levels *cross at a point* $x_* \in \mathbb{R}^2$ if $\lambda^+(x_*) = \lambda^-(x_*)$. Such a crossing is called *conical* if the vectors $\nabla_x v_1(x_*)$ and $\nabla_x v_2(x_*)$ are linearly independent. If all the crossings are conical, the crossing set

$$S = \{x \in \mathbb{R}^2 | \lambda^+(x) = \lambda^-(x)\}$$

is a sub-manifold of *co-dimension two* in \mathbb{R}^2 , cf. (Hagedorn 1994). Assume that the Hamiltonian flows with Hamiltonians λ_n leave invariant the set

$$\Omega = (\mathbb{R}_x^2 \times \mathbb{R}_\xi^2) \setminus S.$$

For $(x, \xi) \in \Omega$, denote by $\chi_n(x, \xi)$ the column eigenvector corresponding to the eigenvalue $\lambda_n(x, \xi)$ and the matrix

$$\Pi_n(x, \xi) = \chi_n(x, \xi)(\chi_n(x, \xi))^\top$$

is the orthogonal projection onto the eigenspace associated to $\lambda_n(x, \xi)$.

By Theorem 6.1 of (Gérard et al. 1997), the matrix-valued Wigner measure $W(t)$ commutes with the projectors Π_n , outside the crossing set S , and thus can be decomposed as

$$W(t, \cdot) = \Pi_1 W(t, \cdot) \Pi_1 + \Pi_2 W(t, \cdot) \Pi_2.$$

Since the eigen-spaces are both one-dimensional, the decomposition is simplified to be

$$W(t, \cdot) = W_1(t, \cdot) \Pi_1 + W_2(t, \cdot) \Pi_2.$$

The scalar functions $W_n(t, x, \xi)$ given by

$$W_n(t, x, \xi) = \text{tr}(\Pi_n W(t, x, \xi)),$$

are then found to satisfy the following Liouville equations

$$\partial_t W_n + \nabla_\xi \lambda_n \cdot \nabla_x W_n - \nabla_x \lambda_n \cdot \nabla_\xi W_n = 0, \quad (t, x, \xi) \in \mathbb{R}^+ \times \Omega, \quad (11.3)$$

subject to initial data

$$W_n(0) = \text{tr}(\Pi_n W), \quad (x, \xi) \in \Omega. \quad (11.4)$$

The scalar functions W_n , $n = 1, 2$, are the phase space probability densities corresponding to the upper and lower energy levels, respectively. One can recover from them the particle densities ρ_n via

$$\rho_n(t, x) = \int_{\mathbb{R}_\xi^2} W_n(t, x, \xi) \, d\xi, \quad n = 1, 2. \quad (11.5)$$

In other words, the Liouville equations (11.3) yields the propagation of the Wigner measures $W_1(t, \cdot)$ and $W_2(t, \cdot)$ on any given time interval, provided that their support do not intersect the eigenvalue crossing set S .

However, analytical and computational challenge arise when their support intersects the set S . In S the dynamics of W_1, W_2 are coupled due to the *non-adiabatic transitions* between the two energy levels and an additional *hopping condition* is needed (analogous to the interface condition considered in Section 10 above).

The Landau-Zener formula

In (Lasser, Swart and Teufel 2007), a heuristic derivation of the non-adiabatic transition probability is given. The derivation is based on the Hamiltonian system corresponding to the Liouville equations (11.3), i.e.

$$\begin{cases} \dot{x}_n(t) = \nabla_{\xi} \lambda_n(t) = \xi_n(t), \\ \dot{\xi}_n(t) = -\nabla_x \lambda_n(t), \quad n = 1, 2. \end{cases} \quad (11.6)$$

The basic idea is to insert the trajectories $(x(t), \xi(t))$ of the Hamiltonian systems (11.6) into the trace-free part of the potential matrix (11.2) to obtain a system of ordinary differential equations, given by

$$i\varepsilon \frac{d}{dt} u^\varepsilon(t) = \begin{pmatrix} v_1(x(t)) & v_2(x(t)) \\ v_2(x(t)) & -v_1(x(t)) \end{pmatrix} u^\varepsilon(t).$$

The non-adiabatic transitions happen in the region where the spectral gap between the eigenvalues becomes minimal. The function

$$h(x(t)) = |\lambda^+(x(t)) - \lambda^-(x(t))| = 2|\vartheta(x(t))|$$

measures the gap between the eigenvalues in phase space along the classical trajectory $(x(t), \xi(t))$, where $\vartheta(x) = (v_1(x), v_2(x))$ and $|\cdot|$ denotes the Euclidean norm. The necessary condition for a trajectory to attain the minimal gap is given by,

$$\frac{d}{dt} |\vartheta(x(t))|^2 = \vartheta(x(t)) \cdot \nabla_x \vartheta(x(t)) \xi(t) = 0,$$

where $\nabla_x \vartheta(x(t))$ is the Jacobian matrix of the vector $\vartheta(x(t))$, and $\xi(t) = \dot{x}(t)$. Hence, a crossing manifold in phase space containing these points is given by

$$S^* = \{(x, \xi) \in \mathbb{R}_x^2 \times \mathbb{R}_\xi^2 : \vartheta(x(t)) \cdot \nabla_x \vartheta(x(t)) \xi(t) = 0\}.$$

The transition probability when one particle hits S^* is assumed to be given by

$$T^\varepsilon(x_0, \xi_0) = \exp\left(-\frac{\pi}{\varepsilon} \frac{(\vartheta(x_0) \wedge \nabla_x \vartheta(x_0) \cdot \xi_0)^2}{|\nabla_x \vartheta(x_0) \cdot \xi_0|^3}\right), \quad (11.7)$$

which is the famous *Landau-Zener formula* (Landau 1932) (Zener 1932). Note that T decays exponentially in x and ξ and

$$\lim_{\varepsilon \rightarrow 0} T^\varepsilon = T_0 = \begin{cases} 1, & (x, \xi) \in S^*, \\ 0, & (x, \xi) \notin S^*, \end{cases}$$

In other words, as $\varepsilon \rightarrow 0$, the transition between the energy bands only occurs on the set S^* , which is consistent with the result in the previous subsections.

11.2. Numerical approaches

Lagrangian surface hopping

One of the widely used numerical approaches to simulate the non-adiabatic dynamics at energy-crossings, is the surface hopping method, first proposed by (Tully and Preston 1971), and further developed in (Tully 1990) and (Sholla and Tully 1998). The basic idea is to combine the classical transports of the system on the individual potential energy surfaces $\lambda^\pm(x)$ that follow (11.6) with an instantaneous transitions at S^* from one energy surface to another. The rate of transition is determined by the Landau-Zener formula (11.7) whenever available, or computed by some quantum mechanical simulation locally around S^* . The hoppings were performed in a Monte-Carlo procedure based on the transition rates. For a review of surface hopping methods see (Drukker 1999).

More recently, surface hopping methods have generated increasing interests in the mathematical community. For molecular dynamical simulations, (Horenko, Salzmann, Schmidt and Schütte 2002) adopted the partial Wigner transform to reduce a full quantum dynamics into the quantum-classical Liouville equation, and then the surface hopping is realized by approximating the quantum Liouville equation using phase space Gaussian wave packets. From the analytical point of view (Lasser and Teufel 2005) and (Fermanian Kammerer and Lasser 2003) analyzed the propagation through conical surface crossings using matrix-valued Wigner measures and proposed a corresponding rigorous surface hopping method based on the semiclassical limit of the time-dependent Born-Oppenheimer approximation. They used a particle method to solve the Liouville equation in (Lasser et al. 2007), (Kube, Lasser and Weber 2009) in which each classical trajectory was subject to a deterministic branching (rather than the Monte-Carlo) process. Branching occurs whenever a trajectory attains one of its local minimal gaps between the eigenvalue surfaces. The new branches are consequently re-weighted according to the Landau-Zener formula for conical crossings

These Lagrangian surface hopping methods are very simple to implement, and in particular, very efficient in high space dimension. However, they require either many statistical samples in a Monte-Carlo framework, or the increase of particle numbers whenever hopping occurs. In addition, as it is typical for Lagrangian methods, a complicated numerical re-interpolation procedure is needed whenever the particle trajectories diverge, in order to maintain uniform accuracy in-time.

Eulerian surface hopping

The Eulerian framework introduced in (Jin, Qi and Zhang n.d.) consists of solving the two Liouville equations (11.3), with a hopping condition that *numerically incorporates the Landau-Zener formula* (11.7). Note that the

Schrödinger equation (11.1) implies conservation of the total mass, which in the semiclassical limit $\varepsilon \rightarrow 0$, locally away from S^* , yields

$$\frac{d}{dt} \int (W_1 + W_2)(t, x, \xi) \, d\xi \, dx = 0. \quad (11.8)$$

For this condition to hold for all x, ξ , the total flux in direction normal to S^* needs to be continuous across S^* . To ensure this, the Landau-Zener transition at S^* should be formulated as a continuity condition for the total flux in the normal direction e_n : Define the flux-function $j_n(x, \xi) \in \mathbb{R}^2$ for each eigenvalue surface via

$$j_n(x, \xi) = (\nabla_\xi \lambda_n, -\nabla_x \lambda_n) W_n(x, \xi), \quad n = 1, 2.$$

Assume, before hopping, that the particle remains on one of the eigenvalue surfaces, i.e.

- (i) $j_1(x_0^-, \xi_0^-) \neq 0$ and $j_2(x_0^-, \xi_0^-) = 0$, or
- (ii) $j_1(x_0^-, \xi_0^-) = 0$ and $j_2(x_0^-, \xi_0^-) \neq 0$.

Then the interface condition is given by

$$\begin{pmatrix} j_1(x_0^+, \xi_0^+) \cdot e_n \\ j_2(x_0^+, \xi_0^+) \cdot e_n \end{pmatrix} = \begin{pmatrix} 1 - T(x_0, \xi_0) & T(x_0, \xi_0) \\ T(x_0, \xi_0) & 1 - T(x_0, \xi_0) \end{pmatrix} \begin{pmatrix} j_1(x_0^-, \xi_0^-) \cdot e_n \\ j_2(x_0^-, \xi_0^-) \cdot e_n \end{pmatrix}$$

where (x^\pm, ξ^\pm) are the (pre- and post-hopping) limits to $(x_0, \xi_0) \in S^*$ along the direction e_n .

Remark 11.2. There is a restriction of this approach based on Liouville equation and the Landau-Zener transition probability. The interference effects generated when two particles from different energy level arrive at S^* at the same time are thereby not accounted, thus important quantum phenomena, such as Berry phase, are missing. One would expect that a Gaussian beam methods could handle this problem, but this remains to be explored.

12. Schrödinger equations with periodic potential

So far we have only considered ε -independent potential $V(x)$. The situation changes drastically if one allows for potentials varying on the fast scale $y = x/\varepsilon$. An important example concerns the case of *highly oscillatory potentials* $V_\Gamma(x/\varepsilon)$, which are *periodic* with respect to a periodic lattice $\Gamma \subset \mathbb{R}^d$. In the following we shall therefore consider Schrödinger equations of the form

$$i\varepsilon \partial_t u^\varepsilon = -\frac{\varepsilon^2}{2} \Delta u^\varepsilon + V_\Gamma\left(\frac{x}{\varepsilon}\right) u^\varepsilon + V(x) u^\varepsilon; \quad u^\varepsilon(0, x) = u_{\text{in}}^\varepsilon(x). \quad (12.1)$$

Here $V \in C^\infty$ denotes some smooth, slowly varying potential and V_Γ a rapidly oscillating potential (not necessarily smooth). For definiteness we shall assume that for some orthonormal basis $\{e_j\}_{j=1}^d$, V_Γ satisfies

$$V_\Gamma(y + 2\pi e_j) = V_\Gamma(y) \quad \forall y \in \mathbb{R}^d, \quad (12.2)$$

i.e. $\Gamma = (2\pi\mathbb{Z})^d$.

Remark 12.1. Equations of the form arise in solid state physics where they are used to describe the motion of electrons under the action of an external field and a periodic potential generated by the ionic cores. This problem has been extensively studied from a physical, as well as from a mathematical point of view, see e.g. (Ashcroft and Mermin 1976), (Bensoussan, Lions and Papanicolaou 1978), (Teufel 2003) and the references given therein. One of the most striking dynamical effect due to the inclusion of a periodic potential V_Γ , is the occurrence of so-called *Bloch oscillations*. These are oscillations exhibited by electrons moving in a crystal lattice under the influence of a constant electric field $V(x) = F \cdot x$, $F \in \mathbb{R}^d$ (see Section 12.2 below).

12.1. Emergence of Bloch bands

In order to better understand the influence of V_Γ , we recall here the basic spectral theory for periodic Schrödinger operators of the form, c.f. (Reed and Simon 1976):

$$H_{\text{per}} = -\frac{1}{2}\Delta_y + V_\Gamma(y).$$

With V_Γ obeying (12.2) we have:

- (i) The fundamental domain of the lattice $\Gamma = (2\pi\mathbb{Z})^d$ is the interval $Y = [0, 2\pi]^d$.
- (ii) The *dual lattice* Γ^* can then be defined as the set of all wave numbers $k \in \mathbb{R}$, for which plane waves of the form $e^{ik \cdot x}$ have the same periodicity as the potential V_Γ . This yields $\Gamma^* = \mathbb{Z}^d$ in our case.
- (iii) The fundamental domain of the dual lattice, i.e. the (first) *Brillouin zone*, Y^* is the set of all $k \in \mathbb{R}$ closer to zero than to any other dual lattice point. In our case $Y^* = [-\frac{1}{2}, \frac{1}{2}]^d$, equipped with periodic boundary conditions, i.e. $Y^* \simeq \mathbb{T}^d$.

By periodicity, it is sufficient to consider the operator H_{per} on the fundamental domain Y only, where we impose the following quasi-periodic boundary conditions:

$$f(y + 2\pi e_j) = e^{2ik_j\pi} f(y) \quad \forall y \in \mathbb{R}, \quad k \in Y^*. \quad (12.3)$$

It is well known (Wilcox 1978) that under mild conditions on V_Γ , the operator H admits a complete set of eigenfunction $\{\psi_m(y, k)\}_{m \in \mathbb{N}}$, parametrized by $k \in Y^*$. These eigenfunctions provide, for each fixed $k \in Y^*$, an orthonormal basis in $L^2(Y)$. Correspondingly there exists a countable family of real eigenvalues $\{E(k)\}_{m \in \mathbb{N}}$, which can be ordered as

$$E_1(k) \leq E_2(k) \leq \dots \leq E_m(k) \leq \dots,$$

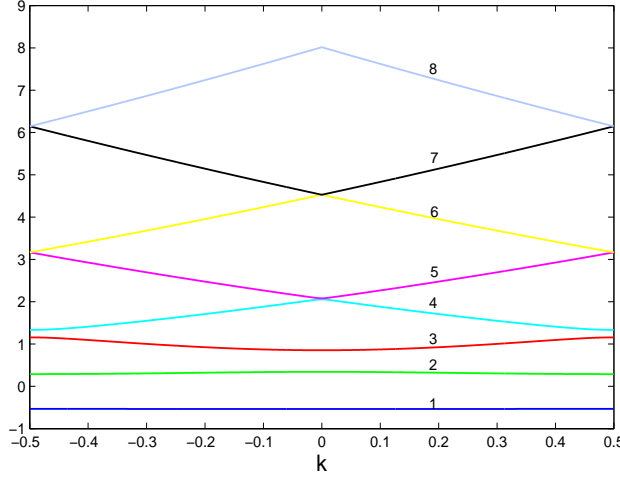


Figure 12.7. The eigenvalues $E_m(k)$, $m = 1, \dots, 8$ for Mathieu's model: $V_\Gamma = \cos y$.

where the respective multiplicities are accounted for in the ordering. The set $\{E_m(k) \mid k \in Y\} \subset \mathbb{R}$ is called the m -th *energy band* of the operator H_{per} . Concerning the dependence on $k \in Y^*$, it has been shown (Wilcox 1978) that for any $m \in \mathbb{N}$ there exists a closed subset $X \subset Y^*$ such that: $E_m(k)$ is analytic and $\psi_m(\cdot, k)$ can be chosen to be a real analytic function for all $k \in Y^* \setminus X$. Moreover

$$E_{m-1} < E_m(k) < E_{m+1}(k) \quad \forall k \in Y^* \setminus X.$$

If this condition indeed holds for all $k \in Y^*$ then $E_m(k)$ is called an *isolated Bloch band*. Moreover, it is known that

$$\text{meas } X = \text{meas} \{k \in Y^* \mid E_n(k) = E_m(k), n \neq m\} = 0. \quad (12.4)$$

This set of Lebesgue measure zero consists of the so called *band crossings*. See Fig. `evaluateexam1` for an example of bands for Mathieu's model with potential $V_\Gamma = \cos y$.

Note that due to (12.3) one can rewrite $\psi_m(y, k)$ as

$$\psi_m(y, k) = e^{ik \cdot y} \chi_m(y, k) \quad \forall m \in \mathbb{N}, \quad (12.5)$$

for some 2π -periodic function $\chi_m(\cdot, k)$, usually called *Bloch functions*. In terms of $\chi_m(y, k)$ the spectral problem for H_{per} becomes (Bloch 1928):

$$\begin{cases} H(k)\chi_m(y, k) = E_m(k)\chi_m(y, k), \\ \chi_m(y + 2\pi e_j, k) = \chi_m(y, k) \quad \forall k \in Y^*, \end{cases} \quad (12.6)$$

where $H(k)$ denotes the shifted Hamiltonian

$$H(k) := e^{-ik \cdot y} H_{\text{per}} e^{ik \cdot y} = \frac{1}{2}(-i\nabla_y + k)^2 + V_\Gamma(y). \quad (12.7)$$

Most importantly, the spectral data obtained from (12.6) allow us to decompose the original Hilbert space $L^2(\mathbb{R}^d)$ into a direct sum of the so-called, *band spaces*: $L^2(\mathbb{R}^d) = \bigoplus_{m=1}^{\infty} \mathcal{H}_m$. This is the well-known *Bloch decomposition method*, which implies that

$$\forall f \in L^2(\mathbb{R}^d): \quad f = \sum_{m \in \mathbb{N}} f_m, \quad f_m \in \mathcal{H}_m. \quad (12.8)$$

The corresponding projection of $f \in L^2(\mathbb{R}^d)$ onto the m -th band space \mathcal{H}_m is thereby given via (Reed and Simon 1976)

$$f_m(y) = \int_{Y^*} \left(\int_{\mathbb{R}^d} f(\zeta) \bar{\psi}_m(\zeta, k) d\zeta \right) \psi_m(y, k) dk. \quad (12.9)$$

In the following, we shall also denote

$$C_m(k) := \int_{\mathbb{R}^d} f(\zeta) \bar{\psi}_m(\zeta, k) d\zeta. \quad (12.10)$$

the coefficient of the Bloch decomposition.

12.2. Two-scale WKB approximation

Equipped with the basic theory of Bloch bands, we recall here an extension of the WKB method presented in Section 2.2 to the case of highly oscillatory periodic potentials. Indeed it has been shown in (Bensoussan et al. 1978) (Guillot, Ralston and Trubowitz 1988) that solutions to (12.1) can be approximated (at least locally in-time) by

$$u^\varepsilon(t, x) \stackrel{\varepsilon \rightarrow 0}{\sim} a(t, x) \chi_m \left(\frac{x}{\varepsilon}, \nabla S \right) e^{iS(t, x)/\varepsilon} + \mathcal{O}(\varepsilon), \quad (12.11)$$

where χ_m is parametrized via $k = \nabla S(t, x)$. The phase function S thereby solves the *semiclassical Hamilton-Jacobi equation*

$$\partial_t S + E_m(\nabla S) + V(x) = 0; \quad S(0, x) = S_{\text{in}}(x). \quad (12.12)$$

The corresponding semiclassical flow $X_t^{\text{sc}} : y \mapsto x(t, y)$ is given by

$$\begin{cases} \dot{x}(t, y) = \nabla_k E_m(k(t, y)); & x(0, y) = y, \\ \dot{k}(t, y) = -\nabla_x V(x(t, y)); & k(0, y) = \nabla S_{\text{in}}(y). \end{cases} \quad (12.13)$$

The wave vector $k \in Y^*$ is usually called *crystal momentum*. In the case of a constant electric field $V = F \cdot x$, the second equation in (12.13) yields

$$k(t, y) = k - tF, \quad k = \nabla S_{\text{in}}(y).$$

Note that since $k \in Y^* \simeq \mathbb{T}^d$, this yields a periodic motion in-time of $x(t, y)$, the so-called Bloch oscillations.

In addition, the leading order amplitude in (12.11) is found to be the solution of the semiclassical transport equation (Carles, Markowich and Sparber 2004):

$$\partial_t a + \nabla_k E_m(\nabla S) \cdot \nabla a + \frac{1}{2} \operatorname{div}_x(\nabla_k E_m(\nabla_x \phi_m)) a_m = (\beta_m \cdot \nabla_x V(x)) a_m, \quad (12.14)$$

where

$$\beta_m(t, x) := \langle \chi_m(y, \nabla S), \nabla_k \chi_m(y, \nabla S) \rangle_{L^2(Y)}, \quad (12.15)$$

denotes the the so-called *Berry phase term* (cf. (Carles et al. 2004), (Panati, Spohn and Teufel 2006)), which is found to be purely imaginary $\beta_m(t, x) \in (i\mathbb{R})^d$. It is importantly related to the Quantum Hall effect (Sundaram and Niu 1999). The amplitude a therefore is necessarily complex-valued and exhibits a non-trivial phase modulation induced by the geometry of V_Γ , see also (Shapere and Wilczek 1989) for more details. Note that (12.14) yields the following conservation law for $\rho = |a|^2$,

$$\partial_t \rho + \operatorname{div}(\rho \nabla_k E_m(\nabla S)) = 0.$$

The outlined two-scale WKB approximation again faces the problem of caustics. Furthermore there is an additional problem of possible band-crossings at which $\nabla_k E_m$ is no longer defined. The right hand side of (12.11) can therefore only be regarded a valid approximation for (possibly very) short times only. Nevertheless it shows the influence of the periodic potential which can be seen to introduce additional high frequency oscillations (Γ -periodic) within u^ε .

Remark 12.2. These types of techniques have also been successfully applied in weakly nonlinear situations (Carles et al. 2004).

12.3. Wigner measures in the periodic case

The theory of Wigner measures discussed in Section 3 can be extended to the case of highly oscillatory potentials. The theory of the so-called Wigner band-series has been developed in (Markowich, Mauser and Poupaud 1994), (Gérard et al. 1997). The basic idea is to use Bloch's decomposition and replace the continuous momentum variable $\xi \in \mathbb{R}^d$ by the crystal momentum $k \in Y^*$.

A more general approach, based on space adiabatic perturbation theory (Teufel 2003), yields in the limit $\varepsilon \rightarrow 0$ a *semiclassical Liouville equation* of the form

$$\partial_t w + \{H_m^{\text{sc}}, w\} = 0; \quad w(0, x, k) = w_{\text{in}}(x, k), \quad (12.16)$$

where $w(t, x, k)$ is the m -th band Wigner measure on the Γ -periodic phase space $\mathbb{R}_x^d \times Y^*$, $\{\cdot, \cdot\}$ denotes the corresponding Poisson-bracket, and

$$H_m^{\text{sc}} = E_m(k) + V(x), \quad (12.17)$$

the m -th band semiclassical Hamiltonian.

13. Numerical methods for the Schrödinger equation with periodic potentials

13.1. Bloch decomposition based time-splitting method

The introduction of a highly oscillatory potential $V_\Gamma\left(\frac{x}{\varepsilon}\right)$ poses numerical challenges in the numerical computation of semiclassical Schrödinger equations. It has been observed in (Gosse 2006) and (Gosse and Markowich 2004) that conventional split step algorithms do not perform well. More precisely, in order to guarantee convergence of the scheme, time steps of order $\mathcal{O}(\varepsilon)$ are required. In order to overcome this problem, a new time-splitting algorithm based on Bloch's decomposition method has been proposed (Huang, Jin, Markowich and Sparber 2007) and further developed in (Huang, Jin, Markowich and Sparber 2008) and (Huang, Jin, Markowich and Sparber 2009). The basic idea is as follows:

Step 1. For $t \in [t_n, t_{n+1}]$ one first solves

$$i\varepsilon\partial_t u^\varepsilon = -\frac{\varepsilon^2}{2} \Delta u^\varepsilon + V_\Gamma\left(\frac{x}{\varepsilon}\right) u^\varepsilon, \quad (13.1)$$

The main point is that, by using the Bloch decomposition method, Step 1 can be solved *exactly*, i.e. only up to numerical errors. In fact, in each band space \mathcal{H}_m , equation (13.1) is equivalent to

$$i\varepsilon\partial_t u_m^\varepsilon = E_m(-i\nabla)u_m^\varepsilon, \quad u_m^\varepsilon \in \mathcal{H}_m, \quad (13.2)$$

where $u_m^\varepsilon \equiv \mathbb{P}_m^\varepsilon u^\varepsilon$ is the (appropriately ε -scaled) projection of $u^\varepsilon \in L^2(\mathbb{R}^d)$ onto \mathcal{H}_m defined in (12.9) and $E_m(-i\nabla)$ is the Fourier-multiplier corresponding to the symbol $E_m(k)$. Using the standard Fourier transformation, equation (13.2) is easily solved by

$$u_m^\varepsilon(t, x) = \mathcal{F}^{-1} \left(e^{iE_m(k)t/\varepsilon} (\mathcal{F}u_m)(0, k) \right), \quad (13.3)$$

where \mathcal{F}^{-1} is the inverse Fourier Transform. In other words, one can solve (13.1) by decomposing u^ε into a sum of band-space functions u_m^ε , each of which is propagated in time via (13.3). After resummation this yields $u^\varepsilon(t_{n+1}, x)$. Once this is done, one proceeds as usual in order to take into account $V(x)$.

Step 2. On the same time interval as before, we solve the ODE

$$i\varepsilon\partial_t u^\varepsilon = V(x)u^\varepsilon, \quad (13.4)$$

where the solution obtained in Step 1 serves as initial condition for Step 2.

In this algorithm, the dominant effects from the dispersion and the periodic lattice potential are computed one step. It thereby maintains their strong interaction and treats the non-periodic potential as a perturbation. Because the split-step error between the periodic and non-periodic parts is relatively small, the time-steps can be chosen *considerably larger* than a conventional time-splitting algorithm (see below). As in a conventional splitting method (cf. Section 5), the numerical scheme conserves the particle density $\rho^\varepsilon = |u^\varepsilon|^2$ on the fully discrete level. More importantly, if $V(x) = 0$, i.e. no external potential, the algorithm preserves the particle density (and hence the mass) in each *individual band space* \mathcal{H}_m .

Remark 13.1. Clearly, the algorithm given above is only first order in time, but this can easily be improved by using the Strang splitting method, cf. Section 5. In this case, the method is unconditionally stable and comprises spectral convergence for the space discretization as well as second order convergence in time.

Numerical calculation of Bloch bands

In the numerical implementation of this algorithm a necessary prerequisite is the computation of Bloch bands $E_m(k)$ and Bloch eigenfunction $\chi_m(y, k)$. This requires to numerically solve the eigenvalue problem (12.6). In one spatial dimension $d = 1$ we proceed as in (Gosse and Markowich 2004), by expanding $V_\Gamma \in C^1(\mathbb{R})$ in its Fourier series

$$V_\Gamma(y) = \sum_{\lambda \in \mathbb{Z}} \widehat{V}(\lambda) e^{i\lambda y}, \quad \widehat{V}(\lambda) = \frac{1}{2\pi} \int_0^{2\pi} V_\Gamma(y) e^{-i\lambda y} dy.$$

Clearly, if $V_\Gamma \in C^\infty(\mathbb{R})$ the corresponding Fourier coefficients $\widehat{V}(\lambda)$ decay faster than any power, as $\lambda \rightarrow \pm\infty$, and which case, we only need to take into account a few coefficients to achieve sufficient accuracy. Likewise, expand the Bloch eigenfunction $\chi_m(\cdot, k)$, in its respective Fourier series

$$\chi_m(y, k) = \sum_{\lambda \in \mathbb{Z}} \widehat{\chi}_m(\lambda, k) e^{i\lambda y}.$$

For $\lambda \in \{-\Lambda, \dots, \Lambda - 1\} \subset \mathbb{Z}$, one consequently approximates the spectral problem (12.6), by the following algebraic eigenvalue problem

$$\mathcal{H}(k) \begin{pmatrix} \widehat{\chi}_m(-\Lambda) \\ \widehat{\chi}_m(1-\Lambda) \\ \vdots \\ \widehat{\chi}_m(\Lambda-1) \end{pmatrix} = E_m(k) \begin{pmatrix} \widehat{\chi}_m(-\Lambda) \\ \widehat{\chi}_m(1-\Lambda) \\ \vdots \\ \widehat{\chi}_m(\Lambda-1) \end{pmatrix} \quad (13.5)$$

where the $2\Lambda \times 2\Lambda$ matrix $\mathcal{H}(k)$ is given by

$$\mathcal{H}(k) = \begin{pmatrix} \widehat{V}(0) + \frac{1}{2}(k-\Lambda)^2 & \widehat{V}(-1) & \dots & \widehat{V}(1-2\Lambda) \\ \widehat{V}(1) & \widehat{V}(0) + \frac{1}{2}(k-\Lambda+1)^2 & \dots & \widehat{V}(2-2\Lambda) \\ \vdots & \vdots & \ddots & \vdots \\ \widehat{V}(2\Lambda-1) & \widehat{V}(2\Lambda-2) & \dots & \widehat{V}(0) + \frac{1}{2}(k+\Lambda-1)^2 \end{pmatrix}.$$

The matrix $\mathcal{H}(k)$ has 2Λ eigenvalues. Clearly, this number has to be large enough to have sufficiently many eigenvalues $E_m(k)$ for the simulation, i.e. we require $m \leq 2\Lambda$. Note however, that the number Λ is *independent* of the spatial grid (in particular independent of ε), thus the numerical costs of this eigenvalue problem are often negligible compared to those of the evolutionary algorithms (see below for more details).

In higher dimensions $d > 1$, computing the eigenvalue problem (12.6) along these lines becomes numerically too expensive to be feasible. In many physical application, however, the periodic potential splits into a sum of one-dimensional potentials, i.e.

$$V_\Gamma(y) = \sum_{j=1}^d V_\Gamma(y_j), \quad V_j(y_j + 2\pi) = V_j(y_j),$$

where $y = (y_1, y_2, \dots, y_d) \in \mathbb{R}^d$. In this case, Bloch's spectral problem can be treated separately (using a fractional step-splitting approach) for each coordinate $y_j \in \mathbb{R}$, as outlined before.

Remark 13.2. In practical applications, the accurate numerical computation of Bloch bands is a highly nontrivial task. Nowadays though, there already exists a huge amount of numerical data detailing the energy band structure of the most important materials used in, e.g., the design of semiconductor devices. In the context of photonic crystals the situation is similar. Thus, relying on such data one can in principle avoid the above given eigenvalue-computations and its generalizations to more dimensions completely. To this end, one should also note that, given the energy bands $E_m(k)$, we do not need any knowledge about V_Γ in order to solve (12.1) numerically. Also, we remark that it was shown in (Huang et al. 2009) that

the Bloch decomposition-based time splitting method is remarkably stable with respect to perturbations of the spectral data.

Implementation of the Bloch decomposition based time-splitting method

In the numerical implementation, we shall assume that V_Γ admits the decomposition (13.1). In this case we can solve (12.1) by using a fractional step method, treating each spatial direction separately, i.e. one only needs to study the one-dimensional equation

$$i\varepsilon\partial_t u^\varepsilon = -\frac{\varepsilon^2}{2}\partial_{xx}u^\varepsilon + V_j\left(\frac{x}{\varepsilon}\right)u^\varepsilon, \quad (13.6)$$

on the time-interval $[t_n, t_{n+1}]$. This equation will be considered on a one-dimensional computational domain $(a, b) \subset \mathbb{R}$, equipped with periodic boundary conditions (necessary in order to invoke Fast Fourier transforms). We suppose that there are $L \in \mathbb{N}$ lattice cells within (a, b) and numerically compute u^ε at $L \times R$ grid points, for some $R \in \mathbb{N}$. In other words we assume that there are R grid points in each lattice cell, which yields the following discretization

$$\begin{cases} k_\ell = -\frac{1}{2} + \frac{\ell-1}{L}, & \text{where } \ell = \{1, \dots, L\} \subset \mathbb{N}, \\ y_r = \frac{2\pi(r-1)}{R}, & \text{where } r = \{1, \dots, R\} \subset \mathbb{N}, \end{cases} \quad (13.7)$$

and thus, $u^n \equiv u(t_n)$ are evaluated at the grid points

$$x_{\ell,r} = \varepsilon(2\pi(\ell-1) + y_r). \quad (13.8)$$

Note that in numerical computations one can use $R \ll L$, whenever $\varepsilon \ll 1$, i.e. only a few grid points are needed within each cell.

Having in mind the basic idea of using Bloch's decomposition, one is facing the problem that the solution u^ε of (13.6) in general does not admit the same periodicity properties as φ_m . A direct decomposition of u^ε into this new basis of eigenfunctions is therefore not possible. This problem can be overcome by invoking the following unitary transformation for $f \in L^2(\mathbb{R})$:

$$f(y) \mapsto \tilde{f}(y, k) := \sum_{\gamma \in \mathbb{Z}} f(\varepsilon(y + 2\pi\gamma)) e^{-i2\pi k\gamma}, \quad y \in Y, \quad k \in Y^*,$$

with the properties

$$\tilde{f}(y + 2\pi, k) = e^{2i\pi k} \tilde{f}(y, k), \quad \tilde{f}(y, k + 1) = \tilde{f}(y, k).$$

In other words $\tilde{f}(y, k)$ admits the same periodicity properties w.r.t. k and y as the eigenfunction $\psi_m(y, k)$. In addition, the following inversion formula holds

$$f(\varepsilon(y + 2\pi\gamma)) = \int_{Y^*} \tilde{f}(y, k) e^{i2\pi k\gamma} dk. \quad (13.9)$$

Moreover, one easily sees that the Bloch coefficient, defined in (12.10), can be equivalently written as

$$C_m(k) = \int_Y \tilde{f}(y, k) \overline{\psi}_m(y, k) \, dy, \quad (13.10)$$

which, in view of (12.5), resembles a Fourier integral. In fact, all of these formulae can be easily implemented by using the Fast Fourier transform. The numerical algorithm needed to perform Step 1 outlined above is then as follows:

Step 1.1. First compute \tilde{u}^ε at time t^n by

$$\tilde{u}^\varepsilon(t_n, x_{\ell,r}, k_\ell) = \sum_{j=1}^L u^\varepsilon(t_n, x_{j,r}) e^{-i2\pi k_\ell \cdot (j-1)},$$

where $x_{\ell,r}$ is as in (13.8).

Step 1.2. Compute the coefficient $C_m^\varepsilon(t_n, k_\ell)$ via (13.10),

$$C_m^\varepsilon(t_n, k_\ell) \approx \frac{2\pi}{R} \sum_{r=1}^R \tilde{u}^\varepsilon(t_n, x_{\ell,r}, k_\ell) \overline{\chi}_m(y_r, k_\ell) e^{-ik_\ell y_r}.$$

Step 1.3. Evolve $C_m^\varepsilon(t_n, k)$ up to time t^{n+1} according to (13.2),

$$C_m^\varepsilon(t_{n+1}, k_\ell) = C_m^\varepsilon(t_n, k_\ell) e^{-iE_m(k_\ell)\Delta t/\varepsilon}.$$

Step 1.4. \tilde{u}^ε can be obtained at time t_{n+1} by summing over all band contributions

$$\tilde{u}^\varepsilon(t_{n+1}, x_{\ell,r}, k_\ell) = \sum_{m=1}^M C_m^\varepsilon(t_{n+1}, k_\ell) \chi_m(y_r, k_\ell) e^{ik_\ell y_r}.$$

Step 1.5. Perform the inverse transformation (13.9),

$$u^\varepsilon(t_{n+1}, x_{\ell,r}, k_\ell) \approx \frac{1}{L} \sum_{j=1}^L \tilde{u}^\varepsilon(t_{n+1}, x_{j,r}, k_j) e^{i2\pi k_j(\ell-1)}.$$

This concludes the numerical procedure performed in Step 1.

The Bloch decomposition based time-splitting method was found to be converging for $\Delta x = \mathcal{O}(\varepsilon)$ and $\Delta t = \mathcal{O}(1)$, see (Huang et al. 2007) for more details. In other words, the time-steps can be chose *independently of* ε , a huge advantage in comparison to the standard time-splitting method used in e.g. (Gosse 2006). Moreover, the numerical experiments done in (Huang et al. 2007) show that of only a few Bloch bands $E_m(k)$ are sufficient to achieve very high accuracy, even in cases where $V(x)$ is no longer smooth

(typically $m = 1, \dots, M$, with $M \approx 8$ is sufficient). Applications of this method are found in the simulation of lattice Bose-Einstein condensates (Huang et al. 2008) and of wave propagation in (disordered) crystals (Huang et al. 2009).

Remark 13.3. For completeness, we recall the numerical complexities for the algorithm outlined above, see (Huang et al. 2007): The complexities of Step 1.1 and 1.5 are $\mathcal{O}(RL \ln L)$, the complexities of Step 1.2 and 1.4 are $\mathcal{O}(MLR \ln R)$, and for Step 1.3 it is $\mathcal{O}(ML)$. The complexity of the eigenvalue problem (13.5) is $\mathcal{O}(\Lambda^3)$. However, since Λ (or R) is independent of ε and since (13.5) needs to be solved only once (as a preparatory step), the computational costs for this step are negligible. In addition, since M and R are independent of ε , one can choose $R \ll L$ and $M \ll L$, whenever $\varepsilon \ll 1$. Finally, one should notice that the complexities in each time step are comparable to the usual time-splitting method.

13.2. Moment closure in Bloch bands

It is straightforward to adapt the moment closure method presented in Section 6 to the case of periodic potentials. To this end, one considers the semiclassical Liouville equation (12.16), i.e.

$$\partial_t w + \nabla_k E_m(k) \cdot \nabla_x w - \nabla_x V(x) \cdot \nabla_k w = 0,$$

and close it with the following ansatz for the Wigner measure

$$w(t, x, k) = \sum_{j=1}^J |a_j(t, x)|^2 \delta_{\sharp}(k - v_j(t, x)),$$

where we denote by δ_{\sharp} the Γ^* -periodic delta distribution, i.e.

$$\delta_{\sharp} = \sum_{\gamma^* \in \Gamma^*} \delta(\cdot - \gamma^*).$$

By following this idea, (Gosse and Markowich 2004) showed the applicability of the moment closure method in the case of periodic potentials in $d = 1$ (see also (Gosse 2006)). In addition, self-consistent Schrödinger-Poisson systems were treated in (Gosse and Mauser 2006). As already mentioned before, extending this method to higher spatial dimensions $d > 1$ is numerical challenging.

13.3. Gaussian beams in Bloch bands

The Gaussian beam approximation, discussed in Sections 8 and 9, can also be extended to Schrödinger equation with periodic potentials. To this end, one adopts the Gaussian beam within each Bloch band of the Schrödinger

equation (12.1). In the following, we shall restrict ourselves to the case $d = 1$, for simplicity.

Lagrangian formulation

Similar to the two-scale WKB ansatz (12.11), we define

$$\varphi_m^\varepsilon(t, x, y_m) = A_m(t, y_m) \chi_m^* \left(\partial_x T_m, \frac{x}{\varepsilon} \right) e^{i T_m(t, x, y_m) / \varepsilon}, \quad (13.11)$$

where $y_m = y_m(t, y_0)$, and

$$T_m(t, x, y_m) = S_m(t, y_m) + p_m(t, y_m)(x - y_m) + \frac{1}{2} M_m(t, y_m)(x - y_m)^2.$$

Here $S_m \in \mathbb{R}$, $p_m \in \mathbb{R}$, $a_m \in \mathbb{C}$, $M_m \in \mathbb{C}$. In addition, we denote by χ_m^* the function obtained by evaluating the usual Bloch function $\chi_m(y, k)$ (with real-valued $k \in Y^*$) at the point $y = x/\varepsilon$ and $k = \partial_x T_m \in \mathbb{C}$. To this end, we impose the following condition:

$$\chi_m^*(y, z) = \chi_m(y, z) \quad \text{for } z \in \mathbb{R}.$$

One can derive a similar derivation of the Lagrangian formulation as in Section 8.1 that corresponds to the semiclassical Hamiltonian (12.17). For more details we refer to (Jin, Wu, Yang and Huang 2010b). Here we only mention, that in order to define the initial values for the Gaussian beams, one first decomposes the initial condition, which is assumed to be given in two-scale WKB form, i.e.

$$u_{\text{in}}^\varepsilon(x) = b_{\text{in}} \left(x, \frac{x}{\varepsilon} \right) e^{i S_{\text{in}}(x) / \varepsilon},$$

in terms of Bloch waves with the help of the stationary phase method, cf. (Bensoussan et al. 1978):

$$u_{\text{in}}^\varepsilon(x) \stackrel{\varepsilon \rightarrow 0}{\sim} \sum_{m=1}^{\infty} a_m^{\text{in}}(x) \chi_m \left(\frac{x}{\varepsilon}, \partial_x S_{\text{in}} \right) e^{i S_{\text{in}}(x) / \varepsilon} + \mathcal{O}(\varepsilon),$$

where the coefficient

$$a_m^{\text{in}}(x) = \int_Y b_{\text{in}}(x, y) \bar{\chi}_m(y, \partial_x S_{\text{in}}) dy.$$

When one computes the Lagrangian beam summation integral, the *complex-valued*

$$\partial_x T_m = p_m + (x - y_m) M_m$$

can be approximated by the real-valued p_m with a Taylor truncation error of order $O(|x - y_m|)$. Since $|x - y_m|$ is of $O(\sqrt{\varepsilon})$, cf. (Tanushev 2008) and (Jin et al. 2008b)), this approximation does not destroy the total accuracy of the Gaussian beam method, yet it provides the benefit that the eigenfunction

$\chi_m^*(k, z)$ is only evaluated for *real-valued* k (and thus, consistent with the Bloch decomposition method) However, because of this, the extension of this method to higher order becomes a challenging task.

Eulerian formulation

Based on the ideas presented in Section 9, an Eulerian Gaussian beam method for Schrödinger equations with periodic potentials has been introduced in (Jin et al. 2010b). It involves solving the (multivalued) velocity $u_m = \partial_x S_m$ from the zero level set of the function Φ_m which satisfies the homogeneous semiclassical Liouville equation (12.16) in the form

$$\mathcal{L}_m \Phi_m = 0,$$

where the m -th band Liouville operator \mathcal{L}_m is defined as

$$\mathcal{L}_m = \partial_t + \partial_k E_m \partial_x - \partial_x V \partial_\xi, \quad (13.12)$$

and Φ_m is the complex-valued d -dimensional level set function for the velocity corresponding to the m -th Bloch band. They also solve the following inhomogeneous Liouville equations for the phase S_m and amplitude a_m :

$$\begin{aligned} \mathcal{L}_m S_m &= k \partial_k E_m - V, \\ \mathcal{L}_m a_m &= -\frac{1}{2} \partial_k^2 E_m M_m a_m + \beta_m a_m \partial_y V, \end{aligned}$$

where \mathcal{L}_m is defined by (13.12) and β_m denoted the Berry phase term as given by (12.15). Above, the Hessian $M_m \in \mathbb{C}$ is obtained from

$$M_m = -\frac{\partial_y \Phi_m}{\partial_\xi \Phi_m}.$$

14. Schrödinger equation with random potentials

Finally, we shall consider (small) *random perturbations* of the potential $V(x)$. It is well known that in one space dimension, linear waves in a random medium get localized even when the random perturbations are small, see, e.g. (Fouque, Garnier, Papanicolaou and Sølna 2007). Thus the analysis here is *restricted to three dimensions*. (The two dimensional case is difficult because it of criticality, i.e. the mean field approximation outlined below is most likely incorrect).

14.1. Scaling and asymptotic limit

Consider the Schrödinger equation with a random potential V_R :

$$i\varepsilon \partial_t u^\varepsilon = -\frac{\varepsilon^2}{2} \Delta u^\varepsilon + V(x) u^\varepsilon + \sqrt{\varepsilon} V_R \left(\frac{x}{\varepsilon} \right) u^\varepsilon; \quad x \in \mathbb{R}^3. \quad (14.1)$$

Here $V_R(y)$ is a mean zero, stationary random function with correlation length of order one. Its correlation length is assumed to be of the same

order as the wavelength. The $\sqrt{\varepsilon}$ -scaling given above is *critical* in the sense that the influence of the random potential is of the same order as the one given by $V(x)$ (see also the remark below). We shall also assume that the fluctuations are statistically homogeneous and isotropic so that

$$\langle V_R(x)V_R(y) \rangle = R(|x - y|), \quad (14.2)$$

where $\langle \cdot \rangle$ denotes statistical average and $R(|x|)$ is the covariance of random fluctuations. The power spectrum of the fluctuations is defined by

$$\widehat{R}(\xi) = (2\pi)^{-3} \int e^{i\xi \cdot x} R(x) dx. \quad (14.3)$$

When (14.2) holds, the fluctuations are isotropic and \widehat{R} is a function of $|k|$ only.

Remark 14.1. Because of the statistical homogeneity, the Fourier transform of the random potential V_R is a generalized random process with orthogonal increments

$$\langle \widehat{V}_R(\xi)\widehat{V}_R(p) \rangle = \widehat{R}(\xi)\delta(\xi + p). \quad (14.4)$$

If the amplitude of these fluctuations is large, then purely random scattering will dominate and waves will be localized, cf. (Fröhlich and Spencer 1983). On the other hand, if the random fluctuations are too weak they will not affect the transport of waves at all. Thus, in order to have scattering induced by the random potential and the influence of the slowly varying background $V(x)$ affect the (energy transport of the) waves in comparable ways, the fluctuations in the random potential must be of order $\sqrt{\varepsilon}$.

Using the ε -scaled Wigner transformation, we can derive the analog of (3.2) in the following form

$$\partial_t w^\varepsilon + \xi \cdot \nabla_x w^\varepsilon - \Theta^\varepsilon[V + V_R]w^\varepsilon = 0; \quad (14.5)$$

where the pseudo-differential operator Θ^ε is given by (3.3). The behavior of this operator as $\varepsilon \rightarrow 0$ is very different from the case without V_R , as can be seen already on the level of formal multi-scale analysis, cf. (Ryzhik, Papanicolaou and Keller 1996).

Let $y = x/\varepsilon$ be a fast spatial variable and introduce an expansion of $w^\varepsilon(t)$ in the following form

$$w^\varepsilon(t, x, \xi) = w(t, x, \xi) + \varepsilon^{1/2}w^{(1)}(t, x, y, \xi) + \varepsilon w^{(2)}(t, x, y, \xi) + \dots \quad (14.6)$$

Note that we hereby assume that the leading term w does not depend on the fast scale. We shall also assume that the initial Wigner distribution $w_{\text{in}}^\varepsilon(x, \xi)$ tends to a smooth, *non-negative function* $w_{\text{in}}(x, \xi)$ which decays sufficiently fast at infinity. Then, as $\varepsilon \rightarrow 0$, one formally finds that $\langle w^\varepsilon(t) \rangle$, i.e. the averaged solution to (14.5), is close to a limiting measure $w(t)$, which

satisfies the following *linear Boltzmann-type transport equation*

$$\partial_t w + \xi \cdot \nabla_x w - \nabla_x V \cdot \nabla_\xi w = Qw.$$

Here, the *linear scattering operator* Q is given by

$$Qw(x, \xi) = 4\pi \int_{\mathbb{R}^3} \widehat{R}(\xi - p) \delta(|\xi|^2 - |p|^2) (w(x, p) - w(x, \xi)) dp, \quad (14.7)$$

with differential scattering cross-section

$$\sigma(k, p) = 4\pi \widehat{R}(\xi - p) \delta(|\xi|^2 - |p|^2) \quad (14.8)$$

and total scattering cross-section

$$\Sigma(k) = 4\pi \int_{\mathbb{R}^3} \widehat{R}(\xi - p) \delta(|\xi|^2 - |p|^2) dp. \quad (14.9)$$

Note that the transport equation (14.7) has two important properties. First, the total mass (or, energy, depending on the physical interpretation) is conserved, i.e.

$$E(t) = \iint_{\mathbb{R}^3 \times \mathbb{R}^3} w(t, x, \xi) d\xi dx = E(0). \quad (14.10)$$

Second, the positivity of $w(t, x, \xi)$ is preserved. Rigorous mathematical results concerning the passage from (14.1) to the transport equation (14.7) can be found in (Spohn 1977), (Dell'Antonio 1983), and (Ho, Landau and Wilkins 1993) (which contains extensive references), and, more recently, in (Erdős and Yau 2000).

14.2. Coupling with other media

One can also study the problems when there are other media, including periodic media and interfaces (flat or random).

In the case of periodic media coupled with random media, one can use the above multi-scale analysis combined with the Bloch decomposition method to derive a system of radiative transport equations, see (Bal, Fannjiang, Papanicolaou and Ryzhik 1999a). In the limit system $\varepsilon \rightarrow 0$, the transport part is governed by the semiclassical Liouville equation (12.16) in each Bloch band, while the right hand side is a nonlocal scattering operator (similar to the one above) coupling all bands.

One can also consider random high frequency waves propagating through a random interface. Away from the interface, one obtains the radiative transport equation (14.7). At the interface, due to the randomness of the interface, one needs to consider a diffusive transmission or reflection process, in which waves can be scattered into all directions (see Fig. 10.6). To this end, a nonlocal interface condition has to be derived, see (Bal et al. 1999b).

So far there has been few numerical works on random Schrödinger equations of the form (14.1). In (Bal and Pinaud 2006) the accuracy of the radiative transport equation (14.7) as an approximation to (14.1) has been studied. In (Jin et al. 2008a) a non-local interface condition for diffusive scattering is discretized, similarly in spirit to the treatment described in Section 10.2. We also mention that the temporal resolution issue for time-splitting approximations of the Liouville equations with random potentials was rigorously studied in (Bal and Ryzhik 2004). Finally, we refer to (Fouque et al. 2007) and (Bal, Komorowski and Ryzhik 2010) for a comprehensive reading on high frequency waves in random media.

15. Nonlinear Schrödinger equations in the semiclassical regime

So far we have only considered linear Schrödinger equations. Nonlinear models however are almost as important, since they describe a large number of physical phenomena in nonlinear optics, quantum superfluids, plasma physics or water waves, see e.g. (Sulem and Sulem 1999) for a general overview. The inclusion of nonlinear effects poses new challenges for mathematical and numerical study.

15.1. Basic existence theory

In the following we consider nonlinear Schrödinger equations (NLS) in the form

$$i\varepsilon\partial_t u^\varepsilon = -\frac{\varepsilon^2}{2}\Delta u^\varepsilon + V(x)u^\varepsilon + \varepsilon^\alpha f(x, |u^\varepsilon|^2)u^\varepsilon; \quad u^\varepsilon(0, x) = u_{\text{in}}^\varepsilon(x), \quad (15.1)$$

with $\alpha \geq 0$ some scaling parameter, measuring (asymptotically) the strength of the nonlinearity. More precisely we shall focus on two important classes of nonlinearities. Namely,

- (i) local gauge invariant nonlinearities, where $f = \pm|u^\varepsilon|^{2\sigma}$, with $\sigma > 0$.
- (ii) Hartree type nonlinearities, where $f = V_0 * |u^\varepsilon|^2$, with $V_0 = V_0(x) \in \mathbb{R}$ some given convolution kernel.

The first case of nonlinearities has important applications in Bose-Einstein condensation and nonlinear optics, whereas the latter typically appears as a mean-field description for the dynamics of quantum particles, say electrons (in which case one usually has $V_0(x) = \pm\frac{1}{|x|}$ in $d = 3$).

Concerning the existence of solutions to (15.1), we shall in the following only sketch the basic ideas. For more details we refer (Cazenave 2003) and (Carles 2008). As a first step we represent the solution to (15.1) using

Duhamel's formula:

$$u^\varepsilon(t) = U(t)u_{\text{in}}^\varepsilon - i\varepsilon^\alpha \int_0^t U^\varepsilon(t-s) (f^\varepsilon(x, |u^\varepsilon|^2)(s)u^\varepsilon(s)) ds. \quad (15.2)$$

where $U^\varepsilon(t)$ is the unitary semi-group generated by the linear Hamiltonian $H = -\frac{1}{2}\Delta + V$ (see the discussion in Section 2.1). The basic idea is to prove that the right hand side of (15.2) defines a contraction mapping (in some suitable topology). To this end, one has to distinguish between the case of *sub-* and *super-critical* nonlinearities. It suffices to say, that the existence of a unique solution $u^\varepsilon \in C([0, \infty); L^2(\mathbb{R}^d))$ can be guaranteed, provided $\sigma < \frac{2}{d}$ and/or V_0 sufficiently smooth and decaying, say $V_0 \in L^\infty(\mathbb{R}^d) \cap L^q(\mathbb{R}^d)$, with $q > \frac{d}{4}$.

Remark 15.1. Unfortunately, this sub-critical range of nonlinearities does not allow to include several physically important examples, such as a cubic nonlinearity $\sigma = 1$ in three spatial dimensions (needed e.g. in the description of Bose-Einstein condensates).

In the case of super-critical nonlinearities $\sigma > \frac{2}{d}$, the space $L^2(\mathbb{R}^d)$ in general is too large to guarantee existence of solutions. Typically, one restricts the initial data to $u^\varepsilon \in H^1(\mathbb{R}^d)$, i.e. initial data with finite kinetic energy, in order to control the nonlinear terms by means of Sobolev's imbedding. Assuming that $u^\varepsilon \in H^1$ local in-time existence can be guaranteed by using Strichartz estimates, see (Cazenave 2003) for more details, and one obtains $u^\varepsilon \in C([-T^\varepsilon, T^\varepsilon]; H^1(\mathbb{R}^d))$, for some (possibly small) existence time $T^\varepsilon > 0$.

Remark 15.2. Strictly speaking, we require $\sigma < \frac{2}{d-2}$ in order to use Sobolev's imbedding to control the nonlinearity. Note however that the case of cubic NLS in $d = 3$ is allowed.

Even though local in-time existence is relatively easy to achieve even in the super-critical case, the existence of a global in-time solution to (15.1) in general does not hold. The reason being the possibility of *finite time blow-up*, i.e. the existence of a time $|T^*| < \infty$, such that

$$\lim_{t \rightarrow T^*} \|\nabla u^\varepsilon\| = +\infty.$$

For $T > T^*$, a strong solutions to (15.1) ceases to exist and one can only hope for weak solutions, which however are usually not uniquely defined. In order to understand better in which situations blow-up can occur, consider, for simplicity, the case of a cubic NLS with $V(x) = 0$:

$$i\varepsilon \partial_t u^\varepsilon = -\frac{\varepsilon^2}{2} \Delta u^\varepsilon \pm |u^\varepsilon|^2 u^\varepsilon; \quad u^\varepsilon(0, x) = u_{\text{in}}^\varepsilon(x). \quad (15.3)$$

Given a local in-time solution to this equation one can invoke the conservation of the (nonlinear) energy, i.e.

$$E[u^\varepsilon(t)] = \frac{\varepsilon^2}{2} \int_{\mathbb{R}^d} |\nabla u^\varepsilon(t, x)|^2 dx \pm \frac{1}{2} \int_{\mathbb{R}^d} |u^\varepsilon(t, x)|^4 dx = E[u_{\text{in}}^\varepsilon].$$

Since $E[u_{\text{in}}^\varepsilon] < \text{const}$, by assumption, we can see that in the case where the nonlinearity comes with '+', the a-priori bound on the energy rules out the possibility of finite time blow-up. These type of nonlinearities are usually referred to as *defocusing*. On the other hand, in the case of a *focusing* nonlinearity, i.e. $f = -|u^\varepsilon|^2$, we can no longer guarantee the existence of a global in-time solutions (in the supercritical regime). Rather, we have to expect finite time blow-up to occur in general. Clearly, this phenomena will also have a significant impact on numerical simulations, in particular for $\varepsilon \ll 1$.

15.2. WKB Analysis of nonlinear Schrödinger equations

In order to understand the influence of nonlinear terms in the limit $\varepsilon \rightarrow 0$ one can again invoke a WKB approximation of form (2.10),

$$u^\varepsilon(t, x) \stackrel{\varepsilon \rightarrow 0}{\sim} a^\varepsilon(t, x) e^{iS(t, x)/\varepsilon}.$$

Let us assume for simplicity that $\alpha \in \mathbb{N}$. Then, upon plugging the ansatz given above into (15.1), and ordering equal powers in ε we see that S solves

$$\partial_t S + \frac{1}{2} |\nabla S|^2 + V(x) = \begin{cases} 0, & \text{if } \alpha > 0, \\ f(x, |a|^2), & \text{if } \alpha = 0. \end{cases} \quad (15.4)$$

We see that in the case $\alpha = 0$ we can no longer solve the Hamilton-Jacobi equation for the phase S independently from the amplitude a . In other words, the amplitude influences the geometry of the rays or characteristics. This is usually referred to as *super-critical geometric optics* (Carles 2008), not to be confused with supercritical regime concerning the existence of solutions as outlined in Section 15.1 above.

Weakly nonlinear geometric optics

In contrast to that, the situation for $\alpha > 0$ (*sub-critical geometric optics*) is similar to the linear situation in the sense that the rays of geometric optics are still given by (2.13) and thus independent of the nonlinearity. In this case, the method of characteristics guarantees the existence of a smooth $S \in C^\infty([-T, T] \times \mathbb{R}^d)$ up to caustics and one can proceed with the asymptotic expansion to obtain the following transport equation for the

leading order amplitude

$$\partial_t a + \nabla S \cdot \nabla a + \frac{a}{2} \Delta S = \begin{cases} 0, & \text{if } \alpha > 1, \\ -if(x, |a|^2), & \text{if } \alpha = 1. \end{cases} \quad (15.5)$$

One sees that if $\alpha > 1$ nonlinear effects are asymptotically negligible for $\varepsilon \ll 1$. The solution is therefore expected to be roughly the same as in the linear situation (at least before caustics). For $\alpha = 1$, however, nonlinear effects show up in the leading order amplitude. Note however, that by multiplying (15.5) with \bar{a} and taking the real part, one again finds

$$\partial_t \rho + \operatorname{div}(\rho \nabla S) = 0$$

which is the same conservation law for $\rho = |a|^2$ as in the linear case. The nonlinear effects for $\alpha = 1$ are therefore solely given by nonlinear phase modulations of the leading order amplitude. In the case of a simple cubic nonlinearity one explicitly finds (Carles 2000):

$$a(t, x) = \frac{a_0(y(t, x))}{\sqrt{J_t(y(t, x))}} e^{iG(t, x)}, \quad |t| \leq T, \quad (15.6)$$

where the slowly varying phase G is given by

$$G(t, x) = - \int_0^t \frac{|a_0(y(\tau, x))|^2}{J_\tau(y(\tau, x))} d\tau.$$

This regime is therefore often called *weakly nonlinear geometric optics* and indeed it is possible to prove a rigorous approximation result analogous to Theorem 2.3 also in this case.

Super-critical geometric optics

On the other hand, the situation for $\alpha = 0$ is much more involved. Indeed it can be easily seen that a naive WKB approximation breaks down since the system of amplitude equation is never closed, i.e. the equation for a_n , obtained at $\mathcal{O}(\varepsilon^n)$, involves a_{n+1} and so on (a problem which is reminiscent of the moment closure problem discussed in Section 6 above). This difficulty was overcome by (Grenier 1998) and (Carles 2007b) (Carles 2007a), who noticed that there exists an exact representation of u^ε in the form

$$u^\varepsilon(t, x) = a^\varepsilon(t, x) e^{iS^\varepsilon(t, x)/\varepsilon}, \quad (15.7)$$

with real-valued phase S^ε (possibly ε -dependent) and *complex*-valued amplitude a^ε . (Essentially the right hand side of (15.7) introduces an additional degree of freedom by invoking complex amplitudes). Plugging (15.7) into (15.1) with $\alpha = 0$ one has the freedom to split the resulting equations for a^ε and S^ε as follows: Upon plugging the ansatz given above into (15.1), and

ordering equal powers in ε one sees that S solves

$$\begin{aligned}\partial_t S^\varepsilon + \frac{1}{2} |\nabla S^\varepsilon|^2 + V(x) + f(x, |a^\varepsilon|^2) &= 0, \\ \partial_t a^\varepsilon + \nabla S^\varepsilon \cdot \nabla a^\varepsilon + \frac{a}{2} \Delta S^\varepsilon - i \frac{\varepsilon}{2} \Delta a^\varepsilon &= 0.\end{aligned}$$

Formally, we expect the limit of this system as $\varepsilon \rightarrow 0$ to give a semiclassical approximation of u^ε , at least locally in-time. Indeed this can be done by first rewriting these equations into a new system for $\rho^\varepsilon = |a^\varepsilon|^2$ and $v^\varepsilon = \nabla S^\varepsilon$. Under some assumptions on the nonlinearity f (satisfied e.g. in the cubic case), the obtained equations form a strictly hyperbolic system in which one can rigorously pass to the limit as $\varepsilon \rightarrow 0$ to obtain

$$\begin{aligned}\partial_t v + v \cdot \nabla v + V(x) + f(\rho) &= 0, \\ \partial_t \rho + \operatorname{div}(\rho v) &= 0.\end{aligned}\tag{15.8}$$

This is a system of (irrotational) Euler equations for a classical fluid with pressure law $p(\rho) = f'(\rho)/\rho$. Following this approach, one can prove that as long as (15.8) admits (local in-time) smooth solutions ρ, v , the quantum mechanical densities (2.6), (2.7) indeed converge

$$\rho^\varepsilon \xrightarrow{\varepsilon \rightarrow 0} \rho, \quad J^\varepsilon \xrightarrow{\varepsilon \rightarrow 0} \rho, \quad \text{in } C([0, T]; L^1(\mathbb{R}^d)) \text{ strongly.}$$

Reconstructing out of these limits an approximate solution of the nonlinear Schrödinger equation in WKB form, i.e.

$$u_{\text{app}}^\varepsilon(t, x) = \sqrt{\rho(t, x)} e^{iS(t, x)/\varepsilon}, \quad v(t, x) := \nabla S(t, x),$$

in general requires some care, though see (Carles 2007b). Essentially one needs to take into account a higher order corrector to ensure that the formal approximation is indeed correct up to errors of order $\mathcal{O}(\varepsilon)$, independent of $t \in [0, T]$.

The semiclassical limit for $\alpha = 0$ for $|t| > T$, i.e. beyond the formation of shocks in (15.8), is a very challenging mathematical problem. In one-dimensional case the only available result is given by (Jin, Levermore and McLaughlin 1999) using the inverse scattering technique. The semiclassical limit of focusing NLS is more delicate, but can also be obtained by inverse scattering, see (Kamvissis, McLaughlin and Miller 2003).

Remark 15.3. Let us close this subsection by noticing that the analysis for Hartree type nonlinearities is found to require slightly less sophistication than for local ones (Alazard and Carles 2007) and that the intermediate case $0 < \alpha < 1$ can be understood as a perturbation of the situation for $\alpha = 0$ (Carles 2007b).

15.3. Wigner measure techniques for nonlinear potentials

One might hope to extend the results for Wigner measures given Section 3 also to nonlinear problems. This would have the considerable advantage of avoiding problems due to caustics. Unfortunately, this idea has not been very successful so far, the reason being that Wigner measures are obtained as weak limits only, which in general is not sufficient to pass to the limit in nonlinear terms. Indeed, one can even prove an ill-posedness result for Wigner measures in the nonlinear case (Carles 2001).

A notable exception is the case of Hartree nonlinearities $f = V_0 * |u^\varepsilon|$ with smooth interaction kernels $V_0 \in C_b^1(\mathbb{R}^d)$ (Lions and Paul 1993). In this case the Wigner measure associated to u^ε is found to be a solution of the self-consistent Vlasov equation:

$$\partial_t w + \xi \cdot \nabla_\xi w - \nabla_x (V_0 * \rho) \cdot \nabla_\xi w = 0, \quad \rho(t, x) = \int_{\mathbb{R}^d} w(t, x, d\xi).$$

The physically more interesting case of a non-smooth interaction kernels, such as $V_0 \sim \frac{1}{|x|}$ which describes the coupling to a Poisson equation, is not covered by this result and can only be established in the particular case of fully mixed quantum state, see (Lions and Paul 1993) and (Markowich and Mauser 1993) for more details and also (Zhang 2002) for a similar result valid for short time, only.

15.4. Numerical challenges

Due to the introduction of nonlinear effects, the numerical difficulties discussed in Sections 4 and 5 are enhanced. The main numerical obstacles are the formation of singularities in focusing nonlinear Schrödinger equations and the creation of new scales at caustics for both focusing and defocusing nonlinearities. Basic numerical studies of semiclassical NLS were conducted in (Bao et al. 2002) and (Bao, Jin and Markowich 2003b), with the result that finite difference methods typically require prohibitively fine meshes to even approximate observables well in semiclassical defocusing and focusing NLS computations. In the case where these very restrictive meshing constraints are bypassed, usual finite-difference schemes for NLS can deliver wrong approximations in the classical limit $\varepsilon \rightarrow 0$ without any particular sign of instability (Carles and Gosse 2007). Time-splitting spectral schemes are therefore the preferred method of choice. To this end, we refer to (Jin, Markowich and Zheng 2004) for the application of the time-splitting spectral method to the Zakharov system, to (Huang, Jin, Markowich, Sparber and Zheng 2005) for the numerical solution of the Dirac-Maxwell system and to (Bao et al. 2003b) for numerical studies of nonlinear Schrödinger equations. In addition, let us mention (Bao, Jaksch and Markowich 2003a), (Bao, Jaksch and Markowich 2004) where numerical simulations of the cu-

bically nonlinear Gross-Pitaevskii equation (appearing in the description of Bose-Einstein condensates) are given using time-splitting trigonometric spectral methods. A numerical study of ground state solutions of the Gross-Pitaevskii equation can be found in (Bao, Wang and Markowich 2005).

Remark 15.4. Note, however, that in the nonlinear case, even for $\varepsilon > 0$ fixed, a rigorous convergence analysis of splitting methods is considerably more difficult than for linear Schrödinger equations, see e.g. (Lubich 2008), (Gauckler and Lubich 2010), and (Faou and Grebert 2010).

Due to the nonlinear creation of new highly oscillatory scales in the limit $\varepsilon \rightarrow 0$, time-splitting methods suffer from more severe meshing restrictions for NLS than for linear Schrödinger equations, in particular after the appearance of the first caustics in the corresponding WKB approximation, see (Bao et al. 2003b), (Carles and Gosse 2007) for more details. In the weakly nonlinear regime the following meshing strategy is sufficient

$$\Delta x = \mathcal{O}(\varepsilon), \quad \Delta t = \mathcal{O}(\varepsilon).$$

(to be compared with (5.5)) whereas in the regime of supercritical geometric optics, one typically requires (even for quadratic observable densities)

$$\Delta x = \mathcal{O}(\varepsilon), \quad \Delta t = o(\varepsilon).$$

i.e. a severe restriction on the time-step. In addition, one may need to invoke *Krasny filter* (Krasny 1986), i.e. high Fourier-mode cut-offs, to avoid artifacts (like symmetry breaking) in focusing NLS computations (Bao et al. 2003b). The latter, however, violates the conservation of mass a clear drawback from the physics point of view. In order to overcome this problem higher order methods (in time), such as exponential time-differencing or the use of integrating factors have to be deployed and we refer to (Klein 2007/08) for a comparison of different fourth order methods for cubic NLS in the semiclassical regime.

Remark 15.5. In the closely related problem of the complex-Ginzburg Landau equation in the large space and time limit, the situation is known to be slightly better, due to the dissipative nature of the equation, see (Degond, Jin and Tang 2008) for a numerical investigation. Finally, we note that the cubic NLS in $d = 1$ is known to be fully integrable by means of inverse scattering. This feature can be used in the design of numerical algorithms, as has been done in e.g. (Zheng 2006). A generalization to higher dimensions or more general nonlinearities seems to be out of reach so far.

The lack of a clear mathematical understanding of the asymptotic behavior of solution to semiclassical NLS beyond the formation of caustics has so far hindered the design of reliable asymptotic schemes. One of the few exceptions is the case of the Schrödinger-Poisson equation in $d = 1$, which

can be analyzed using Wigner measures and which has recently been studied numerically in (Jin, Wu and Yang 2010a) using a Gaussian beam method. In addition, moment closure methods have been employed for this type of nonlinearities, since it is known that the underlying classical problem, i.e. the Euler-Poisson system, allows for a construction of multi-valued solutions. Numerical simulations for the classical system have been conducted in (Wohlbier et al. 2005). In addition the case of the Schrödinger-Poisson equation with periodic potential is treated in (Gosse and Mauser 2006).

REFERENCES

- D. Adalsteinsson and J. A. Sethian (1995), ‘A fast level set method for propagating interfaces’, *J. Comput. Phys.* **118**(2), 269–277.
- T. Alazard and R. Carles (2007), ‘Semi-classical limit of Schrödinger-Poisson equations in space dimension $n \geq 3$ ’, *J. Differential Equations* **233**(1), 241–275.
- L. Ambrosio (2004), ‘Transport equation and Cauchy problem for BV vector fields’, *Invent. Math.* **158**(2), 227–260.
- G. Ariel, B. Engquist, N. Tanushev and R. Tsai (n.d.), ‘Gaussian beam decomposition of high frequency wave fields using expectation-maximization’. submitted.
- D. Armbruster, D. Marthaler and C. Ringhofer (2003), ‘Kinetic and fluid model hierarchies for supply chains’, *Multiscale Model. Simul.* **2**(1), 43–61 (electronic).
- N. W. Ashcroft and N. D. Mermin (1976), *Solid State Physics*, Rinehart and Winston, New York.
- G. Bal and O. Pinaud (2006), ‘Accuracy of transport models for waves in random media’, *Wave Motion* **43**(7), 561–578.
- G. Bal and L. Ryzhik (2004), ‘Time splitting for the Liouville equation in a random medium’, *Commun. Math. Sci.* **2**(3), 515–534.
- G. Bal, A. Fannjiang, G. Papanicolaou and L. Ryzhik (1999a), ‘Radiative transport in a periodic structure’, *J. Statist. Phys.* **95**(1-2), 479–494.
- G. Bal, J. B. Keller, G. Papanicolaou and L. Ryzhik (1999b), ‘Transport theory for acoustic waves with reflection and transmission at interfaces’, *Wave Motion* **30**(4), 303–327.
- G. Bal, T. Komorowski and L. Ryzhik (2010), ‘Kinetic limits for waves in a random medium’, *Kinetic and Related Models* **3**(4), 529–644.
- W. Bao and J. Shen (2005), ‘A fourth-order time-splitting Laguerre-Hermite pseudospectral method for Bose-Einstein condensates’, *SIAM J. Sci. Comput.* **26**(6), 2010–2028 (electronic).
- W. Bao, D. Jaksch and P. A. Markowich (2003a), ‘Numerical solution of the Gross-Pitaevskii equation for Bose-Einstein condensation’, *J. Comput. Phys.* **187**(1), 318–342.
- W. Bao, D. Jaksch and P. A. Markowich (2004), ‘Three dimensional simulation of jet formation in collapsing condensates’, *J. Phys. B: At. Mol. Opt. Phys.* **37**(2), 329–343.
- W. Bao, S. Jin and P. A. Markowich (2002), ‘On time-splitting spectral approximations for the Schrödinger equation in the semiclassical regime’, *J. Comput. Phys.* **175**(2), 487–524.

- W. Bao, S. Jin and P. A. Markowich (2003*b*), ‘Numerical study of time-splitting spectral discretizations of nonlinear Schrödinger equations in the semiclassical regimes’, *SIAM J. Sci. Comput.* **25**(1), 27–64 (electronic).
- W. Bao, H. Wang and P. A. Markowich (2005), ‘Ground, symmetric and central vortex states in rotating Bose-Einstein condensates’, *Commun. Math. Sci.* **3**(1), 57–88.
- N. Ben Abdallah, P. Degond and I. M. Gamba (2002), ‘Coupling one-dimensional time-dependent classical and quantum transport models’, *J. Math. Phys.* **43**(1), 1–24.
- J.-D. Benamou (1999), ‘Direct computation of multivalued phase space solutions for Hamilton-Jacobi equations’, *Comm. Pure Appl. Math.* **52**(11), 1443–1475.
- J.-D. Benamou and I. Sollic (2000), ‘An Eulerian method for capturing caustics’, *J. Comput. Phys.* **162**(1), 132–163.
- J.-D. Benamou, O. Lafitte, R. Sentis and I. Sollic (2003), ‘A geometrical optics-based numerical method for high frequency electromagnetic fields computations near fold caustics. I’, *J. Comput. Appl. Math.* **156**(1), 93–125.
- D. Benedetto, R. Esposito and M. Pulvirenti (2004), ‘Asymptotic analysis of quantum scattering under mesoscopic scaling’, *Asymptot. Anal.* **40**(2), 163–187.
- A. Bensoussan, J. L. Lions and G. Papanicolaou (1978), *Asymptotic analysis for periodic structures*, Vol. 5, North-Holland Publishing Co., Amsterdam.
- F. Bloch (1928), ‘Über die Quantenmechanik der Elektronen in Kristallgittern’, *Z. Phys.* **52**, 555–600.
- F. Bouchut, S. Jin and X. Li (2003), ‘Numerical approximations of pressureless and isothermal gas dynamics’, *SIAM J. Numer. Anal.* **41**(1), 135–158 (electronic).
- S. Bougacha, J.-L. Akian and R. Alexandre (2009), ‘Gaussian beams summation for the wave equation in a convex domain’, *Commun. Math. Sci.* **7**(4), 973–1008.
- Y. Brenier and L. Corrias (1998), ‘A kinetic formulation for multi-branch entropy solutions of scalar conservation laws’, *Ann. Inst. H. Poincaré Anal. Non Linéaire* **15**(2), 169–190.
- R. Carles (2000), ‘Geometric optics with caustic crossing for some nonlinear Schrödinger equations’, *Indiana Univ. Math. J.* **49**(2), 475–551.
- R. Carles (2001), ‘Remarques sur les mesures de Wigner’, *C. R. Acad. Sci. Paris Sér. I Math.* **332**(11), 981–984.
- R. Carles (2007*a*), ‘Geometric optics and instability for semi-classical Schrödinger equations’, *Arch. Ration. Mech. Anal.* **183**(3), 525–553.
- R. Carles (2007*b*), ‘WKB analysis for nonlinear Schrödinger equations with potential’, *Comm. Math. Phys.* **269**(1), 195–221.
- R. Carles (2008), *Semi-classical Analysis for nonlinear Schrödinger equations*, World Scientific Publishing Co. Ltd., Singapore.
- R. Carles and L. Gosse (2007), ‘Numerical aspects of nonlinear Schrödinger equations in the presence of caustics’, *Math. Models Methods Appl. Sci.* **17**(10), 1531–1553.
- R. Carles, P. A. Markowich and C. Sparber (2004), ‘Semiclassical asymptotics for weakly nonlinear Bloch waves’, *J. Statist. Phys.* **117**(1-2), 343–375.
- T. Cazenave (2003), *Semilinear Schrödinger equations*, Vol. 10 of *Courant Lecture Notes in Mathematics*, New York University Courant Institute of Mathematical Sciences, New York.

- V. Cervený (2001), *Seismic ray theory*, Cambridge University Press, Cambridge.
- T. F. Chan and L. Shen (1987), ‘Stability analysis of difference scheme for variable coefficient Schrödinger type equations’, *SIAM J. Numer. Anal.* **24**, 336–349.
- T. Chan, D. Lee and L. Shen (1986), ‘Stable explicit schemes for equations of the Schrödinger type’, *SIAM J. Numer. Anal.* **23**, 274–281.
- L.-T. Cheng, M. Kang, S. Osher, H. Shim and Y.-H. Tsai (2004), ‘Reflection in a level set framework for geometric optics’, *CMES Comput. Model. Eng. Sci.* **5**(4), 347–360.
- L.-T. Cheng, H. Liu and S. Osher (2003), ‘Computational high-frequency wave propagation using the level set method, with applications to the semi-classical limit of Schrödinger equations’, *Commun. Math. Sci.* **1**(3), 593–621.
- R. Courant and D. Hilbert (1962), *Methods of Mathematical Physics Vol. 2*, Interscience Publishers.
- M. G. Crandall and P.-L. Lions (1983), ‘Viscosity solutions of Hamilton-Jacobi equations’, *Trans. Amer. Math. Soc.* **277**(1), 1–42.
- P. Degond, S. Jin and M. Tang (2008), ‘On the time splitting spectral method for the complex Ginzburg-Landau equation in the large time and space scale limit’, *SIAM J. Sci. Comput.* **30**(5), 2466–2487.
- M. Delfour, M. Fortin and G. Payre (1981), ‘Finite-difference solutions of a nonlinear Schrödinger equation’, *J. Comp. Phys.* **44**, 277–288.
- G. F. Dell’Antonio (1983), ‘Large time, small coupling behaviour of a quantum particle in a random field’, *Ann. Inst. H. Poincaré Sect. A (N.S.)* **39**(4), 339–384.
- R. J. DiPerna and P.-L. Lions (1989), ‘Ordinary differential equations, transport theory and Sobolev spaces’, *Invent. Math.* **98**(3), 511–547.
- W. Dörfler (1998), ‘A time- and space adaptive algorithm for the linear time dependent Schrödinger equation’, *Numer. Math.* **73**, 419–448.
- K. Drukker (1999), ‘Basics of surface hopping next term in mixed quantum/classical simulations’, *J. Comp. Phys.* **153**, 225–272.
- J. J. Duistermaat (1996), *Fourier integral operators*, Vol. 130 of *Progress in Mathematics*, Birkhäuser Boston Inc., Boston, MA.
- G. Dujardin and E. Faou (2007a), ‘Long time behavior of splitting methods applied to the linear Schrödinger equation’, *C. R. Math. Acad. Sci. Paris* **344**(2), 89–92.
- G. Dujardin and E. Faou (2007b), ‘Normal form and long time analysis of splitting schemes for the linear Schrödinger equation with small potential’, *Numer. Math.* **108**(2), 223–262.
- B. Engquist and O. Runborg (1996), ‘Multi-phase computations in geometrical optics’, *J. Comput. Appl. Math.* **74**(1-2), 175–192. TICAM Symposium (Austin, TX, 1995).
- B. Engquist and O. Runborg (2003), ‘Computational high frequency wave propagation’, *Acta Numer.* **12**, 181–266.
- L. Erdős and H.-T. Yau (2000), ‘Linear Boltzmann equation as the weak coupling limit of a random Schrödinger equation’, *Comm. Pure Appl. Math.* **53**(6), 667–735.

- E. Faou and B. Grebert (2010), ‘Resonances in long time integration of semi linear hamiltonian pdes’, Preprint available at : <http://www.irisa.fr/ipso/perso/faou/>.
- C. Fermanian Kammerer and C. Lasser (2003), ‘Wigner measures and codimension two crossings’, *J. Math. Phys.* **44**(2), 507–527.
- H. Flaschka, M. G. Forest and D. W. McLaughlin (1980), ‘Multiphase averaging and the inverse spectral solution of the Korteweg-de Vries equation’, *Comm. Pure Appl. Math.* **33**(6), 739–784.
- S. Fomel and J. A. Sethian (2002), ‘Fast-phase space computation of multiple arrivals’, *Proc. Natl. Acad. Sci. USA* **99**(11), 7329–7334 (electronic).
- B. Fornberg (1996), *A practical guide to pseudospectral methods*, Vol. 1 of *Cambridge Monographs on Applied and Computational Mathematics*, Cambridge University Press, Cambridge.
- J.-P. Fouque, J. Garnier, G. Papanicolaou and K. Sølna (2007), *Wave propagation and time reversal in randomly layered media*, Vol. 56 of *Stochastic Modelling and Applied Probability*, Springer, New York.
- J. Fröhlich and T. Spencer (1983), ‘Absence of diffusion in the Anderson tight binding model for large disorder or low energy’, *Comm. Math. Phys.* **88**(2), 151–184.
- L. Gauckler and C. Lubich (2010), ‘Splitting integrators for nonlinear Schrödinger equations over long times’, *Found. Comput. Math.* **10**(3), 275–302.
- P. Gérard, P. A. Markowich, N. J. Mauser and F. Poupaud (1997), ‘Homogenization limits and Wigner transforms’, *Comm. Pure Appl. Math.* **50**(4), 323–379.
- L. Gosse (2002), ‘Using K -branch entropy solutions for multivalued geometric optics computations’, *J. Comput. Phys.* **180**(1), 155–182.
- L. Gosse (2006), ‘Multiphase semiclassical approximation of the one-dimensional harmonic crystal. I. The periodic case’, *J. Phys. A* **39**(33), 10509–10521.
- L. Gosse and F. James (2002), ‘Convergence results for an inhomogeneous system arising in various high frequency approximations’, *Numer. Math.* **90**(4), 721–753.
- L. Gosse and P. A. Markowich (2004), ‘Multiphase semiclassical approximation of an electron in a one-dimensional crystalline lattice. I. Homogeneous problems’, *J. Comput. Phys.* **197**(2), 387–417.
- L. Gosse and N. J. Mauser (2006), ‘Multiphase semiclassical approximation of an electron in a one-dimensional crystalline lattice. III. From ab initio models to WKB for Schrödinger-Poisson’, *J. Comput. Phys.* **211**(1), 326–346.
- L. Gosse, S. Jin and X. Li (2003), ‘Two moment systems for computing multiphase semiclassical limits of the Schrödinger equation’, *Math. Models Methods Appl. Sci.* **13**(12), 1689–1723.
- V. L. Granastein, R. K. Parker and C. Armstrong (1999), ‘Vacuum electronics at the dawn of the twenty-first century’, *Proceedings of the IEEE* **87**, 702–716.
- E. Grenier (1998), ‘Semiclassical limit of the nonlinear Schrödinger equation in small time’, *Proc. Amer. Math. Soc.* **126**(2), 523–530.
- J.-C. Guillot, J. Ralston and E. Trubowitz (1988), ‘Semiclassical asymptotics in solid-state physics’, *Comm. Math. Phys.* **116**(3), 401–415.
- G. A. Hagedorn (1994), ‘Molecular propagation through electron energy level crossings’, *Mem. Amer. Math. Soc.* **111**(536), vi+130.

- E. J. Heller (1981), ‘Frozen gaussians: a very simple semiclassical approximation’, *Journal of Chemical Physics* **75**, 2923–2931.
- E. J. Heller (2006), ‘Guided gaussian wave packets’, *Accounts of Chemical Research* **39**(2), 127–134.
- M. Herman and E. Kluk (1984), ‘A semiclassical justification for the use of non-spreading wavepackets in dynamics calculations’, *Journal of Chemical Physics* **91**, 2923–2931.
- N. Hill (1990), ‘Gaussian beam migration’, *Geophysics* **55**(11), 1416–1428.
- T. G. Ho, L. J. Landau and A. J. Wilkins (1993), ‘On the weak coupling limit for a Fermi gas in a random potential’, *Rev. Math. Phys.* **5**(2), 209–298.
- I. Horenko, C. Salzmann, B. Schmidt and C. Schütte (2002), ‘Quantum-classical liouville approach to molecular dynamics: Surface hopping gaussian phase-space packets’, *Journal of Chemical Physics* **117**, 11075.
- L. Hörmander (1985), *The Analysis of Linear Partial Differential Operators III*, Springer-Verlag, New York.
- Z. Huang, S. Jin, P. A. Markowich and C. Sparber (2007), ‘A Bloch decomposition-based split-step pseudospectral method for quantum dynamics with periodic potentials’, *SIAM J. Sci. Comput.* **29**(2), 515–538 (electronic).
- Z. Huang, S. Jin, P. A. Markowich and C. Sparber (2008), ‘Numerical simulation of the nonlinear Schrödinger equation with multidimensional periodic potentials’, *Multiscale Model. Simul.* **7**(2), 539–564.
- Z. Huang, S. Jin, P. A. Markowich and C. Sparber (2009), ‘On the Bloch decomposition based spectral method for wave propagation in periodic media’, *Wave Motion* **46**(1), 15–28.
- Z. Huang, S. Jin, P. A. Markowich, C. Sparber and C. Zheng (2005), ‘A time-splitting spectral scheme for the Maxwell-Dirac system’, *J. Comput. Phys.* **208**(2), 761–789.
- G. Jiang and E. Tadmor (1998), ‘Nonoscillatory central schemes for multidimensional hyperbolic conservation laws’, *SIAM Journal of Scientific Computing* **19**(1), 1892–1917.
- S. Jin (2009), Recent computational methods for high frequency waves in heterogeneous media, in *Industrial and applied mathematics in China*, Vol. 10 of *Ser. Contemp. Appl. Math. CAM*, Higher Ed. Press, Beijing, pp. 49–64.
- S. Jin and X. Li (2003), ‘Multi-phase computations of the semiclassical limit of the Schrödinger equation and related problems: Whitham vs. Wigner’, *Phys. D* **182**(1-2), 46–85.
- S. Jin and X. Liao (2006), ‘A Hamiltonian-preserving scheme for high frequency elastic waves in heterogeneous media’, *J. Hyperbolic Differ. Equ.* **3**(4), 741–777.
- S. Jin and K. A. Novak (2006), ‘A semiclassical transport model for thin quantum barriers’, *Multiscale Model. Simul.* **5**(4), 1063–1086 (electronic).
- S. Jin and K. A. Novak (2007), ‘A semiclassical transport model for two-dimensional thin quantum barriers’, *J. Comput. Phys.* **226**(2), 1623–1644.
- S. Jin and K. A. Novak (2010), ‘A coherent semiclassical transport model for pure-state quantum scattering’, *Commun. Math. Sci.* **8**(1), 253–275.
- S. Jin and S. Osher (2003), ‘A level set method for the computation of multivalued

- solutions to quasi-linear hyperbolic PDEs and Hamilton-Jacobi equations', *Commun. Math. Sci.* **1**(3), 575–591.
- S. Jin and X. Wen (2005), 'Hamiltonian-preserving schemes for the Liouville equation with discontinuous potentials', *Commun. Math. Sci.* **3**(3), 285–315.
- S. Jin and X. Wen (2006a), 'A Hamiltonian-preserving scheme for the Liouville equation of geometrical optics with partial transmissions and reflections', *SIAM J. Numer. Anal.* **44**(5), 1801–1828 (electronic).
- S. Jin and X. Wen (2006b), 'Hamiltonian-preserving schemes for the Liouville equation of geometrical optics with discontinuous local wave speeds', *J. Comput. Phys.* **214**(2), 672–697.
- S. Jin and Z. Xin (1998), 'Numerical passage from systems of conservation laws to Hamilton-Jacobi equations, relaxation schemes', *SIAM J. Numer. Anal.* **35**(6), 2385–2404 (electronic).
- S. Jin and X. Yang (2008), 'Computation of the semiclassical limit of the Schrödinger equation with phase shift by a level set method', *J. Sci. Comput.* **35**(2-3), 144–169.
- S. Jin and D. Yin (2008a), 'Computation of high frequency wave diffraction by a half plane via the Liouville equation and Geometric Theory of Diffraction', *Comm. Comput. Phys.* **4**, 1106–1128.
- S. Jin and D. Yin (2008b), 'Computational high frequency waves through curved interfaces via the Liouville equation and geometric theory of diffraction', *J. Comput. Phys.* **227**(12), 6106–6139.
- S. Jin and D. Yin (n.d.), 'Computational high frequency wave diffraction by a corner via the Liouville equation and Geometric Theory of Diffraction', to appear.
- S. Jin, C. D. Levermore and D. W. McLaughlin (1999), 'The semiclassical limit of the defocusing NLS hierarchy', *Comm. Pure Appl. Math.* **52**(5), 613–654.
- S. Jin, X. Liao and X. Yang (2008a), 'Computation of interface reflection and regular or diffuse transmission of the planar symmetric radiative transfer equation with isotropic scattering and its diffusion limit', *SIAM J. Sci. Comput.* **30**(4), 1992–2017.
- S. Jin, H. Liu, S. Osher and R. Tsai (2005a), 'Computing multi-valued physical observables for the high frequency limit of symmetric hyperbolic systems', *J. Comput. Phys.* **210**(2), 497–518.
- S. Jin, H. Liu, S. Osher and Y.-H. R. Tsai (2005b), 'Computing multivalued physical observables for the semiclassical limit of the Schrödinger equation', *J. Comput. Phys.* **205**(1), 222–241.
- S. Jin, P. A. Markowich and C. Zheng (2004), 'Numerical simulation of a generalized Zakharov system', *J. Comput. Phys.* **201**(1), 376–395.
- S. Jin, P. Qi and Z. Zhang (n.d.), 'An eulerian surface hopping method for the schrödinger equation with conical crossings', to appear.
- S. Jin, H. Wu and X. Yang (2008b), 'Gaussian beam methods for the Schrödinger equation in the semi-classical regime: Lagrangian and Eulerian formulations', *Commun. Math. Sci.* **6**(4), 995–1020.
- S. Jin, H. Wu and X. Yang (2010a), 'A numerical study of the Gaussian beam methods for Schrödinger-Poisson equations', *J. Comput. Math.* **28**(2), 261–272.

- S. Jin, H. Wu and X. Yang (2011), ‘Semi-eulerian and high order gaussian beam methods for the schrödinger equation in the semiclassical regime’, *Communications in Computational Physics*.
- S. Jin, H. Wu, X. Yang and Z. Huang (2010b), ‘Bloch decomposition-based Gaussian beam method for the Schrödinger equation with periodic potentials’, *J. Comput. Phys.* **229**(13), 4869–4883.
- S. Kamvissis, K. D. T.-R. McLaughlin and P. D. Miller (2003), *Semiclassical soliton ensembles for the focusing nonlinear Schrödinger equation*, Vol. 154 of *Annals of Mathematics Studies*, Princeton University Press, Princeton, NJ.
- K. Kay (1994), ‘Integral expressions for the semi-classical time-dependent propagator’, *Journal of Chemical Physics* **100**, 4437–4392.
- K. Kay (2006), ‘The Herman-Kluk approximation: Derivation and semiclassical corrections’, *Journal of Chemical Physics* **322**, 3–12.
- J. B. Keller and R. M. Lewis (1995), Asymptotic methods for partial differential equations: the reduced wave equation and Maxwell’s equations, in *Surveys in applied mathematics, Vol. 1*, Vol. 1 of *Surveys Appl. Math.*, Plenum, New York, pp. 1–82.
- H. Kitada (1980), ‘On a construction of the fundamental solution for Schrödinger equations’, *J. Fac. Sci. Univ. Tokyo Sect. IA Math.* **27**(1), 193–226.
- C. Klein (2007/08), ‘Fourth order time-stepping for low dispersion Korteweg-de Vries and nonlinear Schrödinger equations’, *Electron. Trans. Numer. Anal.* **29**, 116–135.
- R. Krasny (1986), ‘A study of singularity formation in a vortex sheet by the point-vortex approximation’, *J. Fluid Mech.* **167**, 65–93.
- S. Kube, C. Lasser and M. Weber (2009), ‘Monte Carlo sampling of Wigner functions and surface hopping quantum dynamics’, *J. Comput. Phys.* **228**(6), 1947–1962.
- L. Landau (1932), ‘Zur theorie der energieübertragung. ii.’, *Physics of the Soviet Union* **2**, 46–51.
- C. Lasser and S. Teufel (2005), ‘Propagation through conical crossings: an asymptotic semigroup’, *Comm. Pure Appl. Math.* **58**(9), 1188–1230.
- C. Lasser, T. Swart and S. Teufel (2007), ‘Construction and validation of a rigorous surface hopping algorithm for conical crossings’, *Communications in Mathematical Sciences* **5**(4), 789–814.
- P. D. Lax (1957), ‘Asymptotic solutions of oscillatory initial value problems’, *Duke Math. J.* **24**, 627–646.
- B. Leimkuhler and S. Reich (2004), *Simulating Hamiltonian dynamics*, Vol. 14 of *Cambridge Monographs on Applied and Computational Mathematics*, Cambridge University Press, Cambridge.
- S. Leung and J. Qian (2009), ‘Eulerian gaussian beams for schrödinger equations in the semi-classical regime’, *J. Comput. Phys.* **228**(8), 2951–2977.
- S. Leung, J. Qian and R. Burrige (2007), ‘Eulerian gaussian beams for high frequency wave propagation’, *Geophysics* **72**(2), 61–76.
- C. Levermore (1996), ‘Moment closure hierarchies for kinetic theories’, *Journal of Statistical Physics* **83**(1), 1021–1065.
- X. Li, J. Wohlbier, S. Jin and J. Booske (2004), ‘An eulerian method for computing

- multi-valued solutions to the euler-poisson equations and applications to wave breaking in klystrons', *Phys. Rev. E* **70**(4), 016502.
- P.-L. Lions and T. Paul (1993), 'Sur les mesures de Wigner', *Rev. Mat. Iberoamericana* **9**(3), 553–618.
- H. Liu and J. Ralston (2010), 'Recovery of high frequency wave fields from phase space-based measurements', *Multiscale Model. Simul.* **8**(2), 622–644.
- H. Liu and Z. Wang (2007), 'A field-space-based level set method for computing multi-valued solutions to 1D Euler-Poisson equations', *J. Comput. Phys.* **225**(1), 591–614.
- H. Liu, O. Runborg and N. Yanushev (n.d.), 'Error estimates for gaussian beam superpositions'. submitted.
- J. Lu and X. Yang (n.d.), 'Frozen gaussian approximation for high frequency wave propagation', to appear.
- C. Lubich (2008), 'On splitting methods for Schrödinger-Poisson and cubic nonlinear Schrödinger equations', *Math. Comp.* **77**(264), 2141–2153.
- A. J. Majda, G. Majda and Y. X. Zheng (1994), 'Concentrations in the one-dimensional Vlasov-Poisson equations. I. Temporal development and non-unique weak solutions in the single component case', *Phys. D* **74**(3-4), 268–300.
- P. A. Markowich and N. J. Mauser (1993), 'The classical limit of a self-consistent quantum-Vlasov equation in 3D', *Math. Models Methods Appl. Sci.* **3**(1), 109–124.
- P. A. Markowich and F. Poupaud (1999), 'The pseudo-differential approach to finite differences revisited', *Calcolo* **36**(3), 161–186.
- P. A. Markowich, N. J. Mauser and F. Poupaud (1994), 'A Wigner-function approach to (semi)classical limits: electrons in a periodic potential', *J. Math. Phys.* **35**(3), 1066–1094.
- P. A. Markowich, P. Pietra and C. Pohl (1999), 'Numerical approximation of quadratic observables of Schrödinger-type equations in the semi-classical limit', *Numer. Math.* **81**(4), 595–630.
- V. Maslov, ed. (1981), *Semiclassical Approximations in Quantum Mechanics*, Reidel Dordrecht.
- R. I. McLachlan and G. R. W. Quispel (2002), 'Splitting methods', *Acta Numer.* **11**, 341–434.
- L. Miller (2000), 'Refraction of high-frequency waves density by sharp interfaces and semiclassical measures at the boundary', *J. Math. Pures Appl. (9)* **79**(3), 227–269.
- M. Motamed and O. Runborg (n.d.), 'Taylor expansion and discretization errors in gaussian beam superposition', *Wave Motion*. to appear.
- F. Nier (1995), 'Asymptotic analysis of a scaled Wigner equation and quantum scattering', *Transport Theory Statist. Phys.* **24**(4-5), 591–628.
- F. Nier (1996), 'A semi-classical picture of quantum scattering', *Ann. Sci. École Norm. Sup. (4)* **29**(2), 149–183.
- S. Osher and J. A. Sethian (1988), 'Fronts propagating with curvature-dependent speed: algorithms based on Hamilton-Jacobi formulations', *J. Comput. Phys.* **79**(1), 12–49.

- S. Osher, L.-T. Cheng, M. Kang, H. Shim and Y.-H. Tsai (2002), ‘Geometric optics in a phase-space-based level set and Eulerian framework’, *J. Comput. Phys.* **179**(2), 622–648.
- G. Panati, H. Spohn and S. Teufel (2006), Motion of electrons in adiabatically perturbed periodic structures, in *Analysis, modeling and simulation of multiscale problems*, Springer, Berlin, pp. 595–617.
- D. Pathria and J. Morris (1990), ‘Pseudo-spectral solution of nonlinear Schrödinger equations’, *J. Comp. Phys.*
- D. Peng, B. Merriman, S. Osher, H. Zhao and M. Kang (1999), ‘A PDE-based fast local level set method’, *J. Comput. Phys.* **155**(2), 410–438.
- B. Perthame and C. Simeoni (2001), ‘A kinetic scheme for the Saint-Venant system with a source term’, *Calcolo* **38**(4), 201–231.
- M. M. Popov (1982), ‘A new method of computation of wave fields using Gaussian beams’, *Wave Motion* **4**(1), 85–97.
- J. Qian and L. Ying (2010), ‘Fast gaussian wavepacket transforms and gaussian beams for the schrödinger equation’, *Journal of Computational Physics* **229**, 7848–7873.
- J. Ralston (1982), Gaussian beams and the propagation of singularities, in *Studies in partial differential equations*, Vol. 23 of *MAA Stud. Math.*, Math. Assoc. America, Washington, DC, pp. 206–248.
- M. Reed and B. Simon (1975), *Methods of modern mathematical physics. II. Fourier analysis, self-adjointness*, Academic Press [Harcourt Brace Jovanovich Publishers], New York.
- M. Reed and B. Simon (1976), *Methods of modern mathematical physics. IV. Analysis of operators*, Academic Press [Harcourt Brace Jovanovich Publishers], New York.
- D. Robert (2010), ‘On the herman-kluk semiclassical approximation’, *Rev. Math. Phys.* **22**, 1123–1145.
- O. Runborg (2000), ‘Some new results in multiphase geometrical optics’, *M2AN Math. Model. Numer. Anal.* **34**(6), 1203–1231.
- L. Ryzhik, G. Papanicolaou and J. B. Keller (1996), ‘Transport equations for elastic and other waves in random media’, *Wave Motion* **24**(4), 327–370.
- A. Shapere and F. Wilczek, eds (1989), *Geometric Phases in Physics*, Vol. 5 of *Advances Series in Mathematical Physics*, World Scientific Publishing Co. Inc., Teaneck, NJ.
- D. Sholla and J. Tully (1998), ‘A generalized surface hopping method’, *J. Chem. Phys.* **109**, 7702.
- C. Sparber, P. Markowich and N. Mauser (2003), ‘Wigner functions versus WKB-methods in multivalued geometrical optics’, *Asymptot. Anal.* **33**(2), 153–187.
- H. Spohn (1977), ‘Derivation of the transport equation for electrons moving through random impurities’, *J. Statist. Phys.* **17**(6), 385–412.
- H. Spohn and S. Teufel (2001), ‘Adiabatic decoupling and time-dependent Born-Oppenheimer theory’, *Comm. Math. Phys.* **224**(1), 113–132. Dedicated to Joel L. Lebowitz.
- J. C. Strikwerda (1989), *Finite difference schemes and partial differential equations*, The Wadsworth & Brooks/Cole Mathematics Series, Wadsworth & Brooks/Cole Advanced Books & Software, Pacific Grove, CA.

- C. Sulem and P.-L. Sulem (1999), *The nonlinear Schrödinger equation*, Vol. 139 of *Applied Mathematical Sciences*, Springer-Verlag, New York. Self-focusing and wave collapse.
- G. Sundaram and Q. Niu (1999), ‘Wave-packet dynamics in slowly perturbed crystals: Gradient corrections and berry-phase effects’, *Phys. Rev. B* **59**, 14915–14925.
- T. Swart and V. Rousse (2009), ‘A mathematical justification for the Herman-Kluk propagator’, *Comm. Math. Phys.* **286**(2), 725–750.
- T. Taha and M. J. Ablowitz (1984), ‘Analytical and numerical aspects of certain nonlinear evolution equations II, numerical, nonlinear Schrödinger equations’, *J. Comp. Phys.* **55**, 203–230.
- N. M. Tanushev (2008), ‘Superpositions and higher order Gaussian beams’, *Commun. Math. Sci.* **6**(2), 449–475.
- N. M. Tanushev, B. Engquist and R. Tsai (2009), ‘Gaussian beam decomposition of high frequency wave fields’, *J. Comput. Phys.* **228**(23), 8856–8871.
- L. Tartar (1990), ‘ H -measures, a new approach for studying homogenisation, oscillations and concentration effects in partial differential equations’, *Proc. Roy. Soc. Edinburgh Sect. A* **115**(3-4), 193–230.
- S. Teufel (2003), *Adiabatic perturbation theory in quantum dynamics*, Vol. 1821 of *Lecture Notes in Mathematics*, Springer.
- J. Tully (1990), ‘Molecular dynamics with electronic transitions’, *J. Chem. Phys.* **93**, 1061.
- J. Tully and R. Preston (1971), ‘Trajectory surface hopping approach to nonadiabatic molecular collisions: The reaction of h^+ with d_2 ’, *J. Chem. Phys.* **55**, 562.
- D. Wei, S. Jin, R. Tsai and X. Yang (2010), ‘A level set method for the semiclassical limit of the Schrödinger equation with discontinuous potentials’, *Communications in Computational Physics* **229**, 7440–7455.
- X. Wen (2009), ‘Convergence of an immersed interface upwind scheme for linear advection equations with piecewise constant coefficients. II. Some related binomial coefficient inequalities’, *J. Comput. Math.* **27**(4), 474–483.
- X. Wen (2010), ‘High order numerical methods to three dimensional delta function integrals in level set methods’, *SIAM J. Sci. Comput.* **32**(3), 1288–1309.
- X. Wen and S. Jin (2009), ‘The l^1 -stability of a Hamiltonian-preserving scheme for the Liouville equation with discontinuous potentials’, *J. Comput. Math.* **27**(1), 45–67.
- G. Whitham (1974), *Linear and Nonlinear Waves*, Wiley-Interscience, New York.
- E. P. Wigner (1932), ‘On the quantum correction for thermodynamic equilibrium’, *Phys. Rev.* **40**, 749–759.
- C. H. Wilcox (1978), ‘Theory of Bloch waves’, *J. Anal. Math.* **33**, 146–167.
- S. Wohlbier, S. Jin and S. Sengele (2005), ‘Eulerian calculations of wave breaking and multivalued solutions in a traveling wave tube’, *Physics of Plasmas* **12**(2), 023106–023113.
- L. Wu (1996), ‘Dufort-frankel-type methods for linear and nonlinear schr odinger dufort-Frankel-type methods for linear and nonlinear Schrödinger equations’, *SIAM J. Numer. Anal.* **33**(4), 1526–1533.

- D. Yin and C. Zheng (n.d.), ‘Composite gaussian beam approximation method for multi-phased wave functions’. submitted.
- L. Ying and E. J. Candès (2006), ‘The phase flow method’, *J. Comput. Phys.* **220**(1), 184–215.
- C. Zener (1932), ‘Non-adiabatic crossing of energy levels’, *Proc. Royal Soc. London, Series A* **137**(6), 692–702.
- P. Zhang (2002), ‘Wigner measure and the semiclassical limit of Schrödinger-Poisson equations’, *SIAM J. Math. Anal.* **34**(3), 700–718 (electronic).
- C. Zheng (2006), ‘Exact nonreflecting boundary conditions for one-dimensional cubic nonlinear Schrödinger equations’, *J. Comput. Phys.* **215**(2), 552–565.